Study on the non-precious metal catalyst for cathode in a direct formic acid fuel cell

Dissertation

Study on the non-precious metal catalyst for cathode in a direct formic acid fuel cell

Graduate School of Natural Science & Technology

Kanazawa University

Division of Mechanical Science and Engineering

Student ID Number : 1624032014

Name : Fahimah Binti Abd Lah Halim

Chief Advisor : Associate Professor Dr. Takuya Tsujiguchi

Date of Submission : June 2019

ABSTRACT

Non-precious metal catalysts (NPMCs) based such as iron (Fe) and cobalt (Co) catalysts have been widely studied in direct liquid fuel cells (DLFCs) application as cathode catalyst for oxygen reduction reaction (ORR), especially in direct methanol fuel cells (DMFCs). However, the performance of the single DMFC operation using the NPMCs at the cathode is remains low as compared with the conventional Pt/C catalyst. Therefore, the aim of this study is to achieve high performance in DLFC by applying the NPMC to the direct formic acid fuel cell (DFAFC) cathode. Fe– and Co–nitrogen-dopedcarbon nanotubes (NCNT) catalysts were synthesized and their ORR activity in acidic and alkaline medium was measured. As their ORR activity coexisting the fuel for these catalysts has not been investigated to the best of our knowledge, the ORR activity of the catalysts in coexisting the fuel (formic acid and sodium formate) are investigated in acidic and alkaline medium, respectively. Further, their performance in single DFAFC operation was evaluated and compared with the conventional Pt/C catalyst as well as the other DLFC operations.

This thesis consists of 5 chapters. In Chapter 1, the background about DFAFC, non-precious metal-based catalyst, the motivation and the objectives involved in this study are described. The methodology for this study involving the catalyst preparation, physical and electrochemical characterization of the prepared catalyst and single cell performance measurement are explained in Chapter 2. Herein, Fe–NCNT and Co–NCNT were synthesized using the conventional method by pyrolysis of multi-walled carbon nanotubes, dicyandiamide, and metal salt in a N_2 atmosphere at 800°C. First, effect of pyrolysis step and acid treatment of the catalysts on the ORR activity in acidic and alkaline medium are investigated. Different pyrolysis steps show different effect on ORR activity in acidic and alkaline medium. Both Fe–NCNT and Co–NCNT catalysts have higher formic acid and formate tolerance than the Pt/C catalyst in acidic and alkaline

medium, respectively. Co–NCNT catalyst exhibits excellent stability in both acidic and alkaline medium whereas Fe–NCNT catalyst shows comparable stability with that commercial Pt/C catalyst. These findings on the ORR catalytic activity and the fuel tolerance on the prepared catalyst in acidic and alkaline medium are discussed in Chapter 3.

Next, the Fe−NCNT and Co−NCNT catalysts are applied to the cathode DFAFC and the single cell performance test is measured and discussed in Chapter 4. Single-cell tests with hydrogen–oxygen (PEFC) and DFAFC operations were conducted under various operating conditions to compare the performance of the cells using the prepared catalysts and the conventional Pt/C catalyst. The performances of PEFC with both Fe–NCNT and Co–NCNT catalysts were significantly lower, 94.9 mW cm^{-2} for Fe–NCNT and 164.0 mW cm^{-2} for Co–NCNT at 60°C. Nevertheless, the Co–NCNT catalyst showed the high maximum power density of 160.7 mW cm^{-2} at DFAFC operation with 60°C and 7M formic acid. This value is similar to that for the DFAFC with the Pt/C catalyst, 128.9 mW cm^{-2}, and considerably higher than the value for other DLFCs using a non–Pt catalyst. Therefore, using these TM−NCNT catalysts as the cathode catalyst for DFAFC is promising as substitute for high-cost conventional Pt-based catalyst. Finally, all results corresponding to the objectives of this study are summarized in Chapter 5 and future work to enhance the single cell performance has been suggested.

TABLE OF CONTENT

CHAPTER 1

Introduction

1.1 Direct liquid fuel cell (DLFC)

Direct liquid fuel cells (DLFCs) are one of polymer-electrolyte membrane fuel cell (PEMFC) type that are recently gain more interests due to their high energy density, simple structure and ease of fuel storage and transportation. In DLFC, liquid fuel is fed to the anode where the oxidation reaction occurs, while air or oxygen is fed to the cathode for the reduction reaction. There are numerous types of DLFC such as direct methanol fuel cell (DMFC), direct ethanol fuel cell (DEFC), direct formic acid fuel cell (DFAFC), direct glycerol fuel cell (DGFC), direct dimethyl ether fuel cell (DDEFC) and direct hydrazine acid fuel cell (DHFC). The difference between these types of DLFCs is the liquid fuel fed to the anode side which leads in difference of electrochemical reaction involved, theoretical cell potential and energy density [1]. DMFCs is the most developed type of direct alcohol fuel cell for many applications such as portable power, which methanol is fed directly without require any fuel processor that allow in simple and compact design [2]. Methanol also offers several advantages such as higher energy density of 4820 Wh L^{-1} than liquid hydrogen (180 Wh L^{-1}), high solubility in aqueous electrolytes, low cost, easy to handle and transport [3]. DEFCs are another direct alcohol fuel cell type that attracted much attention in DLFC research, has high energy density of 8030 Wh kg^{-1}. As compared with the methanol, ethanol has lower permeability across the Nafion membrane which leads in less negative effect on the cathode performance [4,5]. Besides that, interest in DFAFCs also increasing in recent years. Formic acid used as the fuel does not have many of the limitations of hydrogen and methanol [6]. The advantages and challenges of DFAFCs will be further explained in the next section (1.1.1).

1.1.1 Direct formic acid fuel cell (DFAFC)

Direct formic acid fuel cells (DFAFCs) considered as a promising power source for portable devices as they offer higher power density and fast electro-oxidation kinetics [7]. Formic acid is a liquid at room temperature and dilute formic acid is recognized as safe since it is on the US Food and Drug Administration list of food additives. This fuel also benefit to proton conducting at the interface of anode catalyst layer and polymer electrolyte membrane and triple phase boundary in the anode catalyst layer [8]. Figure 1-1 shows the schematic of DFAFC which the formic acid oxidation reaction (FAOR) and oxygen reduction reaction (ORR) occur in the anode and cathode, respectively. The electromotive force (EMF) of formic acid (1.45 V) is higher than hydrogen and methanol which is 1.23 V and 1.18 V, respectively [9]. The anode, cathode and overall reaction of DFAFC are described as follows [10]:

Anode : $HCOOH \rightarrow CO_2 + 2H^+ + 2e^- \quad E_a^0 \sim 0.25\,V$ (1)

Cathode : $\frac{1}{2}O_2 + 2H^+ + 2e^- \rightarrow H_2O \quad E_c^0 = 1.23\,V$ (2)

Overall : $HCOOH + \frac{1}{2}O_2 \rightarrow CO_2 + H_2O \quad E^0 = 1.48\,V$ (3)

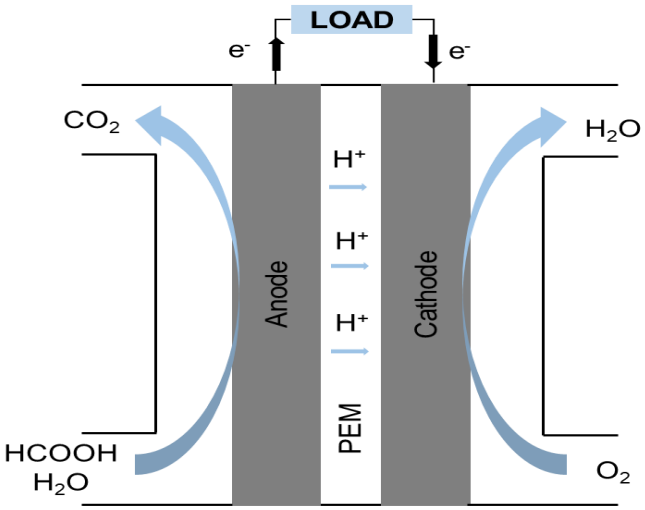

Figure 1-1 Schematic of direct formic acid fuel cell

There are several challenges faced in DFAFC operation in which one of them is caused by its fuel; formic acid. The transportations, storage and uses of formic acid should be handled with care due to its corrosive property. Formic acid also has specific toxic effects such as the exposure to humans could damage optical nerve and kidney. This challenge could be potentially addressed by using the counterpart of formic acid, which is formate salt in alkaline fuel cell. Formate salt is easily to handle as a solid of in solution form, stable, low toxicity and potentially low in cost [11]. This alkaline medium operation also can remarkably improve kinetics of oxygen reduction reaction and formic acid oxidation reaction [12].

Fuel crossover phenomena which is the transport of fuel from the anode to the cathode through a polymer electrolyte membrane is one of the major issues in DLFC operation. This phenomenon causes in reduction of fuel utilizations, degrade the cathode performance and reduction of the overall cell performance [13]. It has been reported by Y.-W. Rhee et al., the formic acid crossover rate through Nafion membrane is much lower than methanol which allows the usage of high fuel concentration in DFAFCs operation [14,15]. However, the formic acid crossover rate

is still significant due to repulsion between the formate anions and the membrane sulfonic groups [16]. Thus, recent studies turned towards to design cathode catalyst that has good tolerant to formic acid decomposition product which is notably CO [17]. Even though the Pt-based electrocatalyst is considered as the most practical oxygen reduction reaction (ORR) catalyst in DLFC cathode, it has low fuel tolerance. Furthermore, the high cost of Pt-based catalyst used at the cathode which increase the overall cost of fuel cell will hinder the large-scale commercialization of the DLFCs. Approaches to reduce the fuel cell cost have been introduced which are by reducing the amount of Pt loading and development of binary and ternary platinum based catalyst in DMFC [18,19]. However, over the long term, usage of non-precious metal catalyst (NPMC) would be better solution to this problem due to low abundance of Pt. Therefore, it is essential to develop alternative, cost-effective catalyst to eliminate the usage of Pt-based catalyst in fuel cell application. The high fuel tolerance, especially methanol on the non-precious metal catalyst (NPMC) based catalyst has been widely developed for DMFC application which will be further discussed in section 1.2 but, there is still limited number of the development of non-Pt based catalyst for DFAFC cathode application.

1.2 Non-precious metal catalyst (NPMC) for oxygen reduction reaction (ORR)

Non-precious metal-based catalyst (NPMC) for oxygen reduction reaction (ORR) was early developed by Jasinski in 1964 by pyrolyzing transition metal-containing macrocycles at temperature exceeding 700°C which significantly enhanced ORR activity and stability as compared with the performance of unheated macrocycles. The effort to replace the conventional Pt-based catalyst was then grew with various sources of nitrogen containing compounds, transition metal salt and carbon used to synthesized the NPMC that considerably improve the ORR activity and stability [20,21]. ORR at the cathode surface can proceed via two pathways. One is 2-electron

reduction pathway also referred as partial reduction that resulting in the production of H_2O_2 and the other is 4-electron reduction pathway which directly produce H_2O as shown in the following equations:

4-electron transfer pathway : $$O_2 + 4H^+ + 4e^- \rightarrow 2H_2O \quad (7)$$

2-electron transfer pathway : $$O_2 + 2H^+ + 2e^- \rightarrow H_2O_2 \quad (8)$$

$$H_2O_2 + 2H^+ + 2e^- \rightarrow 2H_2O \quad (9)$$

NPMCs have been widely developed to facilitate the ORR on cathode electrode in the past few decades, including metal free nitrogen-doped carbon (N-doped C) [22,23], non-precious metal oxides and carbides [24,25], transition metal−coordinating macrocyclic compounds [26,27], and transition metal−coordinating nitrogen-doped carbon catalysts (TM−NC) [28,29]. However, macrocyclic compounds are expensive and the N_4-chelates are eventually decompose into metal-nitrogen-carbon fragments. In addition, NPMCs can also be prepared from other cost-effective nitrogen-rich precursor (e.g. polyaniline, polypyrrole or ethylenediamine), transition metal salt (e.g. sulfates, nitrates, acetates, hydroxides and chlorides) and carbon support [20,30].

To date, the transition metal−nitrogen-doped carbon (TM−NC) catalysts with Fe and/or Co were found as the most effective than other non-precious transition metal such as Ni, Mn, Cu, Zn, Cr and V in both acidic and alkaline media [23,31,32]. The ORR active site for the TM−NC catalyst is formed when transition metal source, nitrogen precursor and carbon precursor are simultaneously going through heat treatment at temperature range from 500 °C to 1000 °C. It has been proposed that the transition metal itself does not play a role in the ORR but specific nitrogen functional group such as pyridinic-N or graphitic-N act as the catalytic sites by enhancing the electron donor properties of nitrogen doped-carbon based catalyst [33]. Nitrogen is considered as

an essential component to form active site for ORR in the catalyst [34]. In general, nitrogen is doped into the graphite structure can exist in the form of pyridinic-N, pyrrolic-N, graphitic-N and pyridinic-N oxide [35]. According to previous studies on transition metal-nitrogen doped-carbon electrocatalyst, the electrocatalytic activity for oxygen reduction reaction (ORR) can be attributed to pyridinic-N, pyrrolic-N and graphitic-N which regarded as ORR active site [33,36,37] . Pyridinic-N has one lone pair of electrons in addition to the one electron donated to the conjugated p bond system, imparting a Lewis basicity to the carbon. It is enable in adsorbing molecular oxygen and its intermediates in the ORR due to an increased electron-donor property of carbon [38]. Graphitic-N, which also known as "Quaternary-N", represents the nitrogen atom bonded to three carbon atoms within a graphite plane, while pyrrolic-N refer to nitrogen atoms that contribute to the p system with two p electron within a five-membered ring [39]. The possible nitrogen bonding configuration in graphitic network is illustrated in Figure 1-2. Some works suggest that higher relative content of pyridinic-N lead to the most active sites for ORR [40]. Therefore, the direct correlation between the type of nitrogen configuration and the ORR activity of the NPMC is remains elusive.

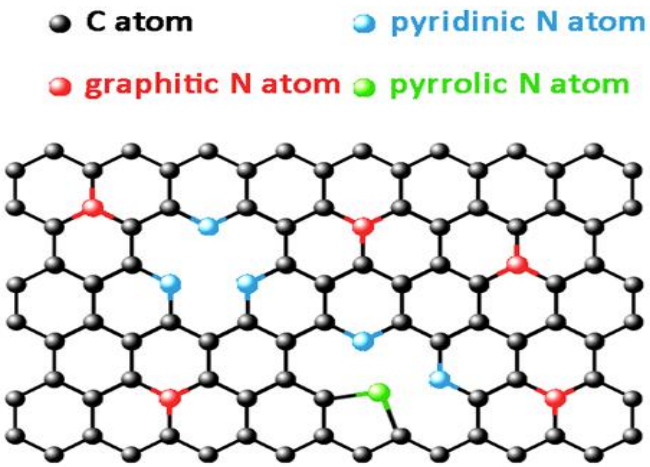

Figure 1-2 Illustration of nitrogen configuration in nitrogen-doped carbon.

Due to their significant ORR activity and stability as well as high fuel tolerance, study on the TM−NC catalyst have been widely reported for acidic and alkaline medium. Numerous types of cheap and abundant metal, nitrogen and carbon precursor are introduced by simple preparation procedure which supporting the effort to develop cost-effective, high catalytic activity and high fuel tolerance TM−NC catalyst as alternative to the Pt-based catalyst.

1.2.1 TM−NC catalyst in acidic medium

Transition metal−nitrogen-doped carbon (TM−NC) catalyst can be prepared by various low-cost and abundance metal or nitrogen precursors. The ORR catalytic activity of this TM−NC catalyst in acidic medium has been extensively studied and various parameters that significantly affect the ORR activity were determined. For instance, pyrolysis temperature, nitrogen or metal content, type of metal and catalyst preparation method. The reported studies on ORR activity of TM−NC catalyst in acidic medium is summarized in Table 1-1. In the study done by H.Xiao et al., carbon black supported Fe-imidazole complexes was prepared by using imidazole as the nitrogen precursor, iron chloride as the metal source and supported on Ketjen black EC300J. The effect of various pyrolysis temperature on the ORR activity of the catalyst was investigated and they found that the pyrolysis temperature influences the surface atomic composition and chemistry of Fe–NC catalysts, such as the iron content, nitrogen content and nitrogen species proportion, which results in different ORR activities. Fe–NC obtained by pyrolysis at 700 °C displays a comparable ORR activity with Pt–C and a better electrochemical stability than Pt–C [32]. R. Kothandaraman et al. prepared Fe−NC by pyrolysis of iron acetate, 2,2’-bipyridine and Ketjenblack in a quartz ampule at high pressure. Nitrogen precursor loading which is 2,2’-bipyridine and pyrolysis temperature were varied to determine their effect on the ORR activity of the synthesized catalyst. From the result, onset potential of the catalyst increases as the N content increases up to 10.3 wt. %.

Increasing N content over this value results in decreases in the onset potential due to excess partially decomposed bipyridine mass that cover or screen out some nitrogen species. The catalyst pyrolyzed at 800 °C showed improved kinetics [41].

S.-H. Liu and J-R. Wu investigated the effect of different nitrogen and metal precursor for Fe−NC catalyst on the ORR activity and stability. Nitrogen precursor namely which are ethylenediamine, tetratethylenepetamine and pentaethylenehexamine and two types of iron precursors, iron (III) chloride and iron (II) ammonium sulphate were used in the study. Catalyst synthesized from pentaethylenehexamine and iron (III) chloride as nitrogen and metal precursor, respectively possess highest electrocatalytic ORR activity and stability as compared with other types of precursors. This is due to the co-existence of pyridinic-N and quaternary-N as two main nitrogen-doping types in the catalyst that considered as the active site for ORR activity [37].

The N-doped carbon in the transition metal-nitrogen-carbon catalyst also can be prepared by using single precursor as reported by C.H. Choi et al.. Dicyandiamide (DCDA) was used as both carbon and nitrogen precursor. DCDA, as a precursor of N-doped carbon is low in cost and easy to handle due to its solid phase and non-flammability. They elucidate the effect of various metal precursor ($MeCl_2 \cdot xH_2O$, Me = Co, Fe and Ni) on the physical and electrochemical characteristics of the N-doped carbon. N-doped carbon from Co exhibited the highest ORR activity in acidic media due to the highest degree of sp^2-carbon structure than the other metal types; Fe and Ni. The type of seed metals also altered the amount of N-doping in carbon, which induced the formation of active sites for ORR. However, the amount of metal sees do not significantly change the electrochemical properties including capacitance, ORR activity and H_2O_2 production, but it affect the yield of DCDA carbonization during the pyrolysis [35]. A facile and cost-effective one-pot approach was utilized in the study done by X.Zhang et al. to prepare Co−NCNT by pyrolysis

of homogenously dispersed cobalt nitrate in melamine formaldehyde. This Co−NCNT catalyst exhibits reasonable activity and excellent durability in acidic media [42].

Instead of using only one transition metal precursor, S.H. Lim et al. 2012 used bimetallic FeCo nanoparticles to synthesize metal−nitrogen−carbon based ORR catalyst. The catalyst was prepared by annealing poly(vinylpyrrolidone)/MWCNTs Fe-Co complex (MWCNT-FeCo) in ammonia at 900 °C for 1 h. This method is considered as a very simple and cost-effective for converting pristine MWCNTs into nitrogen-doped carbon nanotubes. The NPMCs incorporate with binary Fe-Co metals yield better ORR activity than that NPMCs based on single metal precursor. The FeCo−MWCNT catalyst also exhibits excellent stability as compared with commercial Pt/C catalyst. The presence of different metal nanoparticle gives significant influence on the nature of nitrogen dopants [30].

S. Ratso et al. synthesized Fe− and Co− containing N-doped CNT by pyrolysis of multi-walled carbon nanotubes (MWCNTs), dicyandiamide as a nitrogen precursor and metal salt as the transition metal source. Fe-based catalyst is more active than Co-based catalyst in acidic medium but both catalysts were highly tolerant to methanol which could be used as cathode catalysts in DMFC. The stability test showed that Co-based catalyst has higher stability than the Fe-based catalyst [28]. Another simple, low-cost and environmentally friendly method to prepare cobalt-based catalyst for ORR also introduced by Q. Zhao et al.. They synthesized N-doped carbon nanosheet-encased Co nanoparticles (NCN−Co) by simple one-step pyrolysis method using cheap and sustainable corn starch, cobalt acetate and dicyandiamide. The ORR catalytic activity of NCN−Co catalyst outperformed the nitrogen-doped carbon nanosheet (NCN) counterparts. The onset potential of the NCN−Co is still lower than commercial Pt/C catalyst, but it exhibits much higher limiting current density, comparable half-wave potential and high electron transfer number

which indicates its comparable ORR overpotential to the Pt/C catalyst in acidic media [43]. It can be concluded that, TM−NC catalyst which can be prepared by simple and cost-effective method using inexpensive materials exhibits comparable ORR activity, high stability and much higher fuel tolerance than conventional Pt/C catalyst in acidic medium. This indicates the TM−NC catalyst is promising as the cathode catalyst for DLFC applications.

Table 1-1 TM−NC catalyst studied for ORR in acidic medium

Catalyst	Precursor	Preparation method	ORR performance	Number of electrons transfer	References
FeCo−NC	Poly(vinylpyrrolidone), iron (III) chloride hexahydrate, cobalt (II) acetate tetrahydrate, Multi-walled carbon nanotubes (MWCNTs)	Pyrolysis in NH_3	0.82	3.7	[30]
Fe−NC	Poly(vinylpyrrolidone), iron (III) chloride hexahydrate, cobalt (II) acetate tetrahydrate, Multi-walled carbon nanotubes (MWCNTs)	Pyrolysis in NH_3	0.67	2.0	[30]
Co−NC	Poly(vinylpyrrolidone), iron (III) chloride hexahydrate, cobalt (II) acetate tetrahydrate, Multi-walled carbon nanotubes (MWCNTs)	Pyrolysis in NH_3	0.67	1.9	[30]
Fe−NC	Imidazole Iron chloride Ketjen black EC300J (EC300)	Pyrolysis in N_2	0.8	3.95	[32]
			~ 0.8	3.57	[41]

Fe−NC	Iron (II)-acetate 2-2'-bipyridine Ketjen black 600JD	Pyrolysis in N_2			
Fe−NC	pentaethylenehexamine iron (III) chloride Vulcan XC-72	Pyrolysis in N_2	0.83	3.1	[37]
Fe−NC	$FeCl_3$ Dicyandiamide (DCDA) MWCNTs	Pyrolysis in N_2	0.56	~4.0	[28]
Co−NC	$CoCl_2$ Dicyandiamide (DCDA) MWCNTs	Pyrolysis in N_2	0.52	~3.5	[28]
Co−NC	Cobalt nitrate Melamine formaldehyde	Pyrolysis in N_2	0.87	3.95	[42]
Co−NC	Corn starch Cobalt acetate Dicyandiamide	Pyrolysis in Ar	~0.6	3.52~3.86	[43]
Co−NC	2,4,6-tris(2-pyridyl)-1,3,5-triazine (TPTZ, cobalt(II) nitrate hexahydrate MWCNT	Pyrolysis in N_2	~0.8	NA	[44]
Co−NC	Dicyandiamide Cobalt chloride	Pyrolysis in Ar	0.59	NA	[35]

1.2.2 TM−NC catalyst in alkaline medium

Besides acidic condition, the TM−NC catalyst can be well applied in alkaline DLFC as the cathode catalyst due to its comparable ORR activity with the conventional Pt/C catalyst. Extensive studies were reported in the measurement of ORR activity of the TM−NC in alkaline medium. Various low-cost carbon, nitrogen and metal sources with different preparation procedure are used to synthesize the TM−NC catalyst as summarized in Table 1-2. H.Wu et al. synthesized a highly active cobalt-nitrogen doped graphene (Co−NC) catalyst by pyrolysis cheap milk biomass as the nitrogen source, graphene oxide (GO) as the carbon source and $CoCl_2 \cdot 6H_2O$ as the metal source. The acid-treatment was done to facilitate the transformation of quaternary-N and oxidized-N to pyridinic-N and pyrrolic-N species that have been proved as the active site for ORR. This Co−NC catalyst showed superior long-term stability and better methanol tolerance than commercial Pt/C catalyst in alkaline medium. These features are important considerations for the catalyst to be applied as cathode catalyst of fuel cells [45].

In the work done by S. Ratso et al. carbon nanotubes based NPM catalyst was developed. The effect of acid treatment on ORR activity in alkaline medium was investigated. Synthesis of Fe−NC catalyst was carried out by simple pyrolysis using cheap nitrogen (dicyandiamide) and metal precursor (iron chloride) followed by an acid treatment and a second pyrolysis step. The Fe−NC catalyst exhibits a comparable ORR activity but remarkable methanol tolerance and high stability in alkaline medium as compared with the commercial Pt/C catalyst. Comparing between the non-acid treated and acid treated catalyst, the ORR activity was improved approaching to that of commercial Pt/C catalyst for the Fe−NC catalyst obtained from acid leaching and second pyrolysis step was done [46]. Z. Ma et al. reported a facile method to synthesize Co−NC by pyrolysis of single-wall carbon nanotubes with low-cost dual nitrogen sources which are

polyaniline (PANI) and melamine (ME), and metallic cobalt as the transition metal source. The findings show superior methanol tolerance and stability of the prepared catalyst as compared with commercial Pt/C catalyst. They also compare the effect of acid treated and non-acid treated catalyst on the ORR activity. The existence of the metallic Co in the heat-treatment process can enhance the ORR catalytic activity and it needs to be remove during acid treatment process to expose more active sites [47].

N-doped graphene coupled with Co nanoparticles was prepared by one-step pyrolysis of the mixture of sucrose, urea and cobalt nitrate by G. Zhang et al. [48]. The prepared catalyst has comparable ORR catalytic activity to commercial Pt/C catalyst with dominating 4-electron pathway in alkaline condition. Additionally, the Co−NC catalyst synthesized also exhibit outstanding stability and a much better methanol tolerance than Pt/C, which was positive for the application of the electrocatalyst in DMFC. Another low-cost and high performance NPM catalyst was developed in the study done by S. Mutyala and J. Mathiyarasu [49]. Fe−NCNF catalyst was fabricated from pyrolysis of ferric chloride and interfacial synthesized polyaniline (PANI) nanofibers. Even though the ORR catalytic activity is still less than Pt/C catalyst, the durability and methanol tolerance is much better than that commercial Pt/C in alkaline medium. H. Ghanbarlou et al. studied the effect of different supporting material for Fe and Co electrocatalyst on ORR activity. Fe and Co nanoparticles were precipitated on N-doped graphene (NG) and multi-walled carbon nanotubes (MWCNT). NG supported metal exhibited higher ORR activity than those which is supported by MWCNTs. This study concluded that the planar structure of graphene and nitrogen species has important effect on the improved ORR catalytic activity. This is because the ORR active site on the NG supported metal catalyst is induced by the nitrogen atoms [50].

Instead of carbon nanotubes, carbon black and graphene which were commonly used as the carbon precursor, A. Sarapuu et al. used carbon aerogel (CA) as the carbon precursor in preparing TM−NC catalyst and the effect of different transition metal used on the ORR activity was investigated. Two types of transition metal which are Co and Fe, and melamine as the nitrogen precursor were synthesized and their ORR activity was evaluated and compared. Co−N-doped carbon aerogel (Co−NCA) was found to be more active than Fe−NCA catalyst in alkaline medium with good stability and low peroxide yield. As compared with commercial Pt/C catalyst, the half-wave potential for Co−NCA catalyst was slightly lower than that commercial Pt/C catalyst which indicates that the CA as the carbon precursor is a promising material to be used to synthesize TM−NC catalyst for fuel cell cathode catalyst. However, further optimizations on the compositions and surface morphology need to be done to improve electrocatalytic activity of the catalyst [51].

In summary, the TM−NC catalysts that have been widely studied for ORR in alkaline medium shows comparable ORR activity with the conventional Pt/C catalyst but, they have better stability and higher tolerance toward methanol than that Pt/C catalyst. These findings are in accordance with the ORR activity in acidic medium. Therefore, the Fe− and Co−NC catalyst is considered as promising cathode catalyst for single DMFC both in acidic and alkaline condition.

Table 1-2 TM−NC catalyst studied for ORR in alkaline medium

Catalyst	Precursor	Preparation method	Onset potential (V)	Number of electrons transfer	References
Co−NC	milk biomass, GO nanosheets, Cobalt chloride	Pyrolysis in N_2	0.035	3.8	[45]
Fe−NC	Iron nitrate, melamine, Carbon aerogel	Ion-exchange, pyrolysis in N_2	~-0.2	3.2	[51]
Co−NCA	Cobalt nitrate,	Ion-exchange,	-0.1	3.7	

	Melamine, Carbon aerogel	pyrolysis in N_2			[51]
Fe−MWCNT	Iron nitrate MWCNTs	Precipitation	-0.25	-	[50]
Co−MWCNT	Cobalt nitrate MWCNTs	Precipitation	-0.28	-	[50]
Fe−NG	Iron nitrate N-doped graphene (prepare by solvothermal)	Precipitation	-0.20	-	[50]
Co−NG	Cobalt nitrate N-doped graphene (prepare by solvothermal)	Precipitation	-0.14	-	[50]
Co−NC	CNTs, melamine, polyaniline, Cobalt chloride	Ball-milling, Pyrolysis in N_2	~ - 0.05	4.1	[47]
Co−NC	Cobalt nitrate Sucrose Urea	Pyrolysis in Ar	-0.035	3.6	[48]
Fe−NC	Iron chloride PANI nanofibers (prepare by interfacial polymerization)	Pyrolysis in inert atmosphere	~0.15	3.8	[49]
Fe−NC	Iron chloride Dicyandiamide MWCNT	Pyrolysis in N_2	-0.04	close to 4	[46]

1.3 Non-precious metal catalyst (NPMC) in DLFC operation

Since Fe−NC and Co−NC catalyst are proved to have higher methanol tolerance and higher stability than the conventional Pt/C catalyst, these catalysts are successfully applied as the cathode in DMFC operation. However, there is no studies for DFAFC operation with the Fe− and Co−NC as cathode catalyst although there are a few studies on NPMC for DFAFC cathode. In this section,

the performance of single DMFC with Fe− and Co−NC as cathode catalyst from previous studies are reviewed. Other studies reported supporting the effort to replace the Pt-based catalyst for DFAFC application including the modification of Pt-based and development of non-Pt based catalyst are also reviewed in this section

1.3.1 Single cell performance of DMFC with TM−NC cathode

Numerous studies reported on the performance of single DMFC using TM−NC catalysts in the cathode. D. Sebastian et al. carried out performance tests on single DMFC using a Fe–NC cathode catalyst based on heat-treated iron nitrate with a highly nitrogen-rich organic precursor: aminobenzimidazole. The highest maximum power density which is approximately 24 mW cm^{-2} obtained at 90°C operating temperature and 5 M methanol [52]. They also tested single DMFC with a Fe-based cathode catalyst synthesized from another nitrogen precursor, aminoantipyrine. The highest maximum power density obtained was 35 mW cm^{-2} at 90°C and 5 M methanol but, the performance using a conventional Pt/C catalyst was better, with the maximum power density of 65 mW cm^{-2} under similar operating conditions. It is remarkable that there is slightly changes in OCV values with the increase of methanol concentration for Fe-based cathode catalyst. However, a significant decrease of OCV for Pt−based cathode as the methanol concentration increase which indicates the detrimental effect of methanol crossover in DMFC operation with Pt−based cathode catalyst [53].

Next, they evaluated the DMFC performance with a Fe–NC catalyst derived from nicarbazin as the nitrogen precursor, and the cell performance was compared with the conventional Pt/C cathode catalyst at two different operating temperature and methanol concentration. The highest maximum power density achieved by Fe–NC cathode catalyst is approximately 62 mW

cm^{-2} at 90 °C and 5 M methanol concentration while slightly lower than 60 mW cm^{-2} achieved by Pt/C cathode under similar condition as shown in Figure 1-3.

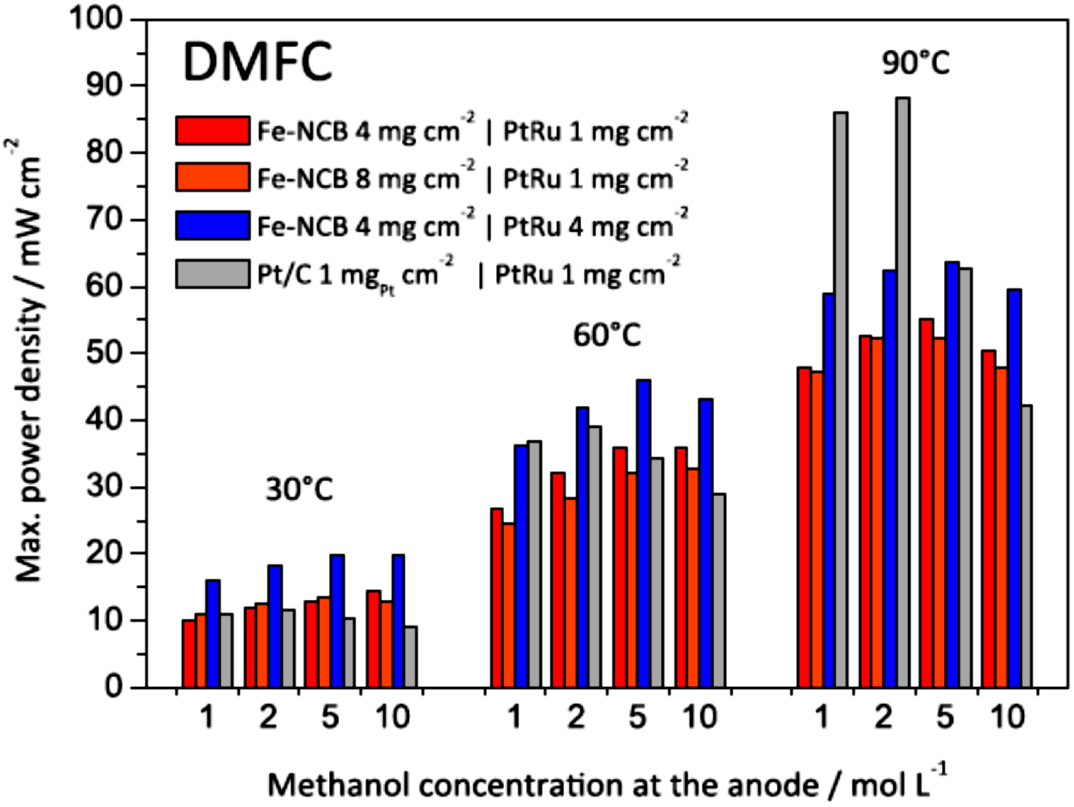

Figure 1-3 Maximum power densities in DMFC operation at different electrode loading, operating temperature and methanol concentration [54].

At the same temperature, as the methanol concentration increase to 10 M, the maximum power density slightly decreases to 60 mW cm^{-2} for Fe–NC and significant decrease to 40 mW cm^{-2} for Pt/C cathode which is caused by the detrimental effect of methanol crossover on the low methanol tolerance Pt-based catalyst. This crossover effect can be observed from the OCV values. The OCV for the MEA with Pt/C cathode (0.5 V) is lower than that with Fe−NC cathode catalyst (0.82 V). This trend also observed when the operating temperature and methanol concentration were increased to 110 °C and 17 M, respectively. It is noteworthy that the OCV for Pt/C cathode-

based MEA is 0.45 V whereas MEA based on Fe−NC cathode exhibit higher than that, 0.78 V. The maximum power density reached is 58 mW cm^{-2} and 26 mW cm^{-2} for Fe−NC and Pt/C, respectively at 110 °C and 7 M methanol concentration. In summary, the higher cell performance for the NPM catalyst in the DMFC operation is related to the superior methanol tolerance properties as compared with the conventional Pt/C catalyst [54].

In the study done by L. Osmieri et al., the DMFC performance was evaluated when using Fe–NC catalysts synthesized from four different carbon supports. However, those catalysts showed lower performance compared to the conventional Pt/C catalyst that showed a maximum power density of 30.9 mW cm^{-2} at 90 °C operating temperature and 2 M methanol concentration. The best catalyst using synthesized mesoporous silica nanoparticles as carbon support (Fe–NMPC) gave a 22.6 mW cm^{-2} maximum power density under the similar operating condition [55]. E.Negro et al. have reported Fe−N supported on graphitic carbon nano-networks which is synthesized by wet-impregnation method. The maximum power density recorded in DMFC operation is 15 mW cm^{-2} at 2 M methanol concentration and 90 °C operating temperature [56]. They also measured the cell performance using different methanol concentration (1, 2 and 10 M) at 60 °C and the highest maximum power density achieved with 2 M methanol. From the single DMFC performance results, higher performance can be obtained by the TM−NC cathode catalyst at higher methanol concentration and operating temperature as attributed to the high methanol tolerance as compared with conventional Pt/C cathode catalyst. Several studies were done on NPMC for DFAFC cathode application in order to find the alternatives for reducing the usage of expensive Pt-based catalyst which will be further discussed in section 1.3.2

1.3.2 Non-precious metal-based cathode catalyst in DFAFC operation

Pt/C catalyst is typically used as the cathode catalyst in direct formic acid fuel cell (DFAFC) operation. In DFAFC, studies were done on the cathode electrocatalyst including modification of Pt-based catalyst and development of non-Pt based catalyst [57–60] which is summarized in Table 1-3. Modification of support for Pt-based catalyst also affects the tolerance toward formic acid as reported by L. Timperman et al. Formic acid tolerance was measured on Pt and Ru_xSe_y deposited onto oxide-carbon composite substrate (TiO_2/C). The formic acid tolerance was improved for Pt/TiO2/C catalyst than Pt/C catalyst where the onset potential recorded for Pt/TiO_2/C is shifted to a higher potential from 0.30 V to 0.38 V as compared to Pt/C catalyst. Inversely, for the Ru_xSe_y catalyst, the onset potential was negatively shifted 90 mV for Ru_xSe_y/TiO_2/C with respect to the Ru_xSe_y/C in the presence of formic acid. As compared with Pt, Ru_xSe_y catalyst is more tolerant to the formic acid [60].

K.Lee et al. synthesized three carbon-supported Iridium (Ir) -based binary catalysts, Ir-Co/C, Ir-Ni/C and Ir-Cr/C for the ORR in acidic medium with and without formic acid. Compared with both Pt/C and Pd/C catalyst, the Ir-based catalysts demonstrated much higher formic acid tolerance indicates that the synthesized catalysts are promising for DFAFC applications [16]. ORR activity on carbon supported transition metal chalcogenides catalyst such as Ru_xSe_y/C, CoSe/C were also tested with and without formic acid in acidic medium. The result indicates that the onset potential of CoSe/C catalyst is approximately 0.1 V lower than Pt/C prepared in the study. However, CoSe/C shows almost full tolerance and inactive for oxidation reaction in the presence of formic acid up to concentration of 10 M which in contrast with Pt/C that shows no tolerance to formic acid [58]. Due to the lower price of palladium (Pd) than Pt, this metal could be a good candidate as an alternative to Pt for ORR catalyst. A. Mikolajczuk-Zychora et al. prepared carbon

supported Pd (Pd/Vulcan) catalyst for DFAFC cathode with functionalizing the carbon support with nitric acid. From the single cell performance test, it was observed that the maximum power density for Pd/C is similar to that commercial 20 wt. % Pt/C (Premetek) catalyst as shown in Figure 1-4 [61]. Based on these literatures discussed, it can be deducted that non-platinum catalysts developed are considered as promising cathode electrocatalyst for DFAFC due to the high formic acid tolerance than Pt-based catalyst.

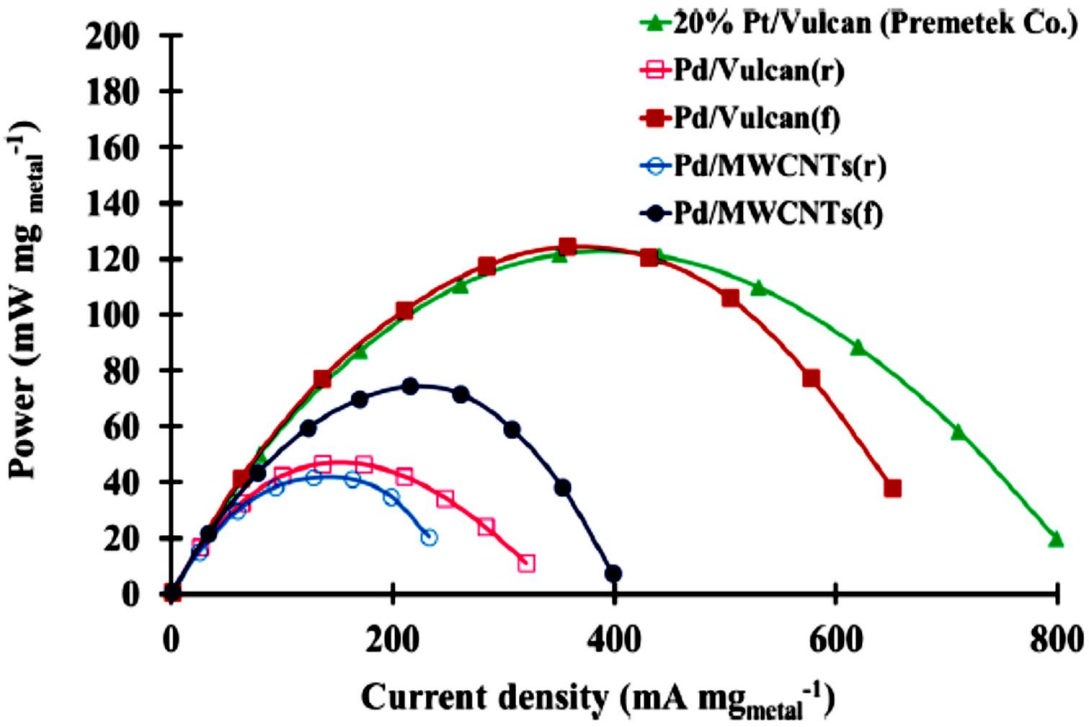

Figure 1-4 Initial power versus current density curves for DFAFC cathode catalysts at 30 ◦C [61].

Table 1-3 Studies on non-precious metal-based catalyst for DFAFC application

Measurement	Operating condition	Anode catalyst	Cathode catalyst	Outcomes	Reference
Half-cell	0.5 M H_2SO_4 0.5 M H_2SO_4 + 0.1 M HCOOH	-	Ir-Co/C	E_{onset} : 0.89 V vs. RHE (without HCOOH) E_{onset} : 0.83 V vs. RHE (with 0.1M HCOOH)	[16]
Half-cell	0.5 M H_2SO_4 0.5 M H_2SO_4 + 0.1 M HCOOH	-	Ir-Ni/C	E_{onset} : 0.89 V vs. RHE (without HCOOH) E_{onset} : 0.83 V vs. RHE (with 0.1M HCOOH)	[16]
Half-cell	0.5 M H_2SO_4 0.5 M H_2SO_4 + 0.1 M HCOOH	-	Ir-Cr/C	E_{onset} : 0.89 V vs. RHE (without HCOOH) E_{onset} : 0.83 V vs. RHE (with 0.1M HCOOH)	[16]
Half-cell	0.5 M H_2SO_4 + 0.5 M HCOOH	-	$Ru_xSe_y/TiO_2/C$	E_{onset} : 0.77 V vs. RHE (with 0.5M HCOOH)	[60]
Half-cell	0.5 M H_2SO_4 + 0.5 M HCOOH	-	Ru_xSe_y/ C	E_{onset} : 0.86 V vs. RHE (with 0.5M HCOOH)	[60]
Half-cell	0.5 M H_2SO_4 0.5 M H_2SO_4 + HCOOH (2-10 M)	-	CoSe/C	E_{onset} : 0.82 V vs. SHE 4-electron transfer for ORR high formic acid tolerance	[58]
Single cell	3M HCOOH (0.5 ml/min) O_2 (125 ml/min)	60 wt. % Pd/Vulcan	20 wt. % Pd/Vulcan	~ 120 mW/mg_{metal} of max. power density	[61]

1.4 Objective and scope of study

Transition metal-nitrogen-doped carbon (TM−NC) catalysts have been studied for DMFC cathode catalyst application as an alternative to the expensive conventional Pt-based catalyst. Fe− and Co−NC were found as the most effective catalyst for ORR as compared to the other non-precious metal-based catalyst. Based on the literatures reported on the ORR activity of these Fe−NC and Co−NC catalyst in acidic and alkaline medium that have been discussed in the previous section, they exhibit comparable ORR activity with the conventional Pt/C catalyst. Moreover, they showed superior methanol tolerance and stability than that conventional Pt/C catalyst in acidic and alkaline medium [28,46]. In addition, the application of Fe− and Co−NC catalysts as the cathode catalyst in DMFC operation also reported [52–55]. From the single cell DMFC performance result, the better methanol tolerance and higher stability of the TM−NC catalysts as compared to Pt/C catalyst was also evidenced especially at higher operating temperature and higher methanol concentration [55]. However, their power density was still low, 22.6 mW cm^{-2}, due to the poor anode reaction kinetics. For the improvement of power density using liquid fuel with TM−NC catalyst, use of formic acid as a fuel of DLFC, i.e. DFAFC, is a promising approach. As the cathode reaction of DMFC is similar to DFAFC, it is expected that any improvements to the DMFC cathode catalyst will be applicable for DFAFC as well [62]. Nevertheless, the formic acid tolerance and the performance of single DFAFC operation using the Fe−NC and Co−NC have not been reported to the best of our knowledge.

Therefore, the aim of this study is to achieve high performance in DLFC operation by employing the TM−NC as the cathode catalyst for DFAFC. The scope of this study involves the half-cell measurement to determine the ORR activity and formic acid tolerance of both TM−NC catalysts and then, they are applied in cathode of DFAFC in which the single cell measurement is

carried out. Fe− and Co−NC catalyst were prepared by referring to the procedure described in literature [28]. The ORR catalytic activity and the tolerance toward formic acid and formate salt on the Fe−NC and Co−NC catalyst was evaluated in acidic and alkaline medium, respectively. Single cell performance was evaluated in PEFC and DFAFC operation with the synthesized Fe−NC and Co−NC as the cathode catalyst. The effect of different of operating condition on the DFAFC performance was determined. Both half-cell and single cell measurements of the NPM catalyst are compared with the conventional Pt/C catalyst.

1.4.1 Objective of study

There are several objectives involved to achieve the aim of this study which stated as followed:

1. To study formic acid tolerance on transition metal nitrogen-doped carbon nanotubes (TM−NCNT) catalysts in acidic and alkaline medium
2. To study the single cell performance of direct formic acid fuel cell (DFAFC) by using TM−NCNT catalyst as the cathode catalyst
3. To compare the performance of DFAFC with TM−NCNT catalyst with the conventional Pt/C catalyst and other DLFC operation

1.5 Structure of thesis

In Chapter 1 of this thesis, the type and operation of direct liquid fuel cell (DLFC) were introduced. DFAFC operation, advantages and challenges are discussed in the Chapter 1 as this study is focusing on the DFAFC. Next, the TM−NC catalysts which have been reported in acidic and alkaline medium especially for DLFC cathode catalyst is further reviewed. Several studies reported on the application of TM−NC as cathode catalyst in DMFC application and few studies for DFAFC with non-precious metal cathode catalyst are also included in Chapter 1. According to the literature, the scope of this study was determined which is also stated in Chapter 1.

Methodology involved for this study was thoroughly explained in Chapter 2. The methodology includes catalyst preparation procedure, ORR catalytic activity measurement and single cell performance evaluation in PEFC and DFAFC operation. In Chapter 3, the result for the first objective which is to study the fuel tolerance on the TM−NCNT in acidic and alkaline medium was discussed. Next, Chapter 4 is involving the second and third objective of this study. Both types of TM−NCNT catalysts prepared was then applied as the cathode catalyst in a single cell PEFC and DFAFC operation, and the cell performance was evaluated and discussed in Chapter 4. The findings for this study are then concluded and summarized in Chapter 5 and further work also suggested. The structure of this thesis is summarized and presented Figure 1-5:

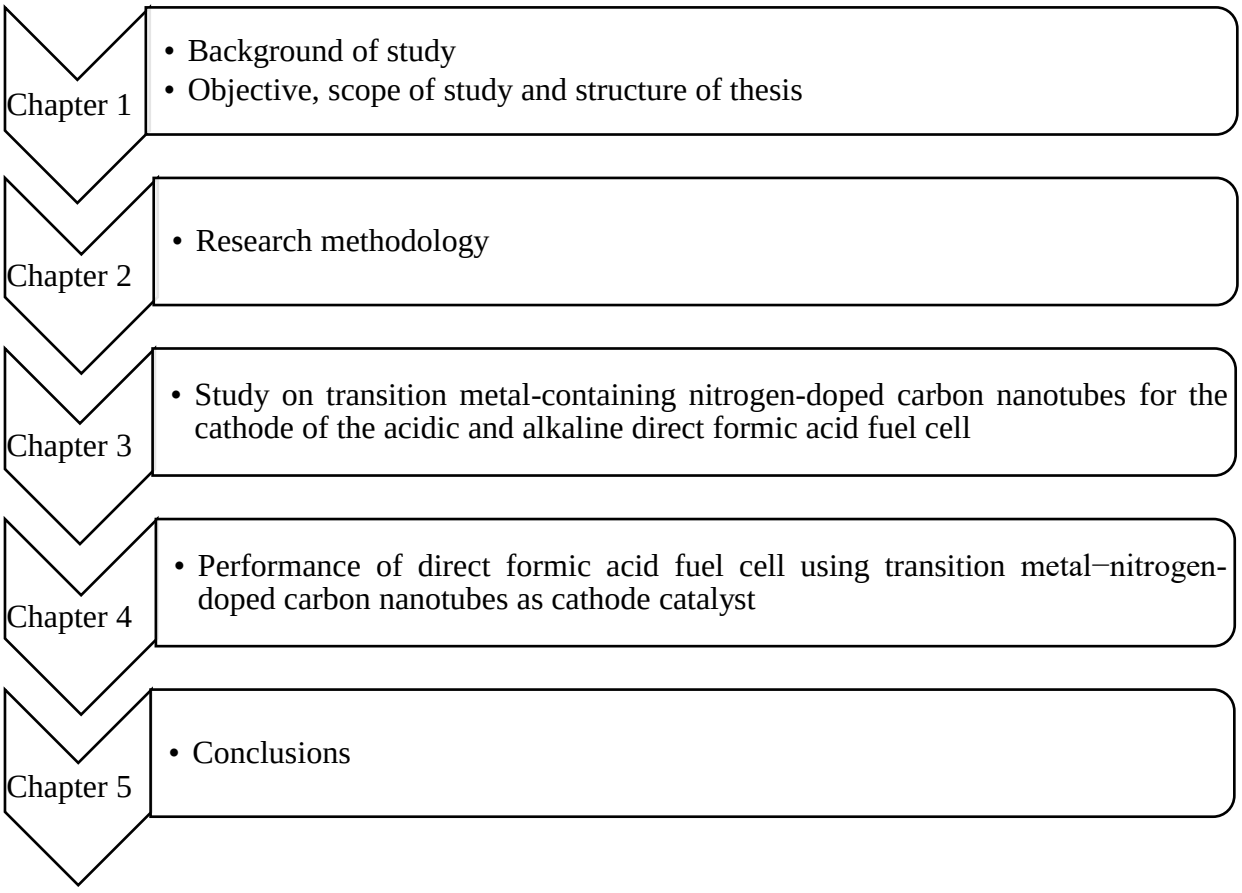

Figure 1-5 Flow chart of the thesis structure

1.6 References

[1] B.C. Ong, S.K. Kamarudin, S. Basri, Direct liquid fuel cells : A review, Int. J. Hydrogen Energy. 42 (2017) 10142–10157. doi:10.1016/j.ijhydene.2017.01.117.

[2] M. Goor, S. Menkin, E. Peled, High power direct methanol fuel cell for mobility and portable applications, Int. J. Hydrogen Energy. 44 (2019) 3138–3143. doi:10.1016/J.IJHYDENE.2018.12.019.

[3] C. Lamy, A. Lima, V. LeRhun, F. Delime, C. Coutanceau, J.-M. Léger, Recent advances in the development of direct alcohol fuel cells (DAFC), J. Power Sources. 105 (2002) 283–296. doi:10.1016/S0378-7753(01)00954-5.

[4] M.Z.F. Kamarudin, S.K. Kamarudin, M.S. Masdar, W.R.W. Daud, Review: Direct ethanol fuel cells, Int. J. Hydrogen Energy. 38 (2013) 9438–9453. doi:10.1016/J.IJHYDENE.2012.07.059.

[5] S. Song, W. Zhou, Z. Liang, R. Cai, G. Sun, Q. Xin, V. Stergiopoulos, P. Tsiakaras, The effect of methanol and ethanol cross-over on the performance of PtRu/C-based anode DAFCs, Appl. Catal. B Environ. 55 (2005) 65–72. doi:10.1016/J.APCATB.2004.05.017.

[6] C.M. Miesse, W.S. Jung, K.-J. Jeong, J.K. Lee, J. Lee, J. Han, S.P. Yoon, S.W. Nam, T.-H. Lim, S.-A. Hong, Direct formic acid fuel cell portable power system for the operation of a laptop computer, J. Power Sources. 162 (2006) 532–540. doi:10.1016/J.JPOWSOUR.2006.07.013.

[7] T. Tsujiguchi, F. Matsuoka, Y. Hokari, Y. Osaka, A. Kodama, Overpotential analysis of the Direct Formic Acid Fuel Cell, Electrochim. Acta. 197 (2016) 32–38. doi:10.1016/j.electacta.2016.03.062.

[8] W. Cai, L. Liang, Y. Zhang, W. Xing, C. Liu, Real contribution of formic acid in direct formic acid fuel cell : Investigation of origin and guiding for micro structure design, Int. J. Hydrogen Energy. 38 (2012) 212–218. doi:10.1016/j.ijhydene.2012.09.155.

[9] S. Ha, B. Adams, R.I. Masel, A miniature air breathing direct formic acid fuel cell, J. Power Sources. 128 (2004) 119–124. doi:10.1016/j.jpowsour.2003.09.071.

[10] X. Yu, P.G. Pickup, Recent advances in direct formic acid fuel cells (DFAFC), J. Power Sources. 182 (2008) 124–132. doi:10.1016/j.jpowsour.2008.03.075.

[11] J. Jiang, A. Wieckowski, Prospective direct formate fuel cell, Electrochem. Commun. 18 (2012) 41–43. doi:10.1016/j.elecom.2012.02.017.

[12] L. Zeng, Z.K. Tang, T.S. Zhao, A high-performance alkaline exchange membrane direct formate fuel cell, Appl. Energy. 115 (2014) 405–410. doi:10.1016/j.apenergy.2013.11.039.

[13] W. Qian, D.P. Wilkinson, J. Shen, H. Wang, J. Zhang, Architecture for portable direct liquid fuel cells, J. Power Sources. 154 (2006) 202–213. doi:10.1016/J.JPOWSOUR.2005.12.019.

[14] K.-J. Jeong, C.M. Miesse, J.-H. Choi, J. Lee, J. Han, S.P. Yoon, S.W. Nam, T.-H. Lim, T.G. Lee, Fuel crossover in direct formic acid fuel cells, J. Power Sources. 168 (2007) 119–125. doi:10.1016/j.jpowsour.2007.02.062.

[15] Y.-W. Rhee, S.Y. Ha, R.I. Masel, Crossover of formic acid through Nafion® membranes, J. Power Sources. 117 (2003) 35–38. doi:10.1016/S0378-7753(03)00352-5.

[16] K. Lee, L. Zhang, J. Zhang, Formic Acid Tolerant Ir-Based Electrocatalysts for Oxygen Reduction Reaction, Int. J. Green Energy. 8 (2011) 295–305. doi:10.1080/15435075.2011.557849.

[17] N. V Rees, R.G. Compton, Sustainable energy: a review of formic acid electrochemical fuel cells, J. Solid State Electrochem. 15 (2011) 2095–2100. doi:10.1007/s10008-011-1398-4.

[18] S. Knani, L. Chirchi, W.T. Napporn, S. Baranton, J.M. Léger, A. Ghorbel, Promising ternary Pt-Co-Sn catalyst for the oxygen reduction reaction, J. Electroanal. Chem. 738 (2015) 145–153. doi:10.1016/j.jelechem.2014.11.023.

[19] J.F. Drillet, A. Ee, J. Friedemann, R. Kötz, B. Schnyder, V.M. Schmidt, Oxygen reduction at Pt and Pt70Ni30 in H2SO4/CH3OH solution, Electrochim. Acta. 47 (2002) 1983–1988. doi:10.1016/S0013-4686(02)00027-0.

[20] G. Wu, P. Zelenay, Nanostructured nonprecious metal catalysts for oxygen reduction reaction, Acc. Chem. Res. 46 (2013) 1878–1889. doi:10.1021/ar400011z.

[21] G. Wu, K.L. More, C.M. Johnston, P. Zelenay, High-Performance Electrocatalysts for Oxygen Reduction Derived from Polyaniline, Iron, and Cobalt, Science (80-.). 332 (2011) 443–447. doi:10.1126/science.1200832.

[22] M. Borghei, P. Kanninen, M. Lundahl, T. Susi, J. Sainio, I. Anoshkin, A. Nasibulin, T. Kallio, K. Tammeveski, E. Kauppinen, V. Ruiz, High oxygen reduction activity of few-walled carbon nanotubes with low nitrogen content, Appl. Catal. B Environ. 158 (2014) 233–241. doi:10.1016/j.apcatb.2014.04.027.

[23] J. Masa, A. Zhao, W. Xia, Z. Sun, B. Mei, M. Muhler, W. Schuhmann, Trace metal residues promote the activity of supposedly metal-free nitrogen-modified carbon catalysts for the oxygen reduction reaction, Electrochem. Commun. 34 (2013) 113–116. doi:10.1016/j.elecom.2013.05.032.

[24] W. Jin, J. Liu, Y. Wang, Y. Yao, J. Gu, Z. Zou, Direct NaBH4-H2O2 fuel cell based on nanoporous gold leaves, Int. J. Hydrogen Energy. 38 (2013) 10992–10997. doi:10.1016/j.ijhydene.2013.01.016.

[25] G. Singla, K. Singh, O.P. Pandey, Study on single step solid state synthesis of WC@C nanocomposite and electrochemical stability of synthesized WC@C & Pt/WC@C for alcohol oxidation (methanol/ethanol), J. Alloys Compd. 665 (2016) 186–196. doi:10.1016/j.jallcom.2015.09.098.

[26] S.N.S. Goubert-renaudin, X. Zhu, A. Wieckowski, Electrochemistry Communications Synthesis and characterization of carbon-supported transition metal oxide nanoparticles — Cobalt porphyrin as catalysts for electroreduction of oxygen in acids, Electrochem. Commun. 12 (2010) 1457–1461. doi:10.1016/j.elecom.2010.06.004.

[27] N.A. Karim, S.K. Kamarudin, Novel heat-treated cobalt phthalocyanine/carbon-tungsten oxide nanowires (CoPc/C-W18O49) cathode catalyst for direct methanol fuel cell, J. Electroanal. Chem. 803 (2017) 19–29. doi:10.1016/j.jelechem.2017.08.050.

[28] S. Ratso, I. Kruusenberg, A. Sarapuu, M. Kook, P. Rauwel, R. Saar, J. Aruväli, K. Tammeveski, Electrocatalysis of oxygen reduction on iron- and cobalt-containing nitrogen-doped carbon nanotubes in acid media, Electrochim. Acta. 218 (2016) 303–310. doi:10.1016/j.electacta.2016.09.119.

[29] L. Lin, Q. Zhu, A. Xu, Noble-Metal-Free Fe − N/C Catalyst for Highly E ffi cient Oxygen Reduction Reaction under Both Alkaline and Acidic Conditions, J. Am. Chem. Soc. 136 (2014) 11027–11033. doi:10.1021/ja504696r.

[30] S.H. Lim, Z. Li, C.K. Poh, L. Lai, J. Lin, Highly active non-precious metal catalyst based

on poly(vinylpyrrolidone)- wrapped carbon nanotubes complexed with iron-cobalt metal ions for oxygen reduction reaction, J. Power Sources. 214 (2012) 15–20. doi:10.1016/j.jpowsour.2012.03.094.

[31] H.-J. Zhang, H.-C. Kong, X. Yuan, Q.-Z. Jiang, J. Yang, Z.-F. Ma, Influence of metal precursors on the catalytic activity and structure of non-precious metal electrocatalysts for oxygen reduction reaction, Int. J. Hydrogen Energy. 37 (2012) 13219–13226. doi:https://doi.org/10.1016/j.ijhydene.2012.03.049.

[32] H. Xiao, Z.G. Shao, G. Zhang, Y. Gao, W. Lu, B. Yi, Fe-N-carbon black for the oxygen reduction reaction in sulfuric acid, Carbon N. Y. 57 (2013) 443–451. doi:10.1016/j.carbon.2013.02.017.

[33] H.S. Oh, H. Kim, The role of transition metals in non-precious nitrogen-modified carbon-based electrocatalysts for oxygen reduction reaction, J. Power Sources. 212 (2012) 220–225. doi:10.1016/j.jpowsour.2012.03.098.

[34] A. Dorjgotov, J. Ok, Y. Jeon, S.-H. Yoon, Y.G. Shul, Nitrogen-doped ordered porous carbon catalyst for oxygen reduction reaction in proton exchange membrane fuel cells, J. Solid State Electrochem. 17 (2013) 2567–2577. doi:10.1007/s10008-013-2135-y.

[35] C.H. Choi, S.H. Park, S.I. Woo, N-doped carbon prepared by pyrolysis of dicyandiamide with various MeCl2·xH2O (Me=Co, Fe, and Ni) composites: Effect of type and amount of metal seed on oxygen reduction reactions, Appl. Catal. B Environ. 119–120 (2012) 123–131. doi:10.1016/j.apcatb.2012.02.031.

[36] A.H.A. Monteverde Videla, L. Osmieri, M. Armandi, S. Specchia, Varying the morphology of Fe-N-C electrocatalysts by templating Iron Phthalocyanine precursor with different

porous SiO2 to promote the Oxygen Reduction Reaction, Electrochim. Acta. 177 (2015) 43–50. doi:10.1016/j.electacta.2015.01.165.

[37] S.H. Liu, J.R. Wu, Influence of nitrogen and iron precursors on the synthesis of FeN x/carbons electrocatalysts toward oxygen reduction reaction in acid solution, Electrochim. Acta. 135 (2014) 147–153. doi:10.1016/j.electacta.2014.04.167.

[38] H. Zhang, H. Kong, X. Yuan, Q. Jiang, J. Yang, Influence of metal precursors on the catalytic activity and structure of non-precious metal electrocatalysts for oxygen reduction reaction, Int. J. Hydrogen Energy. 37 (2012) 13219–13226. doi:10.1016/j.ijhydene.2012.03.049.

[39] F. Roncaroli, E.S. Dal Molin, F.A. Viva, M.M. Bruno, E.B. Halac, Cobalt and Iron Complexes with N-heterocyclic Ligands as Pyrolysis Precursors for Oxygen Reduction Catalysts, Electrochim. Acta. 174 (2015) 66–77. doi:https://doi.org/10.1016/j.electacta.2015.05.136.

[40] F.J. Pérez-Alonso, M.A. Salam, T. Herranz, J.L. Gómez De La Fuente, S.A. Al-Thabaiti, S.N. Basahel, M.A. Peña, J.L.G. Fierro, S. Rojas, Effect of carbon nanotube diameter for the synthesis of Fe/N/multiwall carbon nanotubes and repercussions for the oxygen reduction reaction, J. Power Sources. 240 (2013) 494–502. doi:10.1016/j.jpowsour.2013.04.086.

[41] R. Kothandaraman, V. Nallathambi, K. Artyushkova, S.C. Barton, Non-precious oxygen reduction catalysts prepared by high-pressure pyrolysis for low-temperature fuel cells, Appl. Catal. B Environ. 92 (2009) 209–216. doi:10.1016/j.apcatb.2009.07.005.

[42] X. Zhang, P. Lu, X. Cui, L. Chen, C. Zhang, M. Li, Y. Xu, J. Shi, Probing the electro-

catalytic ORR activity of cobalt-incorporated nitrogen-doped CNTs, J. Catal. 344 (2016) 455–464. doi:10.1016/J.JCAT.2016.10.019.

[43] Q. Zhao, Q. Ma, F. Pan, J. Guo, J. Zhang, Facile synthesis of N-doped carbon nanosheet-encased cobalt nanoparticles as efficient oxygen reduction catalysts in alkaline and acidic media, Ionics (Kiel). (n.d.). doi:10.1007/s11581-016-1748-4.

[44] L. Osmieri, A.H.A. Monteverde Videla, S. Specchia, Activity of Co-N multi walled carbon nanotubes electrocatalysts for oxygen reduction reaction in acid conditions, J. Power Sources. 278 (2015) 296–307. doi:10.1016/j.jpowsour.2014.12.080.

[45] H. Wu, C. Guo, J. Li, Z. Ma, Q. Feng, C. Chen, A graphene-based electrocatalyst co-doped with nitrogen and cobalt for oxygen reduction reaction, Int. J. Hydrogen Energy. 41 (2016) 20494–20501. doi:10.1016/j.ijhydene.2016.09.074.

[46] S. Ratso, I. Kruusenberg, A. Sarapuu, P. Rauwel, R. Saar, U. Joost, J. Aruväli, P. Kanninen, T. Kallio, K. Tammeveski, Enhanced oxygen reduction reaction activity of iron-containing nitrogen-doped carbon nanotubes for alkaline direct methanol fuel cell application, J. Power Sources. 332 (2016) 129–138. doi:10.1016/J.JPOWSOUR.2016.09.069.

[47] Z. Ma, C. Guo, Y. Yin, Y. Zhang, H. Wu, C. Chen, The use of cheap polyaniline and melamine co-modified carbon nanotubes as active and stable catalysts for oxygen reduction reaction in alkaline medium, Electrochim. Acta. 160 (2015) 357–362. doi:10.1016/j.electacta.2015.02.053.

[48] G. Zhang, W. Lu, F. Cao, Z. Xiao, X. Zheng, N-doped graphene coupled with Co nanoparticles as an efficient electrocatalyst for oxygen reduction in alkaline media, J. Power Sources. 302 (2016) 114–125. doi:10.1016/j.jpowsour.2015.10.055.

[49] S. Mutyala, J. Mathiyarasu, Noble metal-free FeN-CNFs as an efficient electrocatalyst for oxygen reduction reaction, Int. J. Hydrogen Energy. 43 (2018) 4746–4753. doi:10.1016/J.IJHYDENE.2017.06.133.

[50] H. Ghanbarlou, S. Rowshanzamir, M.J. Parnian, F. Mehri, Comparison of nitrogen-doped graphene and carbon nanotubes as supporting material for iron and cobalt nanoparticle electrocatalysts toward oxygen reduction reaction in alkaline media for fuel cell applications, Int. J. Hydrogen Energy. 41 (2016) 14665–14675. doi:10.1016/j.ijhydene.2016.06.005.

[51] A. Sarapuu, L. Samolberg, K. Kreek, M. Koel, L. Matisen, K. Tammeveski, Cobalt- and iron-containing nitrogen-doped carbon aerogels as non-precious metal catalysts for electrochemical reduction of oxygen, J. Electroanal. Chem. 746 (2015) 9–17. doi:10.1016/j.jelechem.2015.03.021.

[52] D. Sebastián, A. Serov, K. Artyushkova, P. Atanassov, A.S. Aricò, V. Baglio, Performance, methanol tolerance and stability of Fe-aminobenzimidazole derived catalyst for direct methanol fuel cells, J. Power Sources. 319 (2016) 235–246. doi:10.1016/j.jpowsour.2016.04.067.

[53] D. Sebastián, V. Baglio, A.S. Aricò, A. Serov, P. Atanassov, Performance analysis of a non-platinum group metal catalyst based on iron-aminoantipyrine for direct methanol fuel cells, Appl. Catal. B Environ. 182 (2016) 297–305. doi:10.1016/j.apcatb.2015.09.043.

[54] D. Sebastián, A. Serov, I. Matanovic, K. Artyushkova, P. Atanassov, A.S. Aricò, V. Baglio, Insights on the extraordinary tolerance to alcohols of Fe-N-C cathode catalysts in highly performing direct alcohol fuel cells, Nano Energy. 34 (2017) 195–204. doi:10.1016/J.NANOEN.2017.02.039.

[55] L. Osmieri, R. Escudero-Cid, M. Armandi, A.H.A. Monteverde Videla, J.L. García Fierro, P. Ocón, S. Specchia, Fe-N/C catalysts for oxygen reduction reaction supported on different carbonaceous materials. Performance in acidic and alkaline direct alcohol fuel cells, Appl. Catal. B Environ. 205 (2017) 637–653. doi:10.1016/j.apcatb.2017.01.003.

[56] E. Negro, A.H.A.M. Videla, V. Baglio, A.S. Aricò, S. Specchia, G.J.M. Koper, Fe–N supported on graphitic carbon nano-networks grown from cobalt as oxygen reduction catalysts for low-temperature fuel cells, Appl. Catal. B Environ. 166–167 (2015) 75–83. doi:10.1016/J.APCATB.2014.10.074.

[57] Y. Shi, S. Yin, Y. Ma, D. Lu, Y. Chen, Y. Tang, T. Lu, Oleylamine-functionalized palladium nanoparticles with enhanced electrocatalytic activity for the oxygen reduction reaction, J. Power Sources. 246 (2014) 356–360. doi:10.1016/j.jpowsour.2013.07.099.

[58] P. Nekooi, M. Akbari, M.K. Amini, CoSe nanoparticles prepared by the microwave-assisted polyol method as an alcohol and formic acid tolerant oxygen reduction catalyst, Renew. Energy. 35 (2010) 6392–6398. doi:10.1016/j.ijhydene.2010.03.134.

[59] S. Yang, D.Y. Chung, Y.J. Tak, J. Kim, H. Han, J.S. Yu, A. Soon, Y.E. Sung, H. Lee, Electronic structure modification of platinum on titanium nitride resulting in enhanced catalytic activity and durability for oxygen reduction and formic acid oxidation, Appl. Catal. B Environ. 174–175 (2015) 35–42. doi:10.1016/j.apcatb.2015.02.033.

[60] L. Timperman, A.S. Gago, N. Alonso-Vante, Oxygen reduction reaction increased tolerance and fuel cell performance of Pt and RuxSeyonto oxide-carbon composites, J. Power Sources. 196 (2011) 4290–4297. doi:10.1016/j.jpowsour.2010.11.083.

[61] A. Mikolajczuk-zychora, A. Borodzinski, P. Kedzierzawski, B. Mierzwa, Highly active

carbon supported Pd cathode catalysts for direct formic acid fuel cells, Appl. Surf. Sci. 388 (2016) 645–652. doi:10.1016/j.apsusc.2016.02.065.

[62] S.L. Blair, W.L. (Simon) Law, Electrocatalysis in Other Direct Liquid Fuel Cells, Electrocatal. Direct Methanol Fuel Cells. (2009). doi:doi:10.1002/9783527627707.ch14.

CHAPTER 2

Research Methodology

2.1 Introduction

Transition metal-nitrogen-doped carbon nanotubes catalysts namely; Fe−NCNT and Co−NCNT were synthesized by pyrolysis of metal salt, dicyandiamide and multi-walled carbon nanotube. The oxygen reduction reaction (ORR) activity on each catalyst was measured in acidic and alkaline medium. The catalyst prepared also physically characterized by X-ray diffraction (XRD) and X-ray photoelectron spectroscopy (XPS). Then, their performance in single cell was measured in direct formic acid fuel cell (DFAFC) operation. The overall research methodology involved in this study was summarized in the following flow chart shown in Figure 2-1.

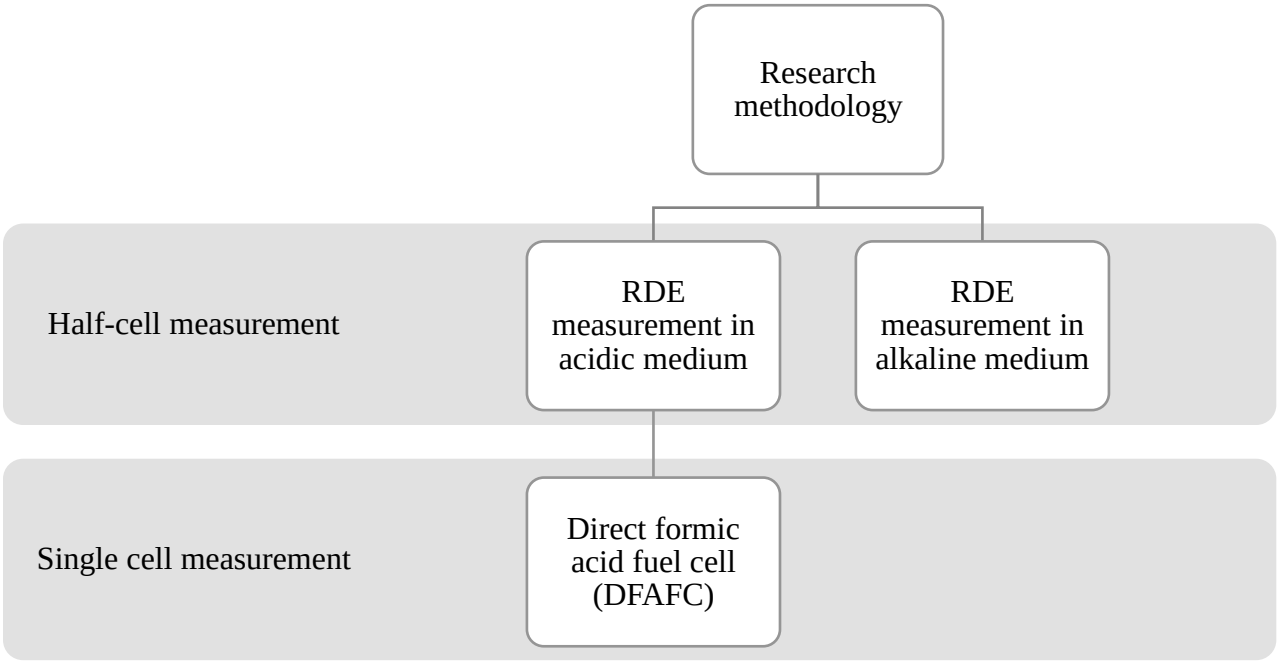

Figure 2-1 Flow chart of overall research methodology for this study

2.2 Materials

Multi-walled carbon nanotubes (MWCNTs) and dicyandiamide (DCDA) were purchased from Tokyo Chemical Industry Co. Ltd., which were used as carbon support and nitrogen precursor, respectively. The metal sources were obtained from anhydrous metal salt which are iron chloride ($FeCl_3$) and cobalt chloride ($CoCl_2$), supplied by Wako Pure Chemical Industries, Ltd. Polyvinylpyrrolidone (PVP), H_2SO_4 ($\geq$ 95 %) and HNO_3 ($\leq$ 70 %) were also purchased from Wako Pure Chemical Industries, Ltd.

2.3 Catalyst preparation

The procedure to synthesize TM−NCNT catalyst is following the procedure described in a previous work [1]. Anhydrous metal chloride ($FeCl_3$ or $CoCl_2$), dicyandiamide (DCDA) and multi-walled carbon nanotubes (MWCNTs) were used as metal, nitrogen and carbon precursor, respectively. Two types of TM−NCNT catalysts, including iron (Fe−NCNT) and cobalt (Co−NCNT) catalysts, were prepared. Before the catalyst synthesis, the MWCNTs was purified in a concentrated acid solution containing H_2SO_4 and HNO_3 with a 1:1 volume ratio under reflux condition for 2 hours at 55°C, followed by 3 hours at 80°C as shown in Figure 2-2. The MWCNTs were subsequently washed with DI water until a pH 7 was obtained; further, they were dried in vacuum oven for 15 hours. The purified MWCNTs were suspended in ethanol (10 mg ml^{-1}) by sonication for 30 minutes to obtain a homogeneous solution. The $FeCl_3$ or $CoCl_2$ was added to the solution with the content of Fe and Co constituted 2.5 % and 5 % of the MWCNT weight, respectively. DCDA with a weight ratio of 20:1 with respect to MWCNTs was added, and PVP was added as the dispersing agent with a weight ratio of 2:1 with respect to the metal salt. The solution was sonicated for 2 hours and was dried in vacuum oven at 70 °C. Then, the obtained dried powder was pyrolyzed in N_2-flowing tube furnace for 2 hours at 800 °C. The temperature

increasing rate is 10°C min^{-1}. Finally, the catalyst powder was cooled and collected. The obtained catalysts were denoted as Fe−NCNT and Co−NCNT. The catalyst preparation process is illustrated in Figure 2-3.

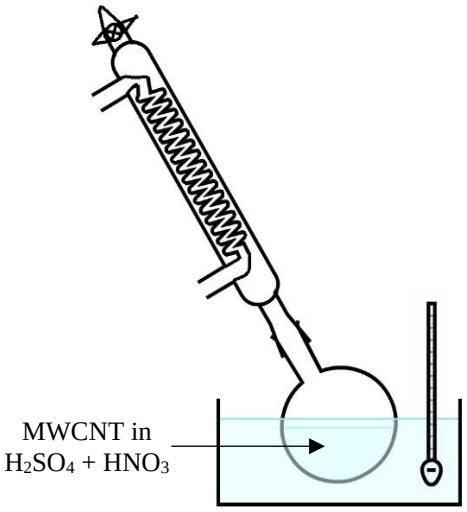

Figure 2-2 Purification of MWCNT in concentrated acid mixture

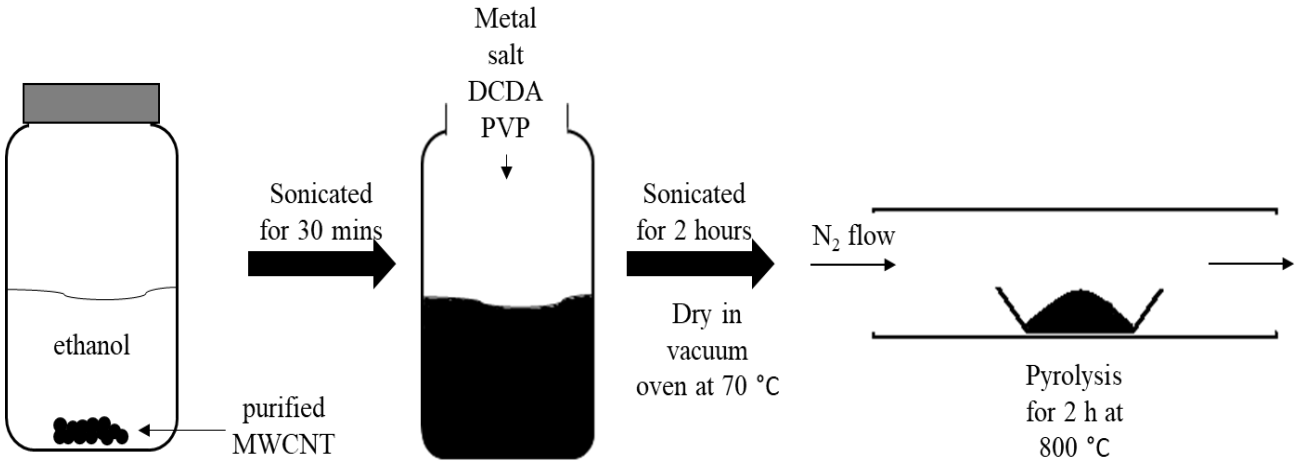

Figure 2-3 Catalyst preparation process

2.4 Catalyst characterization

2.4.1 Physical characterization

The analysis of X-ray diffraction (XRD) was conducted by MiniFlex, Rigaku diffractometer with a Cu Kα radiation operated at 2.7 kV and 30 mA. X-ray photoelectron spectroscopy (XPS) was utilized to analyze the surface composition and to determine the nitrogen configuration in the synthesized catalyst. The XPS spectra were acquired by a JPS-9010 Photoelectron Spectrometer (JEOL Ltd.) using the Mg Kα source at 500 W. Wide scans were recorded in an energy of 0 to 1000 eV with a pass energy and step size of 50 and 1.0 eV, respectively. Then, a narrow scan was repeated thrice for the selected element peaks to reduce the noise with a pass energy and step size of 10 and 0.1 eV, respectively. Further, atomic percentage quantification and curve fitting were obtained using a Shirley-type background and Gauss-Lorentz equation. The binding energy scale was adjusted by referring to the C 1s peak (284.6 eV), and the analysis of data was performed using the SpecSurf (ver. 1.9.3, JEOL) analysis software

2.4.2 Electrochemical characterization

The catalyst ink was prepared by ultrasonically mixing 1 mg catalyst powder with 1 ml ethanol and 10 µL of a 5% Nafion ionomer for 1 hour. The catalyst ink was repeatedly dropped on the glassy carbon (GC) electrode with a geometric area of 0.196 cm^2, yielding 200 µg cm^{-2} of catalyst loading as shown in Figure 2-4 (a). Further, the catalyst-ink-coated electrode was dried at ambient condition. The electrochemical measurement of the synthesized electrocatalysts was conducted in a conventional three-electrodes electrochemical cell configuration. The cell comprised the catalyst-ink-coated GC disk as working electrode, Pt wire as the counter electrode and reversible hydrogen electrode (RHE) as the reference electrode. Before conducting the measurement, the electrolyte solution (0.5 M H_2SO_4 or 0.1 M KOH) was bubbled with N_2 gas for

30 minutes. Then, cyclic voltammetry (CV) was performed in a potential range from 0 V to 1.2 V (vs. RHE) at scan rate of 10 mVs^{-1} and stable curve was recorded after 20 cycles of continuous scanning. The oxygen reduction reaction (ORR) polarization curve was recorded by using rotating disk electrode (RDE) technique in O_2-saturated 0.5 M H_2SO_4 and 0.1 M KOH solution for acidic and alkaline medium, respectively, with various rotations rate from 360 rpm to 4600 rpm using RRDE-3A Rotating Ring Disk Electrode Apparatus (ALS Co., Ltd) with measurement error of less than 1.0% as shown in Figure 2-4 (b). The catalyst tolerance toward formic acid (acidic medium) and formate salt (alkaline medium) and stability test were also conducted. All electrochemical measurements were carried out at room temperature and ambient pressure. These RDE measurements were also conducted for commercial Pt/C (TEC10E50E, Tanaka Holdings Co., Ltd.) with the Pt loading of 60 ug cm^{-2} on the GC electrode for comparison.

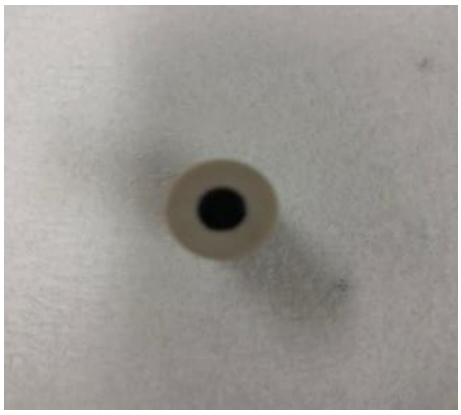

(a) GC electrode

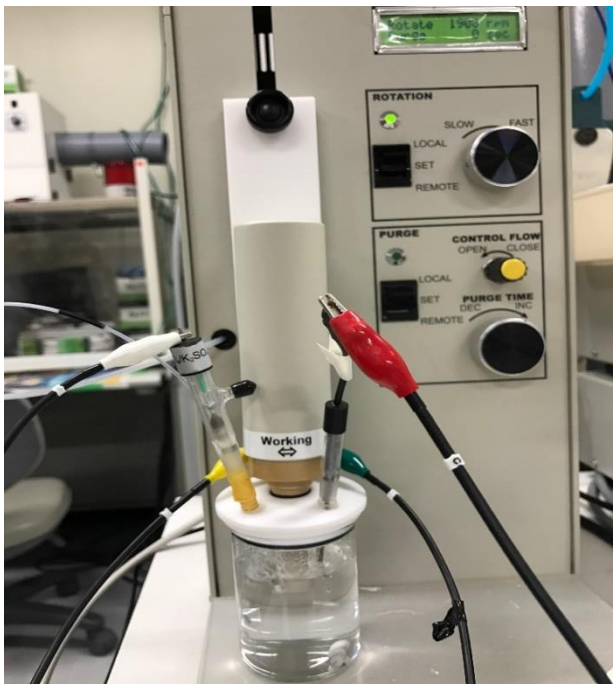

(b) Rotating disk electrode (RDE) measurement setup

Figure 2-4 Electrochemical measurement by using RDE technique

2.5 Single-cell performance measurement

2.5.1 Membrane electrode assemblies (MEA) fabrication

Membrane electrode assemblies (MEA) were prepared using commercial Pd/C (Ishifuku Metal Industry Co., Ltd.) as the anode catalyst and Fe−NCNT or Co−NCNT as the cathode catalyst for single-cell testing. Catalyst ink for the cathode was prepared by mixing the catalyst powder with 5 wt % Nafion solution, 2-propanol and water. A homogeneous ink solution was obtained after 30 minutes of sonication. The catalyst layers were prepared by using ultrasonic spraying technique as reported by A. Zainoodin et al. as shown in Figure 2-5 [2]. The catalyst ink for the cathode was sprayed on a carbon paper (Toray TGP-H-060) with loading of 4.6 mg cm^{-2} and 3.3 mg cm^{-2} for Fe−NCNT and Co−NCNT, respectively. For the anode catalyst ink, the commercial Pd/C was dispersed in a solution containing 5 wt% Nafion solution, 2-propanol, and water. The

Pd/C ink was further coated on a carbon cloth (CC plain, Etek) with a Pd loading of 2.0 mg cm^{-2}. For comparison, MEA with a commercial Pt/C (TEC10E50E, Tanaka Holdings Co., Ltd.) cathode electrode with 2 mg cm^{-2} of Pt loading was also fabricated. The ionomer content was 50 wt % of the catalyst loading for both anode and cathode sides. MEA was fabricated by sandwiching NR212 membrane between the anode and the cathode using hot press at 140 °C and 5MPa for 3 minutes as shown Figure 2-6. A silicone gasket (thickness: 200 μm) was used for the anode side, whereas gaskets having thicknesses of 150 to 350 μm were used for the cathode side depending on the thickness of the electrode. The active area of the electrode is 4.84 cm^2.

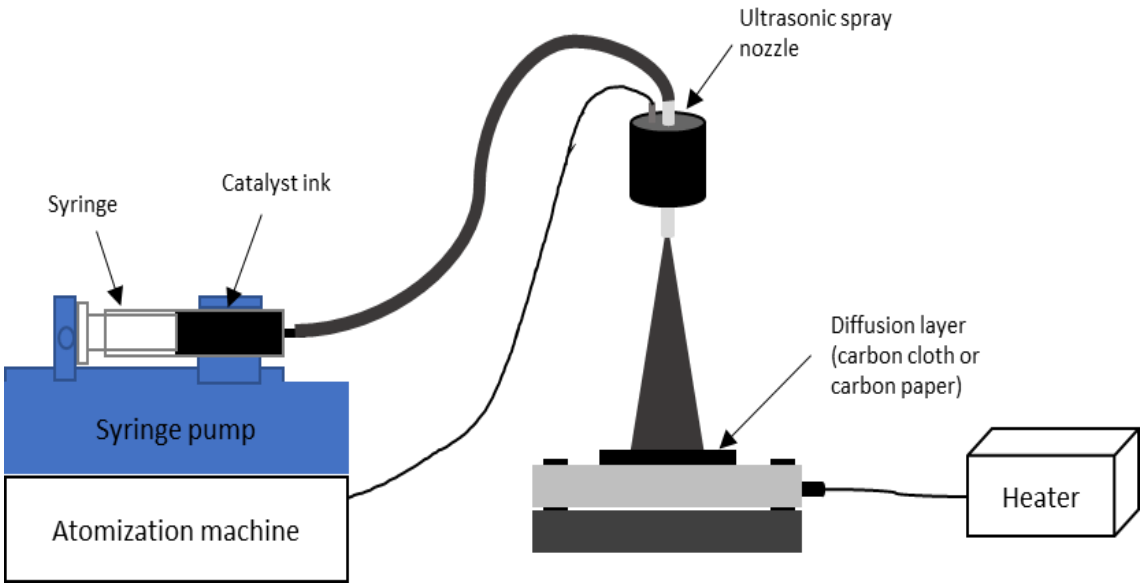

Figure 2-5 Schematic diagram of electrode preparation by ultrasonic spraying method

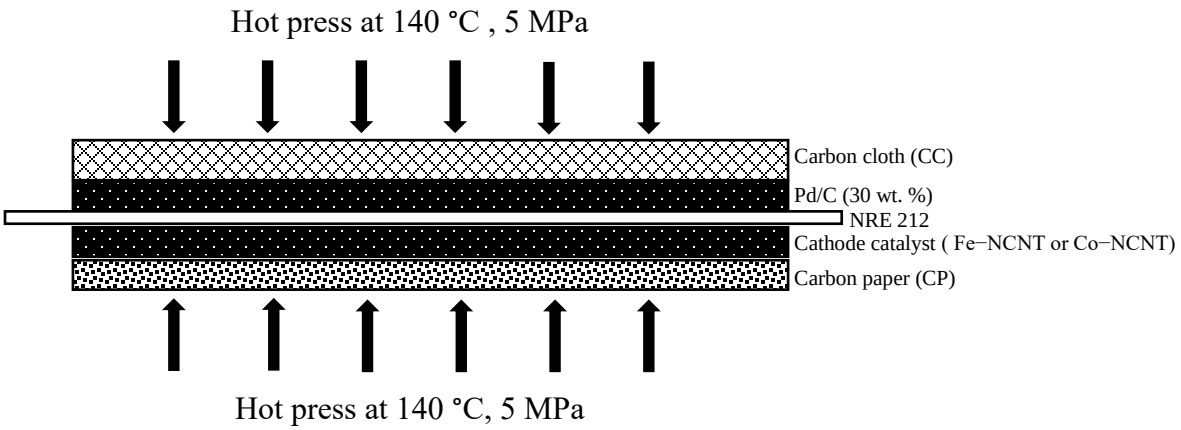

Figure 2-6 Membrane electrode assembly fabrication

2.5.2 Single cell test

The MEA was mounted on a single cell (FC-05-02-H2R, ElectroChem, Inc.) comprising current collectors, graphite block containing flow field channels and silicone sheets, which acted as gasket. Before conducting the performance test, the single cell was pretreated by feeding humidified hydrogen and dry oxygen to the anode and cathode side, respectively. The current-time (i-t) test was conducted for 1hour, and the i-V test was done at a cell temperature of 60 °C. The i–t and i–V were repeatedly measured for several times as a pretreatment to achieve table performance. The i-V measurement was performed at a scan rate of 5 mV s^{-1}. The single-cell performance was measured by a potentiostat (HZ-7000, Hokuto Denko Corp.) with the potential measurement accuracy of ± 0.05 % of reading ±1 mV and a current measurement accuracy of ±0.2 % of full-scale range. For the DFAFC operation, the MEAs were operated at the operating temperature of 60°C, 5 M formic acid concentration, and 500 ml min^{-1} dry oxygen flow rate as a pre-treatment for the formic acid operation. The dry oxygen was used to avoid flooding problem which will affect the oxygen availability for ORR (especially for DFAFC operation). A regeneration process was conducted because of catalyst poisoning, degrading the anode

performance. During the performance tests in the DFAFC operation, fresh water was fed to the anode side to wash the anode surface after each power generation because the catalyst was poisoned by the formic acid solution. The washing process was stopped once the cell voltage decreased to 0.1 V. Note that the anode performance can be recovered to its original level, as reported in previous studied [3,4].

2.6 References

[1] S. Ratso, I. Kruusenberg, A. Sarapuu, M. Kook, P. Rauwel, R. Saar, J. Aruväli, K. Tammeveski, Electrocatalysis of oxygen reduction on iron- and cobalt-containing nitrogen-doped carbon nanotubes in acid media, Electrochim. Acta. 218 (2016) 303–310. doi:10.1016/j.electacta.2016.09.119.

[2] A.M. Zainoodin, T. Tsujiguchi, M.S. Masdar, S.K. Kamarudin, Y. Osaka, A. Kodama, Performance of a direct formic acid fuel cell fabricated by ultrasonic spraying, Int. J. Hydrogen Energy. 43 (2018) 6413–6420. doi:10.1016/J.IJHYDENE.2018.02.024.

[3] Y. Zhou, J. Liu, J. Ye, Z. Zou, J. Ye, J. Gu, T. Yu, A. Yang, Poisoning and regeneration of Pd catalyst in direct formic acid fuel cell, Electrochim. Acta. 55 (2010) 5024–5027. doi:10.1016/J.ELECTACTA.2010.04.014.

[4] T. Tsujiguchi, F. Matsuoka, Y. Hokari, Y. Osaka, A. Kodama, Overpotential analysis of the Direct Formic Acid Fuel Cell, Electrochim. Acta. 197 (2016) 32–38. doi:10.1016/j.electacta.2016.03.062.

CHAPTER 3

Study on transition metal-containing nitrogen-doped carbon nanotubes for the cathode of the acidic and alkaline direct formic acid fuel cell

3.1 Introduction

Recently, research on direct formic acid fuel cells (DFAFCs) which is one of the direct liquid fuel cell (DLFC) type gained much interest as they offer higher power density and lower fuel crossover flux than DMFC [1]. However, the large-scale commercialization of the fuel cells is limited by their high cost especially the cost of the platinum (Pt) catalyst used for oxygen reduction reaction (ORR) at the cathode. Moreover, Pt catalyst also suffer stability problems during long-term operation and low tolerance to the presence of organic fuels such as methanol, ethanol and formic acid [2,3]. High fuel tolerance is important for ORR electrocatalyst in DLFC due to fuel crossover problem which defined as transport of fuel from anode to cathode through the membrane. This phenomenon will cause mixed potential at the cathode and thus, lower the electrical efficiency and power density of DLFCs [4]. Development of binary and ternary platinum based catalyst were introduced in DMFC to reduce amount of Pt used [2,5]. However, over the long term, usage of non-precious metal catalyst (NPMC) would be better solution to this problem due to low abundance of Pt. Therefore, it is essential to develop alternative, cost-effective catalyst to eliminate the usage of Pt-based catalyst in fuel cell application. To date, transition metal−nitrogen-doped carbon (TM−N−C) catalyst with Fe and Co as the transition metal have been widely reported for DMFC cathode application due to their high methanol tolerance and better stability than the commercial Pt/C catalyst in acidic and alkaline medium [6–17].

For DFAFC operation, even though the formic acid crossover is lower than the methanol, it is still significant in limiting the performance of DFAFCs [18]. Only few studies were reported on the formic acid tolerance of NPMCs such as $Ru_xSe_y/TiO_2/C$ and CoSe/C that exhibits better formic acid tolerance than the conventional Pt/C catalyst [19,20]. As the ORR at the cathode side is similar for both DMFC and DFAFC operation, it is expected that any improvement to the cathode catalyst for DMFC or other DLFC types will be applicable to the DFAFC. Other challenge that hindered the commercialization of DFAFC, is the handling and transportation of formic acid due to its corrosive property. Formic acid also has specific toxic effects if expose to humans that could damage optical nerve and kidney. This challenge can be overcome by using formate salt in an alkaline operation. Formate salts are easy to handle either in solid or in solutions, have low toxicity and potentially low in cost [21,22]. Thus, recently, alkaline fuel cell with formate as a fuel has received increasing attention due to these characteristics [23]. However, there is no study reported for tolerance of formic acid and formate salt on the TM−N−C catalyst; especially Fe- and Co-based catalyst for ORR in acidic and alkaline medium.

In this chapter, TM−N−C catalysts were prepared and their ORR activity and tolerance toward formic acid (HCOOH) and sodium formate (HCOONa) in acidic and alkaline medium were measured. TM−N−C catalysts were synthesized by pyrolysis of metal salt, which is anhydrous $FeCl_3$ and $CoCl_2$, dicyandiamide (DCDA) and multiwalled carbon nanotubes (MWCNTs) are used as nitrogen precursor and carbon support, respectively. Effect of once pyrolysis step and twice pyrolysis step with and without acid treatment of the catalyst samples on the ORR activity was studied. Pyrolysis step was done twice because catalytic activity can be improved due to increases of microporosity of the catalyst and to remove the HSO_4^- adsorbed during acid treatment step [13,24]. The ORR activity of each catalyst in acidic and alkaline medium were determined in this

study. Since the catalysts synthesized in this study will be applied as cathode catalyst for direct formic acid fuel cell (DFAFC) and direct formate fuel cell (DFFC), the tolerance toward formic acid and sodium formate also tested as it has not been investigated in other studies. These measurements were also done for commercial Pt/C (50 wt %) catalyst for comparison.

3.2 Experimental method

Fe−NCNT and Co−NCNT catalysts were prepared by following the procedure described in literature [13] which was explained in detail in Chapter 2. Three catalyst samples were prepared for each type of catalyst for this study. Catalyst obtained from once pyrolysis step is denoted as Fe−NCNT1 and Co−NCNT1. Second samples, Fe−NCNT2 and Co−NCNT2 are from catalyst that subjected to twice identical pyrolysis steps. Third catalyst samples also prepared which the catalyst from first pyrolysis was acid treated in mixture of 0.5 M H_2SO_4 and 0.5 M HNO_3 at 50 °C for 8 h and next subjected to second pyrolysis designated as Fe−NCNT2A and Co−NCNT2A. All catalyst samples were physical characterized by XRD and XPS. Their tolerance toward formic acid in acidic medium and formate salt in alkaline medium were measured. For acidic medium, formic acid (HCOOH) tolerance was studied in O_2-saturated 0.5 M H_2SO_4 solution containing 1 M and 3 M formic acid while for alkaline medium, sodium formate (HCOONa) tolerance was studied in O_2-saturated 0.1 M KOH containing 1 M HCOONa solution. For stability testing, chronoamperometry measurements were performed at a constant voltage, 0.20 V (vs. RHE) in acidic medium and 0.70 V (vs. RHE) in alkaline medium for 6 hours. The ORR activity in the presence of fuel and stability test were performed at rotation rate of 1900 rpm. These RDE measurements also carried out for commercial Pt/C (50 wt. %) for comparison.

3.3 Result and discussion

3.3.1 X-ray diffraction analysis

Figure 3-1 shows X-ray diffractogram peaks for Fe−NCNT and Co−NCNT catalyst. From the pattern, a sharp diffraction peak at 26 ° and a broad diffraction peak at 43 ° were observed in all catalyst samples which can be attributed to the (002) and (101) plane reflection feature of graphitic carbon. For Fe−NCNT, there is a sharp peak at 35.6° which indicates the existence of crystalline Fe_2O_3 phase for all catalyst samples even after the catalyst was subjected to acid treatment before second pyrolysis step was done. For Co−NCNT catalyst, cobalt oxide peak at 36.8 ° was observed for Co−NCNT1 and Co−NCNT2. In contrast with Co−NCNT2A, there is no CoO peak detected which was removed during the acid treatment by H_2SO_4 and HNO_3. The crystallite size for the oxide phase is from 10 nm to 30 nm. However, the existence of metal oxide may not contribute to the ORR activity enhancement of the catalyst significantly [25]. Therefore, XPS measurement was performed to determine the elemental compositions of each catalyst sample and the existence of nitrogen species, which may function as the ORR active sites.

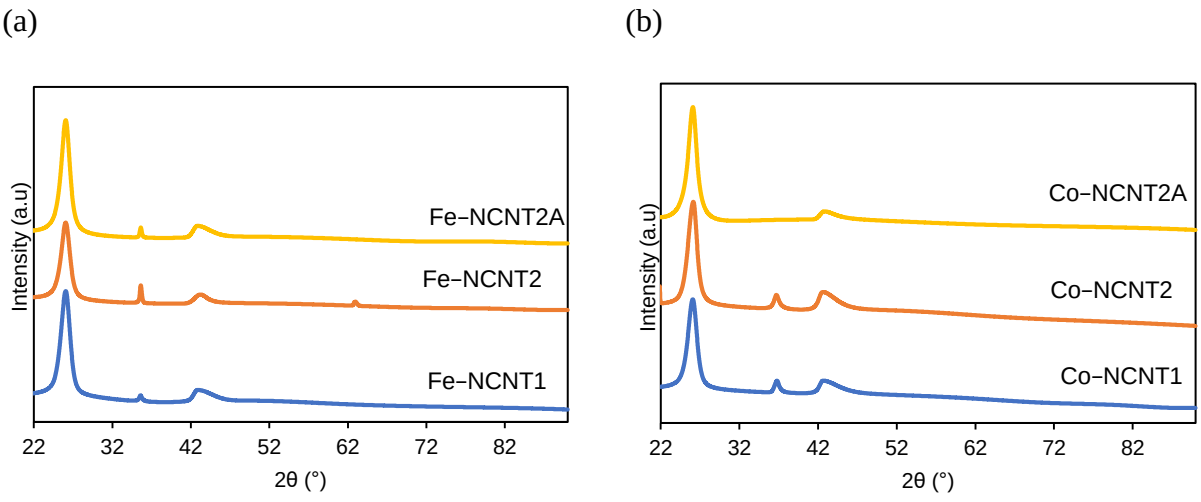

Figure 3-1 XRD pattern for (a) Fe−NCNT and (b) Co−NCNT catalyst

3.3.2 X-ray photoelectron spectroscopy analysis

XPS measurements were carried out to determine the elemental compositions of each catalyst sample and the existence of different binding configurations of nitrogen species, which may function as the ORR active site. Figure 3-2 (a) and (b) show the XPS wide scan spectra for Fe−NCNT and Co−NCNT catalyst, respectively. A C1s peak, O1s peak, N1s peak and metal (Fe2p and Co2p) peak are observed which confirming the incorporation of N and metal in the MWCNT carbon structure for all catalyst samples. The atomic percentage for each element of the catalysts is summarized in Table 3-1. It was found that the metal content for both types of catalyst decreasing after the catalyst was acid treated and subsequently subjected to second pyrolysis. Fe content was slightly decrease from 2.34 at. % to 2.22 at. % whereas Co decrease from 3.18 at. % to 1.17 at. % which indicate that large amount of Co was removed during the acid treatment process. Even though the metal content was removed during the acid treatment process, higher amount of Fe content than Co was observed because there is still Fe may survive from the acid treatment and pyrolysis process due to the metallic nanoparticles are encapsulated into carbon layers [13]. The existence of some metal residues after acid treatment also found in the study done by C.Choi 2012 where carbon layers that deposited on the metal surface prevent from metal dissolution during the acid treatment. This carbon layer was formed by carbonization of carbon atoms in DCDA through pyrolysis of the mixture of transition metal chloride and DCDA [26]. This is in accordance with the peak observed in XRD pattern in Figure 3-1 for Fe−NCNT2A which is Fe_2O_3 also indicates the high Fe content in the Fe−NCNT2A catalyst detected from XPS spectra, but no oxide peak detected in Co−NCNT2A catalyst. Along with the metal, nitrogen content also reduced for Fe−NCNT2A and Co−NCNT2A catalyst. However, the amount of oxygen element increases for Fe−NCNT2A and Co−NCNT2A might be due to the defects of CNT resulting from the acid

treatment [27]. The high oxygen content for Fe−NCNT2A also attributed to the Fe_2O_3 that survived from the acid treatment and the pyridinic-N oxide species which detected in Fe−NCNT2A as referred to the N1s spectra in Figure 3-3. Whereas there is no pyridinic-N oxide detected for Co−NCNT2A catalyst sample.

Catalyst that synthesized via second pyrolysis without acid treatment shows increment of metal content to 3.76 at. % for Fe while Co was slightly reduced to 3.11 at. %. In contrast with nitrogen content which decreases for Fe−NCNT2 but increases for Co−NCNT2. The amount of Fe metal increases after the second pyrolysis could be due to the carbon gasification because metal atoms do not form volatile compound during the pyrolysis. This change in metal content after heat treatment also observed in study done by F. Jaouen and J-P Dodelet [28]. The slightly decrease of Co content after second pyrolysis is due to incorporation of some Co into the bulk of the carbon network, thus decreasing the Co contribution to the XPS signal [29,30].

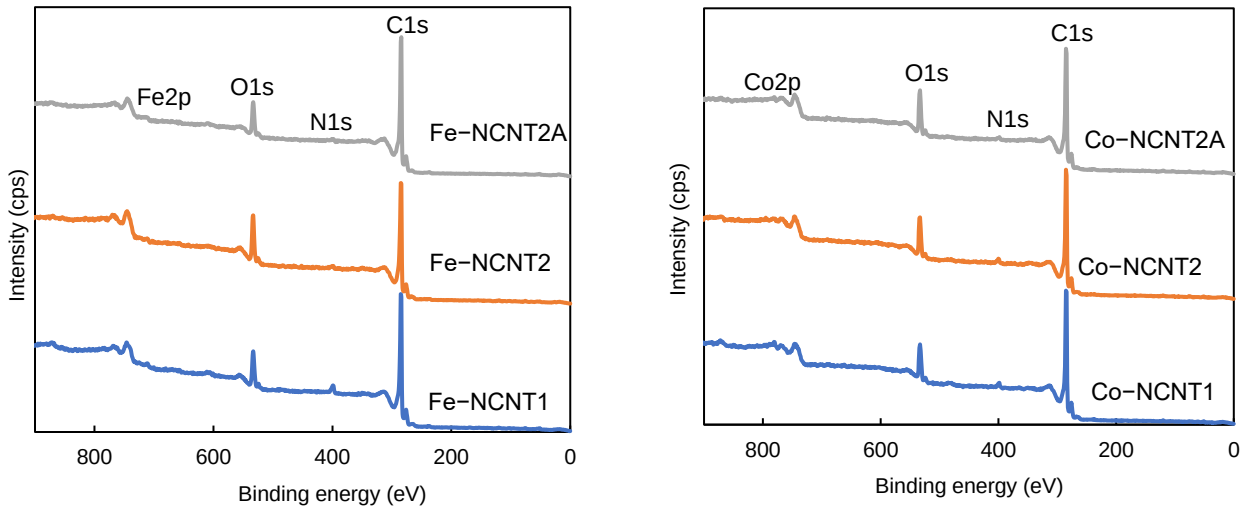

(a) Fe−NCNT (b) Co−NCNT

Figure 3-2 XPS spectra for (a) Fe−NCNT and (b) Co−NCNT catalyst

Table 3-1 Elemental surface composition of Fe−NCNT and Co−NCNT

Element	C	N	O	Fe or Co
Catalyst sample	Composition (at. %)			
Fe−NCNT1	90.09	3.33	4.24	2.34
Fe−NCNT2	85.16	1.76	9.32	3.76
Fe−NCNT2A	82.55	1.29	13.93	2.22
Co−NCNT1	88.05	2.76	6.01	3.18
Co−NCNT2	88.40	3.38	5.11	3.11
Co−NCNT2A	88.90	1.54	8.39	1.17

Nitrogen can exist in various form in the carbon structure which has distinct binding energy. In general, nitrogen is doped into the graphite structure can exist in the form of pyridinic-N, pyrrolic-N, graphitic-N and pyridinic-N oxide [26]. According to previous studies on non-precious metal nitrogen doped carbon electrocatalyst, the electrocatalytic activity for oxygen reduction reaction (ORR) can be attributed to pyridinic-N, pyrrolic-N and graphitic-N which regarded as ORR active site [31–33] . The XPS narrow scans of the N 1s spectra with the curve deconvolution for Fe−NCNT and Co−NCNT catalyst are presented in Figure 3-3 and the relative concentration derived from the N1s peak is summarized in Table 3-2. As shown in Figure 3-3, all catalysts show two major peaks at ~398 eV and ~400 eV which corresponding to pyridinic-N and pyrrolic-N. Additional peaks were also observed like graphitic-N and pyridinic-N oxide for samples that subjected to second pyrolysis either with or without acid treatment. For Fe−NCNT catalyst, pyridinic-N and pyrrolic-N species were observed for all catalyst samples but graphitic-N species was existed in Fe−NCNT2 and Fe−NCNT2A catalyst samples. Graphitic-N species observed after the second pyrolysis either with or without acid treatment was probably due to the rearrangement of the MWCNT support structure during the second pyrolysis [24]. The pyridinic-N species might also converted to graphitic-N species during the second pyrolysis [34]. Besides that, there is

another peak referred to pyridinic-N oxide species in Fe−NCNT2A. This nitrogen species observed in Fe−NCNT2A is in accordance with the Fe−NCNT synthesized in S. Ratso et al. after the acid treatment combined with second pyrolysis step [13]. In Co−NCNT catalyst, pyridinic-N and pyrrolic-N were also exhibit in all samples. Both Co−NCNT2 and Co−NCNT2A exhibits graphitic-N species but no pyridinic-N oxide detected in Co−NCNT2A.

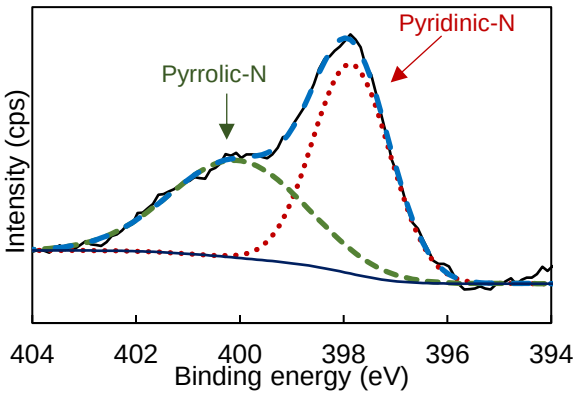

(a) Fe−NCNT1

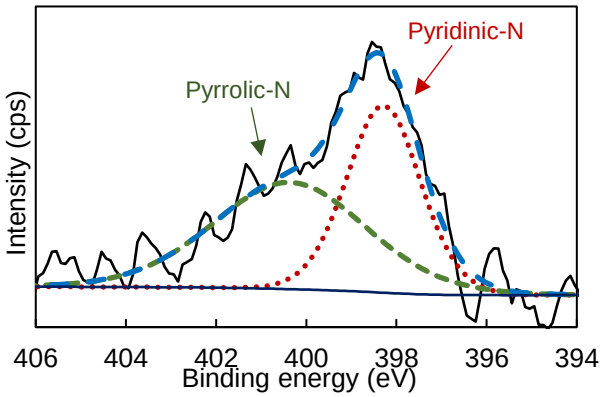

(b) Co−NCNT1

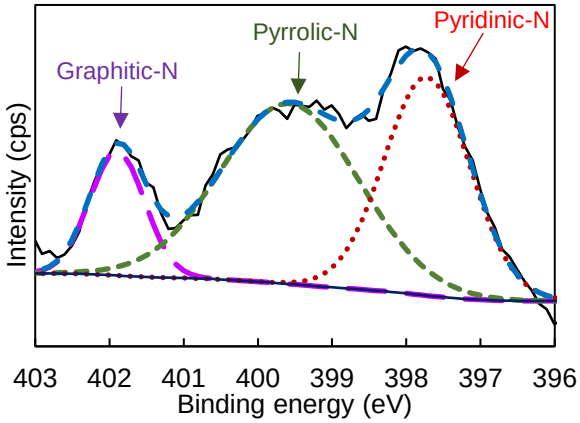

(c) Fe−NCNT2

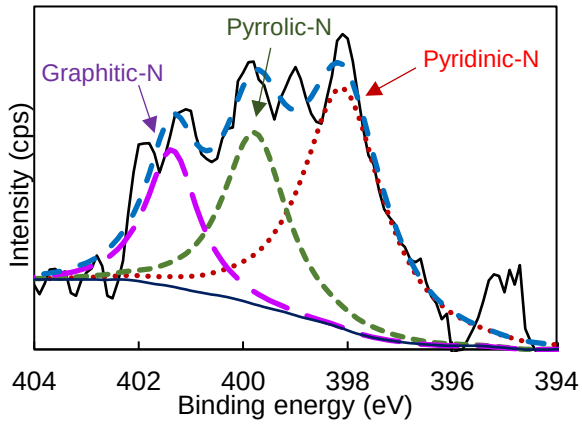

(d) Co−NCNT2

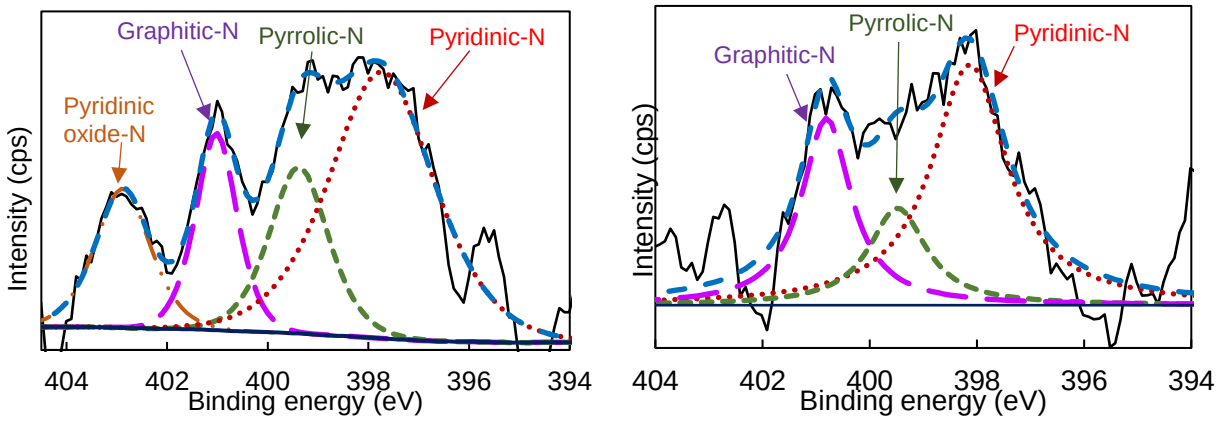

(e) Fe−NCNT2A (f) Co−NCNT2A

Figure 3-3 XPS N1s spectra for Fe−N−CNT (a,c,e) and Co−N−CNT (b,d,f) catalyst

Table 3-2 Relative concentration of nitrogen species in all catalyst samples

Nitrogen species	Pyridinic-N	Pyrrolic-N	Graphitic-N	Pyridinic oxide-N
Catalyst	**Relative concentration (%)**			
Fe−NCNT1	55.15 (397.9 eV)	44.85 (400 eV)	-	-
Fe−NCNT2	37.16 (397.7 eV)	49.30 (399.6 eV)	13.54 (401.9 eV)	-
Fe−NCNT2A	52.30 (397.7 eV)	18.38 (399.4 eV)	15.31 (401.0 eV)	14.01 (402.9 eV)
Co−NCNT1	45.88 (398.3 eV)	54.12 (400.4 eV)	-	-
Co−NCNT2	51.91 (398.1 eV)	29.21 (399.8 eV)	18.88 (401.36 eV)	-
Co−NCNT2A	45.87 (398.1 eV)	18.53 (399.5 eV)	35.60 (400.8 eV)	

3.3.3 Catalytic activity in acidic and alkaline medium

The reduction curve for ORR activity on TM−NCNT catalyst synthesized in this study and commercial Pt/C catalyst in acidic medium and alkaline medium are presented in Figure 3-4 (a) and (b), respectively. These reduction curves are obtained by subtracting the capacitance current recorded in the N_2-saturated electrolyte from the reduction current in the O_2-saturated electrolyte.

The onset potential is determined when the reduction current is initially observed (-0.1 mA cm^{-2}) that is greater than the background capacitance current [29]. In acidic medium, it was observed that the onset potential for Fe−NCNT1 catalyst is approximately 0.63 V. This value is shifted negative to 0.49 V and 0.51 V for Fe−NCNT2 and Fe−NCNT2A, respectively. This result indicates that Fe−NCNT1 give higher ORR activity than Fe−NCNT2 and Fe−NCNT2A. The onset potential decreases as the catalyst was subjected to second pyrolysis combined with acid treatment might be caused by some of the active Fe species are also removed. The higher activity of Fe−NCNT1 is due to the highest amount of pyridinic-N (55.15 %) species available in the Fe−NCNT1 than Fe−NCNT2 and Fe−NCNT2A. For Co-containing catalyst, the highest onset potential obtained by Co−NCNT1 which is 0.62 V. This value shifted negative to 0.57 V and 0.54 V for Co−NCNT2A and Co−NCNT2, respectively. From the XPS result, higher pyrrolic-N species content (54.12 %) in the Co−NCNT1 than other Co−NCNT2 and Co−NCNT2A might contributes to its high ORR activity.

It was suggested in literature that for N-doped carbon based electrocatalyst, the electrocatalytic ORR activity can be attributed to pyridinic-N and/or pyrrolic-N as the active site, whereas other authors suggested that graphitic-N is more important for the ORR activity [31]. Some other studies proposed that both pyridinic-N and graphitic-N, and pyrrolic-N are important for the ORR activity [35]. Based on this result, high content of pyridinic-N and pyrrolic-N are contributing for electrocatalytic ORR activity which is supported by previous studies reported for acidic medium [12,36]. As compared with commercial Pt/C catalyst, the onset potential of Fe−NCNT and Co−NCNT catalyst synthesized in this study is 0.2 V lower than that achieved by commercial Pt/C which is 0.8 V.

In alkaline medium, comparing between the two types of metal used, the onset potential of the ORR is more positive for Co−NCNT catalyst than Fe−NCNT catalyst thus, indicates that Co−NCNT catalyst has better ORR activity than Fe−NCNT. It was found that the different pyrolysis steps did not affect the onset potential for Co−NCNT catalyst in alkaline medium as the onset potentials are similar for all Co−NCNT catalyst samples which is 0.89 V. For Fe-containing catalyst, onset potential for Fe−NCNT1 is 0.85 V which is then shifted positive to 0.87 V for both Fe−NCNT2 and Fe−NCNT2A catalyst samples. This indicates that after second pyrolysis the ORR activity increases for Fe-containing catalyst. It was observed that the onset potential value for the TM−NCNT catalysts in this study is 100 mV less than that commercial Pt/C catalyst alkaline medium. The smaller difference of onset potential in alkaline medium as compared with the acidic medium indicates that the ORR activity for the Fe−NCNT and Co−NCNT catalysts are more comparable with the commercial Pt/C in alkaline medium than in the acidic medium. This condition also showed in previous studies reported on the non-precious metal N-doped carbon based catalyst that the ORR activity was comparable or even higher than the commercial Pt/C catalyst in alkaline medium [37–39].

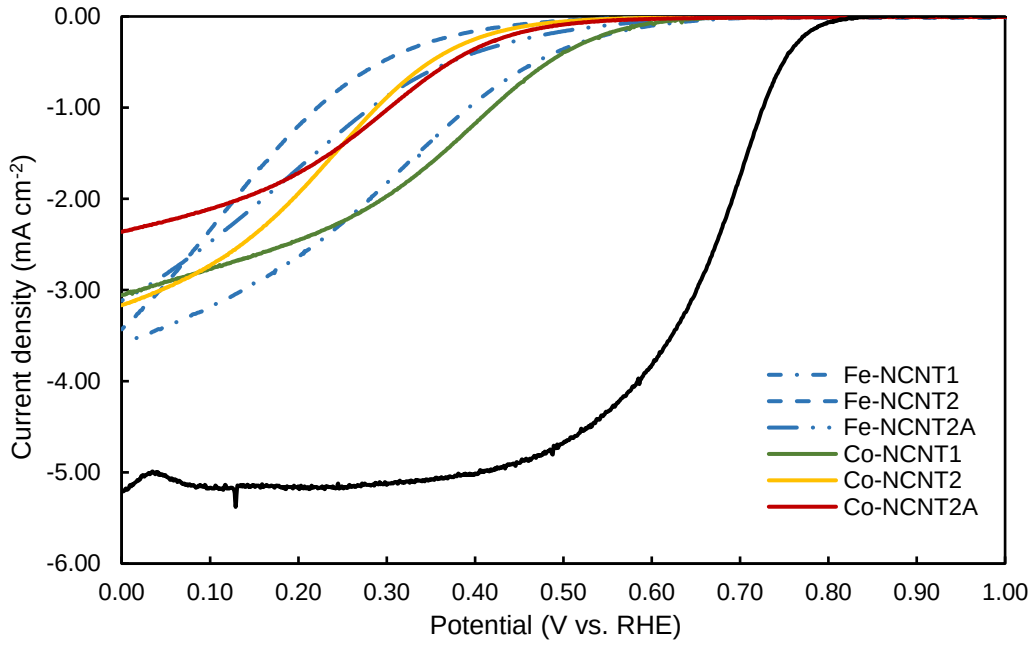

(a) Acidic medium

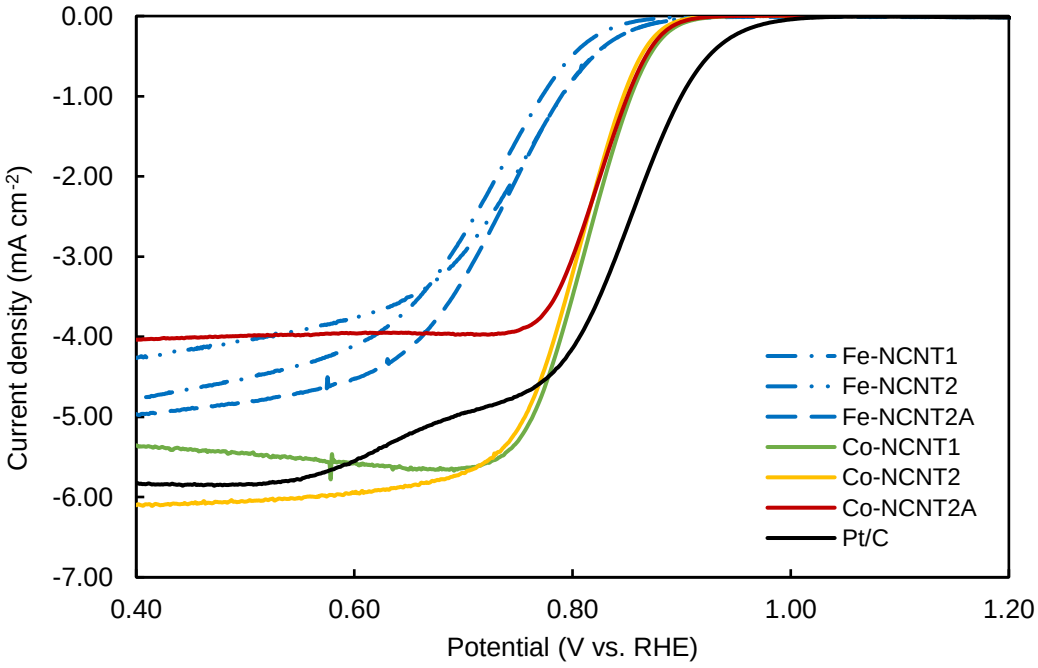

(b) Alkaline medium

Figure 3-4 RDE polarization curve of ORR on Fe−NCNT, Co−NCNT and commercial Pt/C catalyst in (a) 0.5 M H_2SO_4 and (b) 0.1 M KOH at rotations rate of 1900 rpm and potential scan rate of 10 mVs^{-1}

The ORR activity on the TM−NCNT in acidic and alkaline medium were further characterized by rotating disk electrode (RDE) method at different rotations rates to determine the number of electrons transfer for each catalyst sample. Generally, ORR can take place via two reaction pathways. One is 2-electron transfer pathway which produces H_2O_2, and the other is 4-electron transfer pathway which produces water. A reliable catalyst for ORR should follow the 4-electron transfer pathway. According to the Koutecky-Levich (K-L) theory, number of electrons transfer can be calculated by RDE data recorded at different rotations rate using the following K-L equation:

$$\frac{1}{I} = \frac{1}{I_k} + \frac{1}{I_d} = \frac{1}{I_k} + \frac{1}{0.62\, n\, FAD_{O_2}^{2/3} v^{-1/6} C_{O_2}^{b} \omega^{1/2}} \qquad (1)$$

Where I, I_k and I_d are the experimental, kinetic and diffusion-limited currents, respectively, n is the number of electron transferred per O_2 molecule, F is the Faraday constant (96485 C mol^{-1}), A is the geometric area of the electrode (0.196 cm^2), ω is the electrode rotation rate (rad s^{-1}), $C_{O_2}^{b}$ is the concentration of O_2 in 0.5 M H_2SO_4 (1.13×10^{-6} mol cm^{-3}), D_{O_2} is the diffusion coefficient of O_2 ($1.8 \times 10^{-5} cm^2\ s^{-1}$) and v is the kinematic viscosity of the solution (0.01 $cm^2\ s^{-1}$) [13].

The RDE polarization curve at various rotations rate from 360 rpm to 4600 rpm and K-L plots for Fe−NCNT and Co−NCNT catalyst in acidic medium are presented in Figure 3-5 and Figure 3-6. These K-L plots were further analyzed to determine the number of electrons transfer for the catalysts which was summarized in Table 3-3. Electrons transfer calculation can be done at any potential as long as the current is a combination between kinetic and diffusion currents [40]. Therefore, the potential range selected for calculation is 0 V to 0.20 V (vs. RHE) for acidic medium while 0.4 V to 0.6 V (vs. RHE) for alkaline medium. For acidic medium, it was found that between

Fe–NCNT and Co–NCNT, the number of electrons transfer on Fe–NCNT is higher than Co–NCNT which is closer to 4.0 indicates ORR proceed in 4-electron transfer pathway. Fe–NCNT2 catalyst give the highest number of electrons transfer which is 3.7, followed by 3.5 for Fe–NCNT1 and 2.9 for Fe–NCNT2A. Similar trend was observed for Co–NCNT, the electrons transfer obtained to be 2.3, 2.7 and 1.8 for Co–NCNT1, Co–NCNT2 and Co–NCNT2A, respectively.

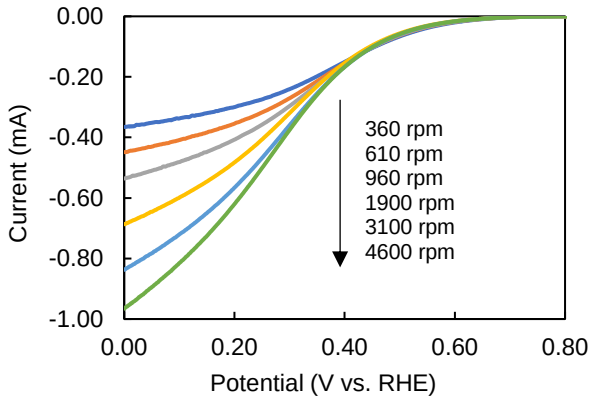

(a) Fe–NCNT1

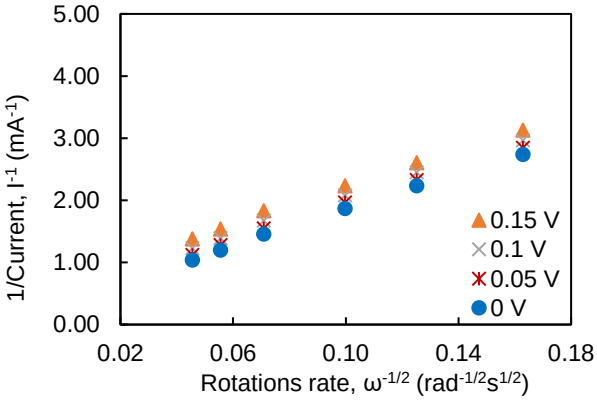

(b) Fe–NCNT1

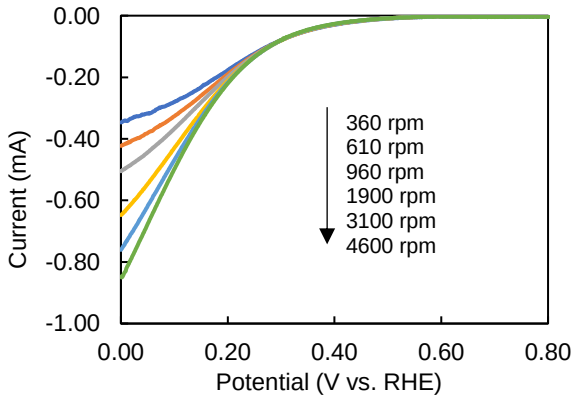

(c) Fe–NCNT2

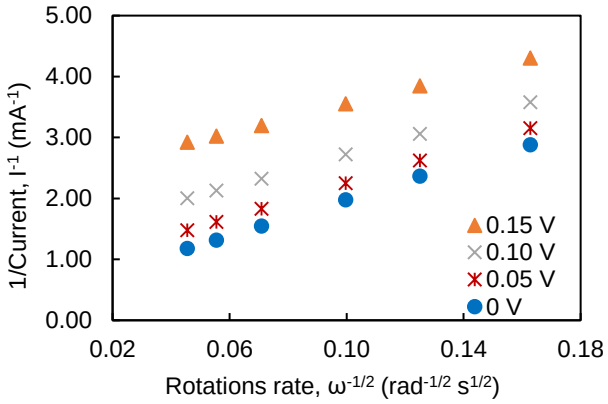

(d) Fe–NCNT2

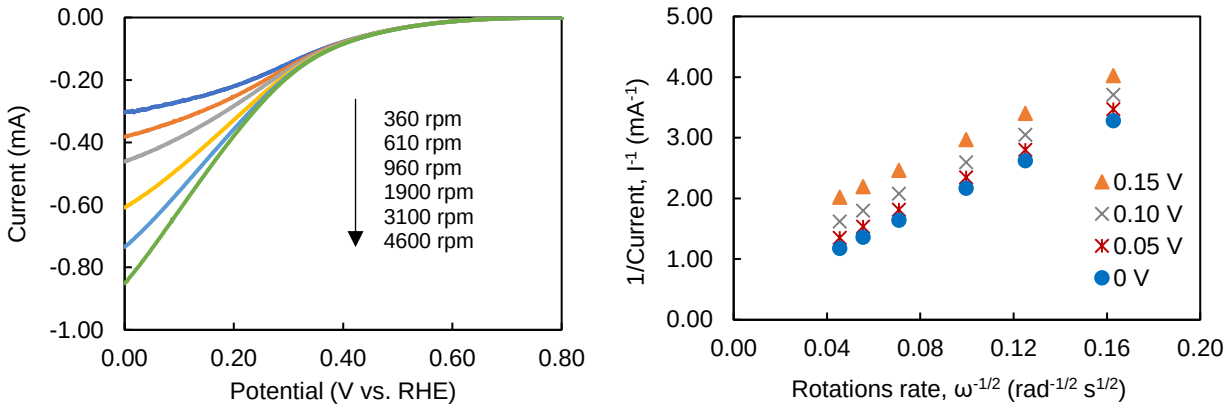

(e) Fe−NCNT2A (f) Fe−NCNT2A

Figure 3-5 RDE polarization curve at various rotations rate for (a) Fe−NCNT1, (c) Fe−NCNT2, (e) Fe−NCNT2A catalyst and K-L plots for (b) Fe−NCNT1, (d) Fe−NCNT2, (f) Fe−NCNT2A catalyst in O_2-saturated 0.5 M H_2SO_4

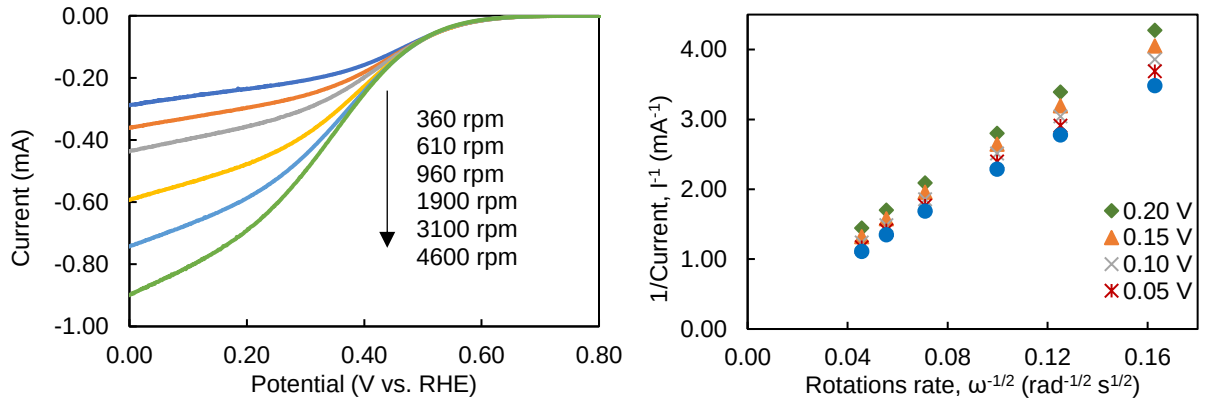

(a) Co−NCNT1 (b) Co−NCNT1

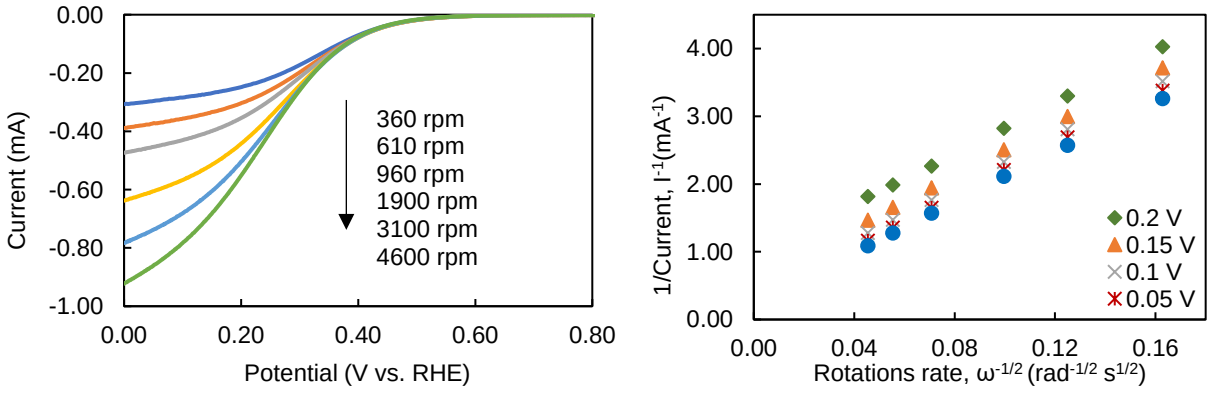

(c) Co−NCNT2 (d) Co−NCNT2

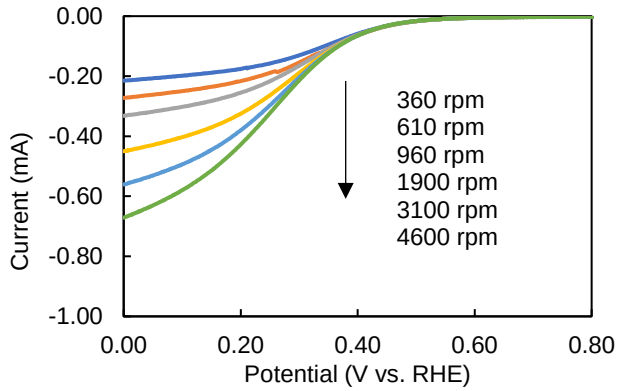

(e) Co−NCNT2A

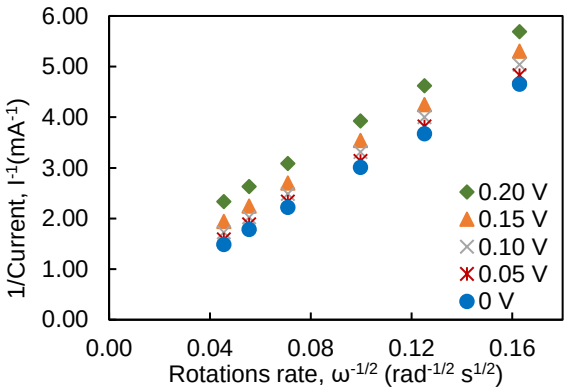

(f) Co−NCNT2A

Figure 3-6 RDE polarization curve at various rotations rate for (a) Co−NCNT1, (c) Co−NCNT2, (e) Co−NCNT2A catalyst and K-L plots for (b) Co−NCNT1, (d) Co−NCNT2, (f) Co−NCNT2A catalyst in O_2-saturated 0.5 M H_2SO_4

The RDE polarization curve recorded at various rotations rate and K-L plots in alkaline medium are shown in Figure 3-7 for Fe−NCNT and Figure 3-8 for Co−NCNT. The number of electrons transfer of the catalysts were calculated by K-L equation (1) with the value of $C_{O_2}^b$ is the concentration of O_2 in the 0.1 M KOH (1.2×10^{-6} mol cm^{-3}), D_{O_2} is the diffusion coefficient of O_2 ($1.8 \times 10^{-5} cm^2\ s^{-1}$) and v is the kinematic viscosity of the solution (0.01 $cm^2\ s^{-1}$) [41]. As referred to the data summarized in Table 3-3, Co−NCNT catalyst showed higher electrons transfer that closer to 4.0 as compared with Fe−NCNT catalyst in alkaline medium, which is 3.8, 4.3, and 3.0 for Co−NCNT1, Co−NCNT2 and Co−NCNT2A, respectively. For Fe-containing catalyst, the number of electron transfer calculated to be 3.5 for Fe−NCNT1 and Fe−NCNT2A while 3.1 for Fe−NCNT2. For the number of electrons transfer obtained that slightly above 4.0 is due to the uneven structure of the catalyst layer on the GC electrode [15].

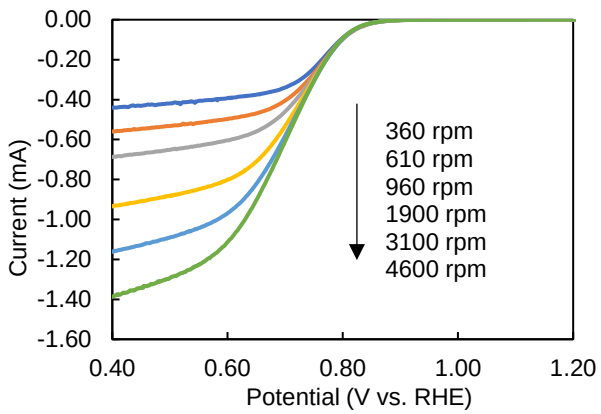

(a) Fe−NCNT1

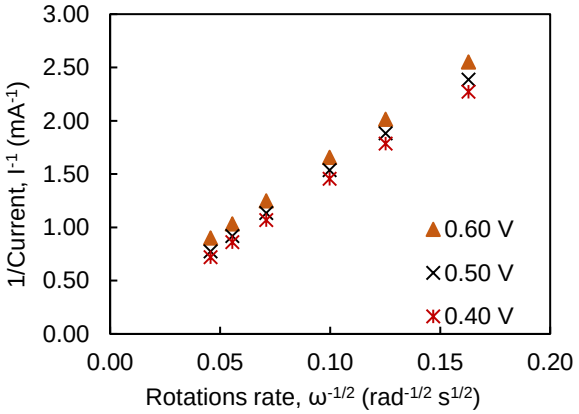

(b) Fe−NCNT1

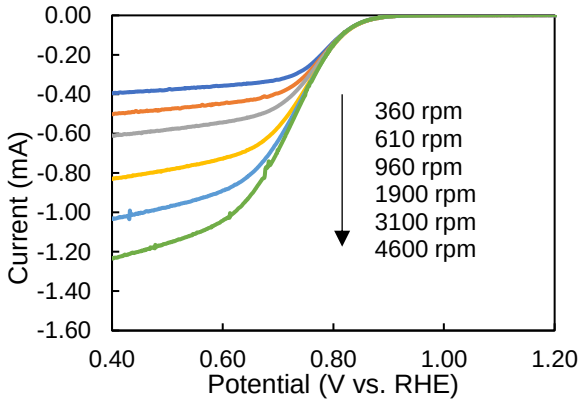

(c) Fe−NCNT2

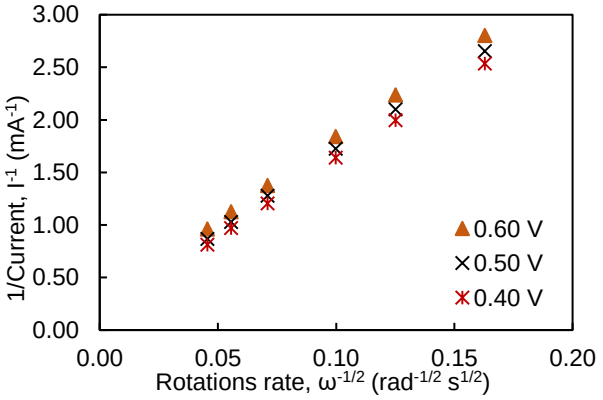

(d) Fe−NCNT2

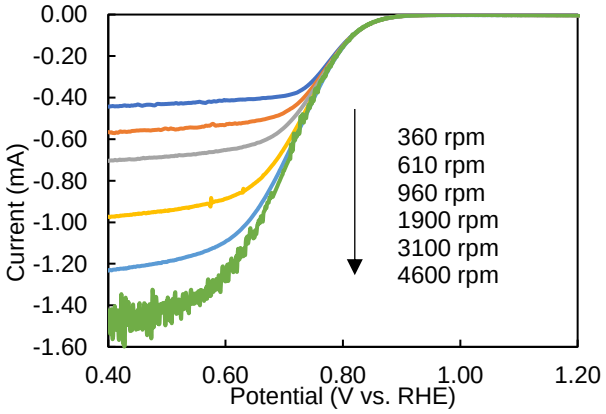

(e) Fe−NCNT2A

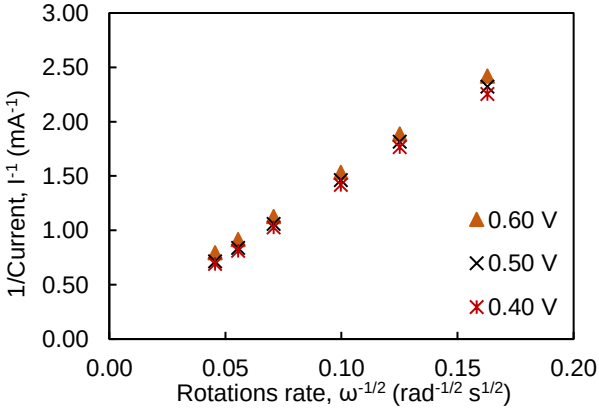

(f) Fe−NCNT2A

Figure 3-7 RDE polarization curve at various rotations rate for (a) Fe−NCNT1, (c) Fe−NCNT2, (e) Fe−NCNT2A catalyst and Koutecky-Levich (K-L) plots generated from K-L equation for (b) Fe−NCNT1, (d) Fe−NCNT2, (f) Fe−NCNT2A catalyst in O_2-saturated 0.1 M KOH

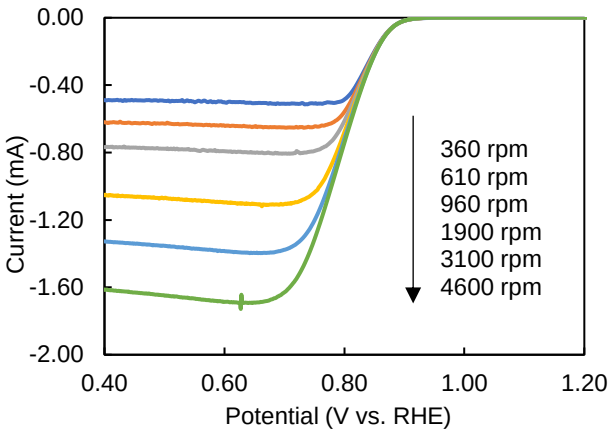

(a) Co−NCNT1

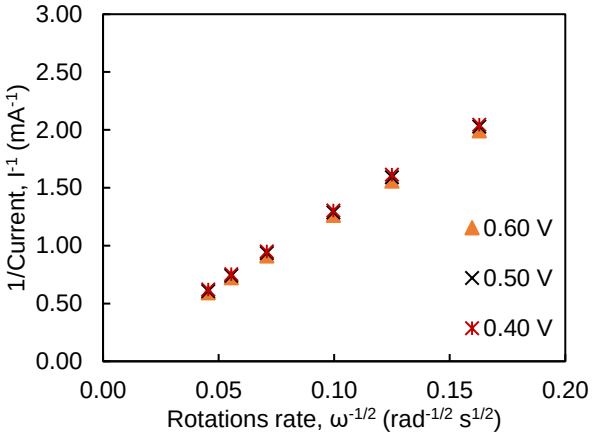

(b) Co−NCNT1

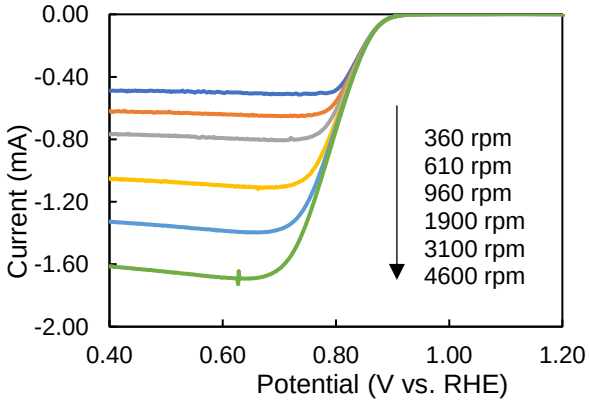

(c) Co−NCNT2

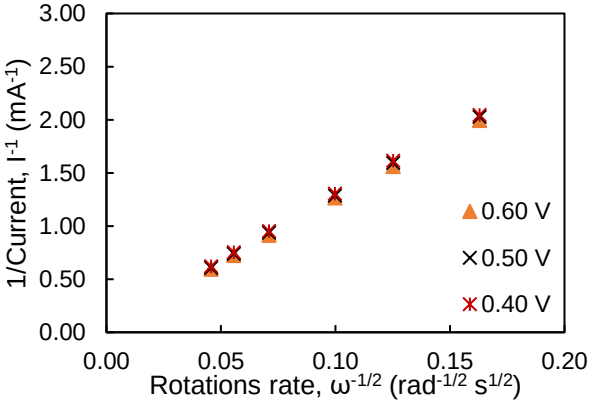

(d) Co−NCNT2

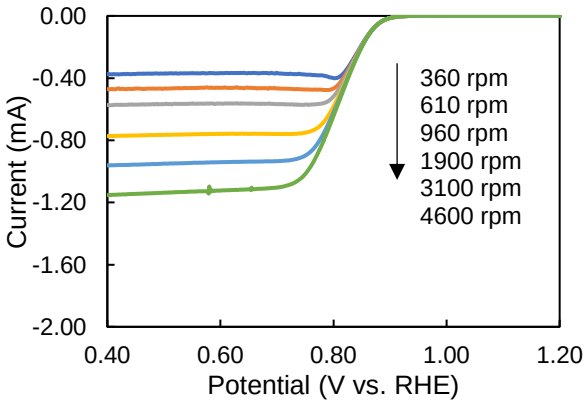

(e) Co−NCNT2A

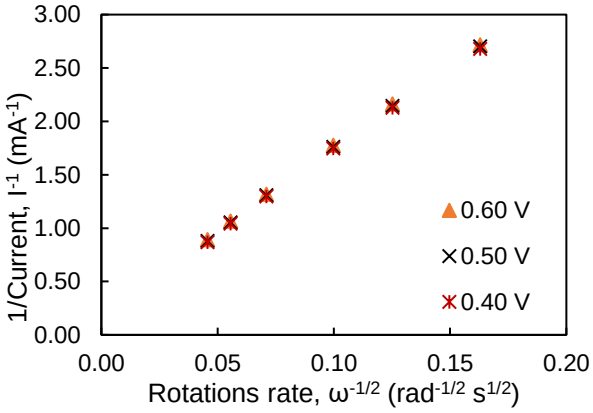

(f) Co−NCNT2A

Figure 3-8 RDE polarization curve at various rotations rate (a) Co−NCNT1, (c) Co−NCNT2, (e) Co−NCNT2A catalyst and K-L plots for (b) Co−NCNT1, (d) Co−NCNT2, (f) Co−NCNT2A catalyst in O_2-saturated 0.1 M KOH

Table 3-3 Catalytic activity parameter for catalyst sample in acidic and alkaline medium

Medium	Acidic		Alkaline	
Catalyst	Onset potential (V vs. RHE)	Number of electron transfer	Onset potential (V vs. RHE)	Number of electron transfer
Fe−NCNT1	0.64	3.5	0.85	3.5
Fe−NCNT2	0.50	3.7	0.87	3.1
Fe−NCNT2A	0.61	2.9	0.87	3.5
Co−NCNT1	0.62	2.3	0.89	3.8
Co−NCNT2	0.54	2.7	0.89	4.3
Co−NCNT2A	0.57	1.8	0.89	3.0
Commercial Pt/C	0.80	4.4	0.97	4.2

3.3.4 Fuel tolerance

For fuel-cell applications, another important parameter to investigate is the fuel tolerance of the catalyst. As reported in the previous studies, a non-Pt-based catalyst containing Fe or Co has high tolerance toward methanol and does not exhibit any activity for the methanol oxidation reaction (MOR). Thus, it is expected that the catalysts synthesized in this study would show high tolerance to formic acid as well. The results for formic acid tolerance in acidic medium are presented in Figure 3-9. The measurements were done in the presence of 1 M and 3 M formic acid, which is the concentration of formic acid used as the feed for the anode DFAFC. The onset potentials for Fe–NCNT1 in the presence of 1 M and 3 M formic acid are 0.54 V and 0.52 V, respectively. The onset potential for Co–NCNT1 does not seem to be affected by the presence of 1 M and 3M formic acid, but as the concentration of formic acid increases, the limiting current density for both catalysts decreases. This is because there could be a weak interaction between formic acid and the ORR active sites or a decrease of O_2 solubility due to the presence of formic acid [6,42].

On the other hand, for the Pt/C catalyst, a high peak in formic acid oxidation is observed in the presence of formic acid, as shown in Figure 3-9 (c), which indicates that formic acid oxidation reaction (FAOR) occurs on the Pt/C catalyst, and thus the Pt/C catalyst has lower tolerance toward formic acid as compared to the non-Pt catalysts synthesized in this study. The onset potential of the Pt/C catalyst in the presence of formic acid is reduced to 0.2 V, reflecting a 75% decay from the onset potential obtained without formic acid. Therefore, the Fe–NCNT1 and Co–NCNT1 catalysts have higher selectivity toward ORR in the presence of formic acid than the Pt/C catalyst and can be considered as promising cathode catalysts for DFAFC.

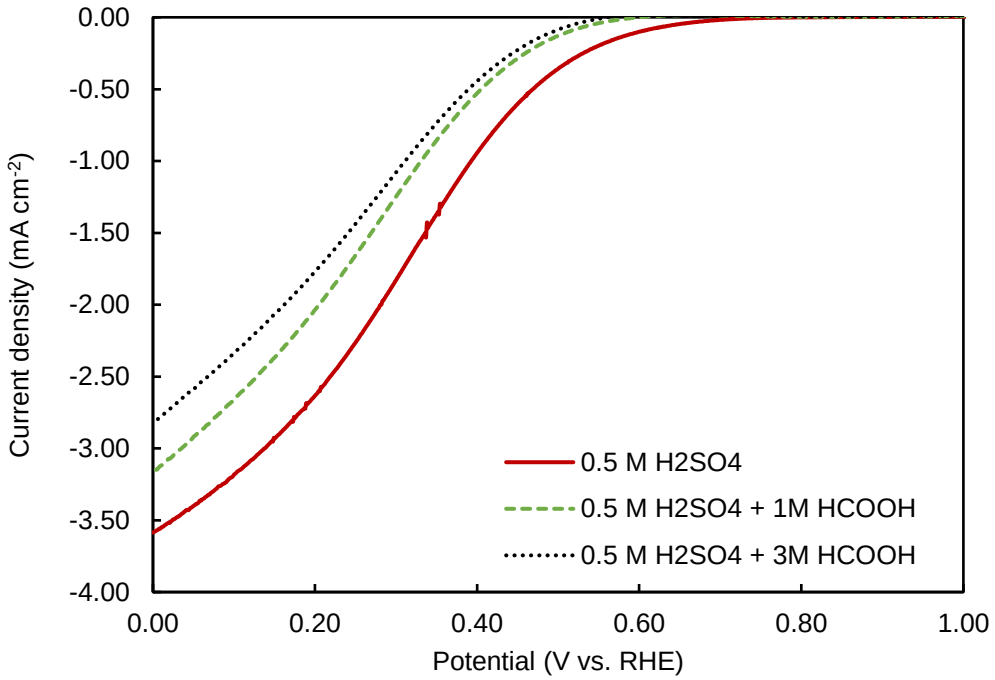

(a) Fe−NCNT1

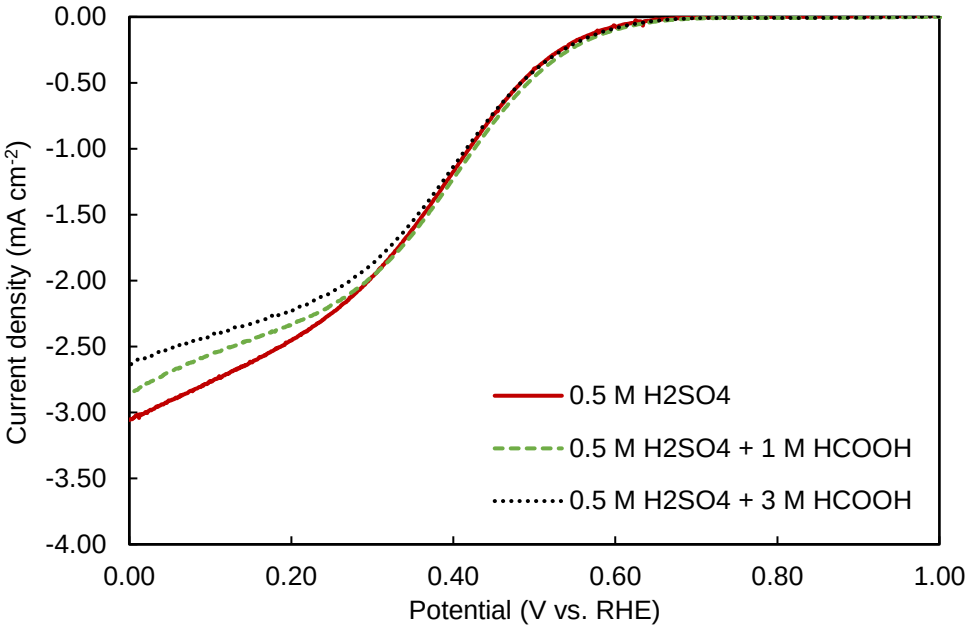

(b) Co−NCNT1

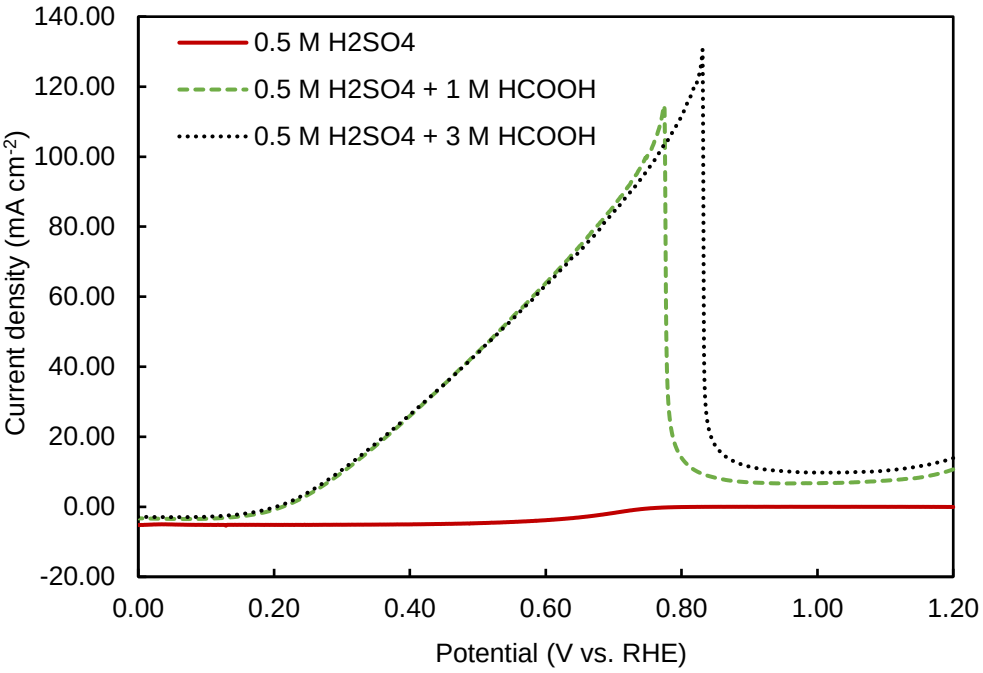

(c) Pt/C

Figure 3-9 ORR activity curve for (a) Fe−NCNT1 (b) Co−NCNT1 and (c) Pt/C catalyst (50 wt. %) in O_2-saturated 0.5 M H_2SO_4 with and without formic acid (HCOOH) at rotation rate of 1900 rpm

Catalyst tolerance toward sodium formate (HCOONa) also investigated for the Fe−N−CNT2A, Co−N−CNT2 catalyst that showed highest catalytic activity in alkaline medium. The reduction curve for ORR activity on the Fe−N−CNT2A, Co−N−CNT2 and commercial Pt/C catalyst without and with the presence of HCOONa in alkaline solution were shown in Figure 3-10. It was observed that there are no significant changes of the onset potential for both TM−NCNT catalysts in the presence of HCOONa in the solution that indicates they have high tolerance toward HCOONa. In comparison with the commercial Pt/C catalyst, there is obvious peak of formate oxidation observed which shows no tolerance of the commercial Pt/C catalyst toward HCOONa in alkaline medium.

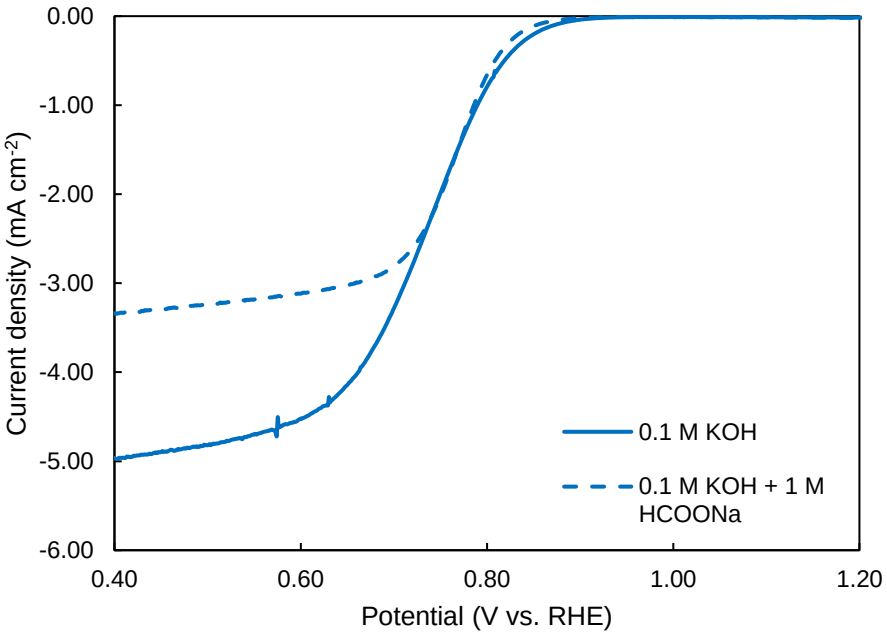

(a) Fe−NCNT2A

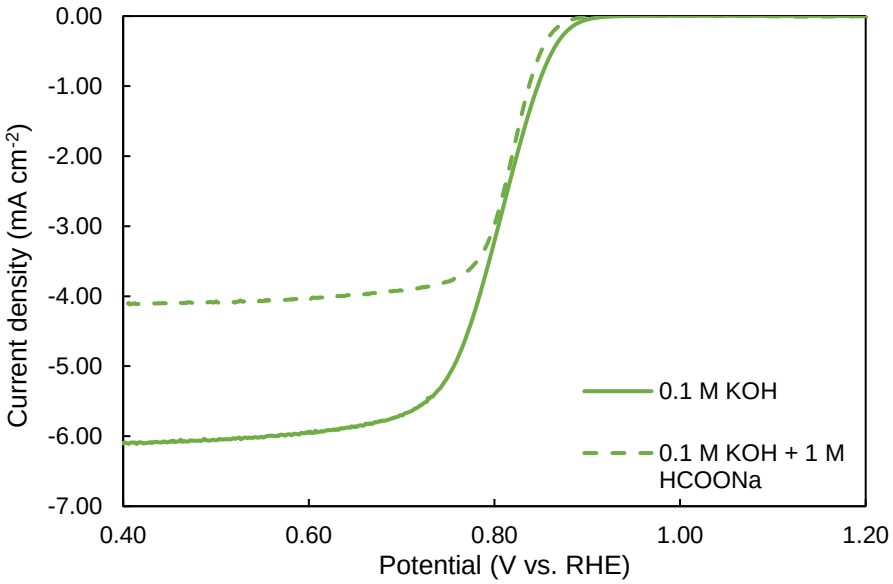

(b) Co−NCNT2

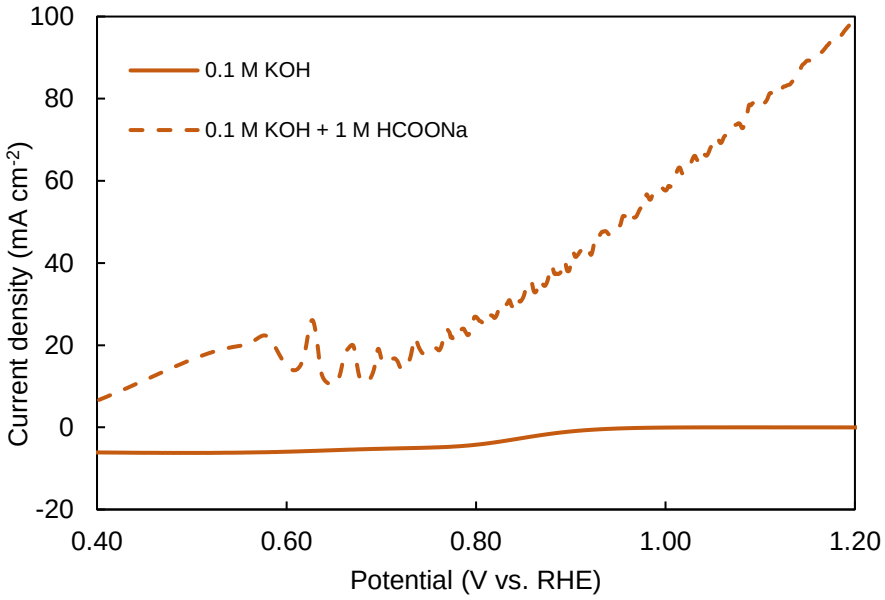

(c) Pt/C

Figure 3-10 ORR activity curve for (a) Fe−NCNT2A, (b) Co−NCNT2 and (c) commercial Pt/C catalyst (50 wt. %) in O_2-saturated 0.1 M KOH with and without sodium formate (HCOONa) at rotation rate of 1900 rpm

3.3.5 Stability test

The stability for Fe−NCNT and Co−NCNT catalyst samples were measured and compared with the stability for commercial Pt/C in both acidic and alkaline medium. The chronoamperometry test was conducted for 6 h at the potential of 0.2 V (vs. RHE) for the acidic medium, as shown in Figure 3-11. The Co–NCNT1 catalyst exhibits better stability than the Fe–NCNT1 catalyst and the commercial Pt/C catalyst. The Co–NCNT1 catalyst shows the highest relative current of 86% after 20000 s, but the Fe–NCNT1 catalyst and the commercial Pt/C catalyst show decreases in the current to 65 % and 64%, respectively. Similar behavior was observed in S. Ratso et al. [13] where the Co-based catalyst has superior stability in acidic medium. Low stability of Pt/C catalyst is might due to the weak interaction between carbon support and the metal. The good stability of Fe−NCNT and Co−NCNT was attributed to the presence of nitrogen binding species exists in the catalyst [43]. However, loss of stability with time was experienced by both TM−NCNT catalysts due to the protonation of the pyridinic-N and pyrrolic-N species in acidic medium, which then become inactive sites for ORR [44].

In alkaline medium, Co−NCNT2 shows the best stability than the other catalysts tested with 95 % of current retention after 20000 s operation while current was reduced to 89 % for commercial Pt/C and 66 % for Fe−NCNT2A catalyst as shown Figure 3-12. Stability of Co−NCNT2 achieved in alkaline medium for this study is in accordance with the other previous Co-carbon-based catalyst developed by Hosna Ghanbarlou et al. They reported that the Co−NG and Co−MWCNT exhibited 90 % and 75 % current retention, respectively which are higher than commercial Pt/C (60 %). The high stability was contributed by the existence of nitrogen atom as doping agent for the metal to the carbon support and thus enhances the interaction between metal and carbon support [45,46]. It can be concluded that the TM−NCNT catalyst in this study exhibits

better stability in alkaline medium as the higher current retention after 20000 s operation in alkaline than acidic medium. This result is in good agreement with the previous stability test result reported by X. Li et al. that indicates the non-precious metal catalyst was much more stable in alkaline medium than in acidic medium. Thus, the high stability in alkaline medium for the Fe−NCNT and Co−NCNT catalyst prepared in this study shows the compatibility to be applied as cathode catalyst for alkaline fuel cell.

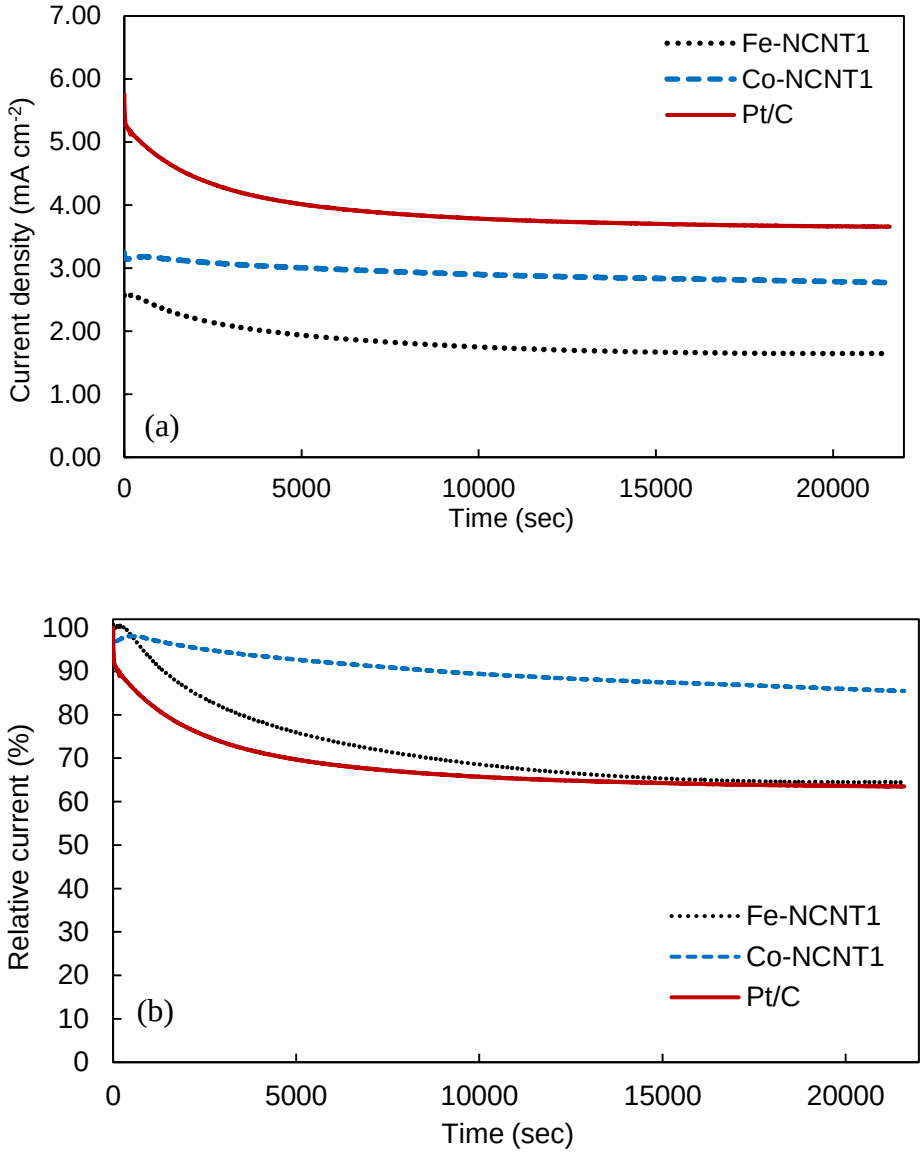

Figure 3-11 Chronoamperometric responses of Fe−NCNT, Co−NCNT and commercial Pt/C in O_2-saturated 0.5 M H_2SO_4 solution at rotations rate of 1900 rpm.

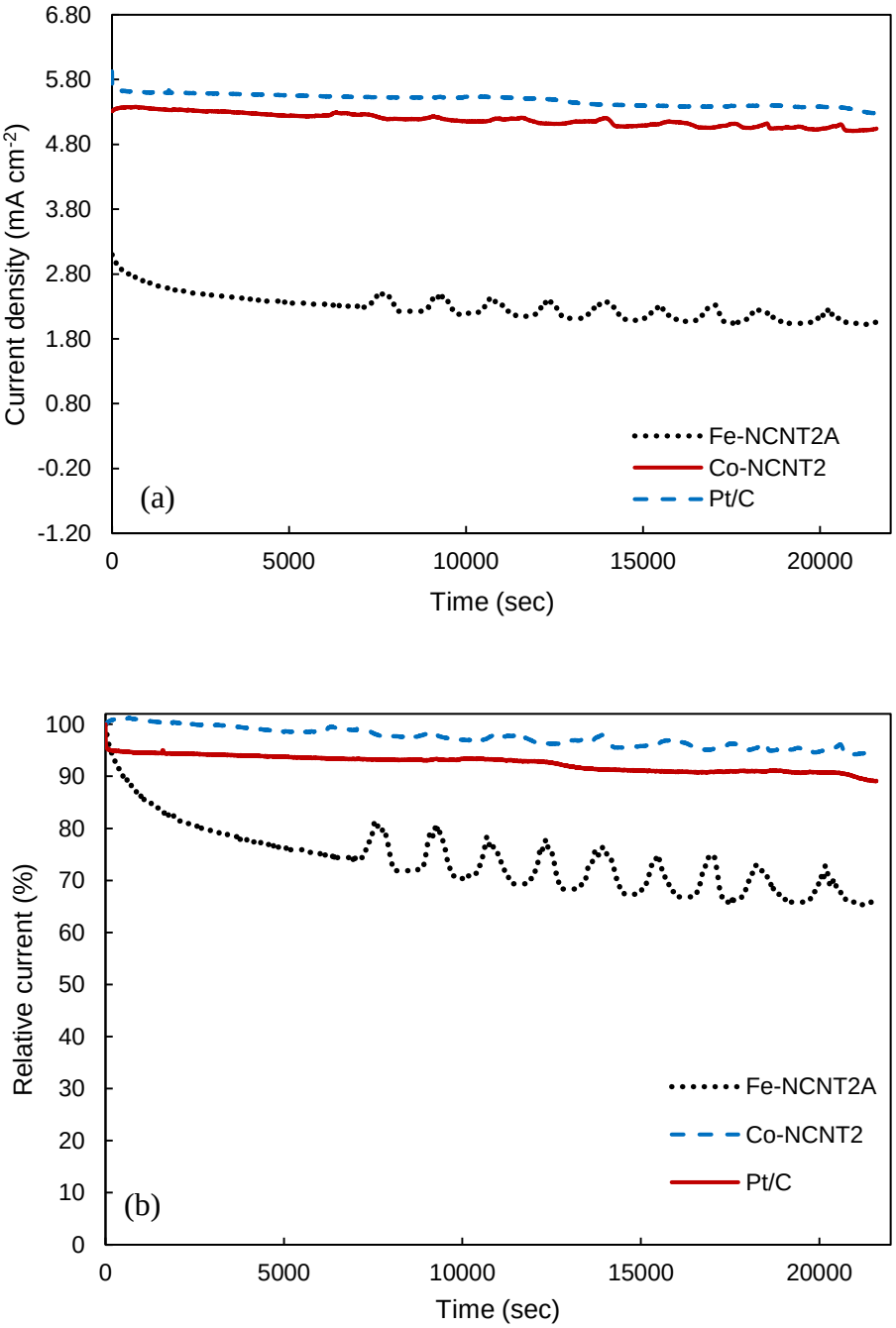

Figure 3-12 Chronoamperometric responses of Fe−NCNT, Co−NCNT and commercial Pt/C in O_2-saturated 0.1 M KOH solution at rotations rate of 1900 rpm

3.4 Conclusions

In summary, transition metal nitrogen doped carbon nanotubes catalyst namely, Fe−NCNT and Co−NCNT were synthesized and the ORR activity on each catalyst samples were investigated in acidic and alkaline medium. The effect of pyrolysis step of each catalyst on the ORR activity was different in acidic and alkaline medium. Catalyst from first pyrolysis, Fe−NCNT1 and Co−NCNT1 perform better than other samples in acidic medium. For alkaline medium, acid-treated combined with second pyrolyzed Fe-containing catalyst (Fe−NCNT2A) and twice pyrolyzed Co-containing catalyst (Co−NCNT2) perform better in alkaline medium. It can be concluded that Fe−NCNT catalyst was found to be more active for ORR in acidic medium whereas Co−NCNT catalyst is more active for ORR in alkaline medium. In comparison with commercial Pt/C catalyst, the ORR activity of these Fe−NCNT and Co−NCNT catalysts are still lower, but they have better fuel tolerance than that commercial Pt/C catalyst in acidic and alkaline medium. The Co−NCNT catalyst exhibits superior stability than Fe−NCNT and comparable with commercial Pt/C catalyst in both medium. These characteristics make the TM−NCNT catalyst prepared in this study as a promising for DFAFC application either in acidic or alkaline condition.

3.5 References

[1] T. Tsujiguchi, F. Matsuoka, Y. Hokari, Y. Osaka, A. Kodama, Overpotential analysis of the Direct Formic Acid Fuel Cell, Electrochim. Acta. 197 (2016) 32–38. doi:10.1016/j.electacta.2016.03.062.

[2] J.F. Drillet, A. Ee, J. Friedemann, R. Kötz, B. Schnyder, V.M. Schmidt, Oxygen reduction at Pt and Pt70Ni30 in H2SO4/CH3OH solution, Electrochim. Acta. 47 (2002) 1983–1988. doi:10.1016/S0013-4686(02)00027-0.

[3] Y. Shi, S. Yin, Y. Ma, D. Lu, Y. Chen, Y. Tang, T. Lu, Oleylamine-functionalized

palladium nanoparticles with enhanced electrocatalytic activity for the oxygen reduction reaction, J. Power Sources. 246 (2014) 356–360. doi:10.1016/j.jpowsour.2013.07.099.

[4] C.O. Colpan, D. Ouellette, A. Glüsen, M. Müller, D. Stolten, Reduction of methanol crossover in a flowing electrolyte-direct methanol fuel cell, Int. J. Hydrogen Energy. 42 (2017) 21530–21545. doi:https://doi.org/10.1016/j.ijhydene.2017.01.004.

[5] S. Knani, L. Chirchi, W.T. Napporn, S. Baranton, J.M. Léger, A. Ghorbel, Promising ternary Pt-Co-Sn catalyst for the oxygen reduction reaction, J. Electroanal. Chem. 738 (2015) 145–153. doi:10.1016/j.jelechem.2014.11.023.

[6] D. Sebastián, V. Baglio, A.S. Aricò, A. Serov, P. Atanassov, Performance analysis of a non-platinum group metal catalyst based on iron-aminoantipyrine for direct methanol fuel cells, Appl. Catal. B Environ. 182 (2016) 297–305. doi:10.1016/j.apcatb.2015.09.043.

[7] R. Janarthanan, A. Serov, S.K. Pilli, D.A. Gamarra, P. Atanassov, M.R. Hibbs, A.M. Herring, Direct Methanol Anion Exchange Membrane Fuel Cell with a Non-Platinum Group Metal Cathode based on Iron-Aminoantipyrine Catalyst, Electrochim. Acta. 175 (2015) 202–208. doi:10.1016/j.electacta.2015.03.209.

[8] B. Liu, B. Huang, C. Lin, J. Ye, L. Ouyang, Applied Surface Science Porous carbon supported Fe-N-C composite as an efficient electrocatalyst for oxygen reduction reaction in alkaline and acidic media, Appl. Surf. Sci. 411 (2017) 487–493. doi:10.1016/j.apsusc.2017.03.150.

[9] L. Osmieri, R. Escudero-Cid, M. Armandi, A.H.A. Monteverde Videla, J.L. García Fierro, P. Ocón, S. Specchia, Fe-N/C catalysts for oxygen reduction reaction supported on different carbonaceous materials. Performance in acidic and alkaline direct alcohol fuel cells, Appl.

Catal. B Environ. 205 (2017) 637–653. doi:10.1016/j.apcatb.2017.01.003.

[10] N.A. Karim, S.K. Kamarudin, Novel heat-treated cobalt phthalocyanine/carbon-tungsten oxide nanowires (CoPc/C-W18O49) cathode catalyst for direct methanol fuel cell, J. Electroanal. Chem. 803 (2017) 19–29. doi:10.1016/j.jelechem.2017.08.050.

[11] N.A. Karim, S.K. Kamarudin, K.S. Loh, Performance of a novel non-platinum cathode catalyst for direct methanol fuel cells, Energy Convers. Manag. 145 (2017) 293–307. doi:10.1016/j.enconman.2017.05.003.

[12] R. Zhang, Y. Peng, Z. Li, K. Li, J. Ma, Y. Liao, L. Zheng, X. Zuo, D. Xia, Oxygen Electroreduction on Heat - treated Multi - walled Carbon Nanotubes Supported Iron Polyphthalocyanine in Acid Media, Electrochim. Acta. 147 (2014) 343–351. doi:10.1016/j.electacta.2014.09.064.

[13] S. Ratso, I. Kruusenberg, A. Sarapuu, M. Kook, P. Rauwel, R. Saar, J. Aruväli, K. Tammeveski, Electrocatalysis of oxygen reduction on iron- and cobalt-containing nitrogen-doped carbon nanotubes in acid media, Electrochim. Acta. 218 (2016) 303–310. doi:10.1016/j.electacta.2016.09.119.

[14] Z. Ma, C. Guo, Y. Yin, Y. Zhang, H. Wu, C. Chen, The use of cheap polyaniline and melamine co-modified carbon nanotubes as active and stable catalysts for oxygen reduction reaction in alkaline medium, Electrochim. Acta. 160 (2015) 357–362. doi:10.1016/j.electacta.2015.02.053.

[15] S. Ratso, I. Kruusenberg, M. Käärik, M. Kook, R. Saar, P. Kanninen, T. Kallio, J. Leis, K. Tammeveski, Transition metal-nitrogen co-doped carbide-derived carbon catalysts for oxygen reduction reaction in alkaline direct methanol fuel cell, Appl. Catal. B Environ. 219

(2017) 276–286. doi:10.1016/j.apcatb.2017.07.036.

[16] Y. Liu, J. Ruan, S. Sang, Z. Zhou, Q. Wu, Iron and nitrogen co-doped carbon derived from soybeans as efficient electro-catalysts for the oxygen reduction reaction, Electrochim. Acta. 215 (2016) 388–397. doi:10.1016/J.ELECTACTA.2016.08.090.

[17] L. Lin, Q. Zhu, A. Xu, Noble-Metal-Free Fe − N/C Catalyst for Highly E ffi cient Oxygen Reduction Reaction under Both Alkaline and Acidic Conditions, J. Am. Chem. Soc. 136 (2014) 11027–11033. doi:10.1021/ja504696r.

[18] X. Yu, P.G. Pickup, Recent advances in direct formic acid fuel cells (DFAFC), J. Power Sources. 182 (2008) 124–132. doi:10.1016/j.jpowsour.2008.03.075.

[19] L. Timperman, A.S. Gago, N. Alonso-Vante, Oxygen reduction reaction increased tolerance and fuel cell performance of Pt and RuxSeyonto oxide-carbon composites, J. Power Sources. 196 (2011) 4290–4297. doi:10.1016/j.jpowsour.2010.11.083.

[20] P. Nekooi, M. Akbari, M.K. Amini, CoSe nanoparticles prepared by the microwave-assisted polyol method as an alcohol and formic acid tolerant oxygen reduction catalyst, Renew. Energy. 35 (2010) 6392–6398. doi:10.1016/j.ijhydene.2010.03.134.

[21] J. Jiang, A. Wieckowski, Prospective direct formate fuel cell, Electrochem. Commun. 18 (2012) 41–43. doi:10.1016/j.elecom.2012.02.017.

[22] X. Yu, A. Manthiram, Catalyst-selective, scalable membraneless alkaline direct formate fuel cells, Appl. Catal. B Environ. 165 (2015) 63–67. doi:10.1016/j.apcatb.2014.09.069.

[23] L. An, R. Chen, Direct formate fuel cells: A review, J. Power Sources. 320 (2016) 127–139. doi:10.1016/j.jpowsour.2016.04.082.

[24] L. Osmieri, A.H.A. Monteverde Videla, S. Specchia, Activity of Co-N multi walled carbon nanotubes electrocatalysts for oxygen reduction reaction in acid conditions, J. Power Sources. 278 (2015) 296–307. doi:10.1016/j.jpowsour.2014.12.080.

[25] H. Peng, F. Liu, X. Liu, S. Liao, C. You, X. Tian, H. Nan, F. Luo, H. Song, Z. Fu, P. Huang, Effect of transition metals on the structure and performance of the doped carbon catalysts derived from polyaniline and melamine for ORR application, ACS Catal. 4 (2014) 3797–3805. doi:10.1021/cs500744x.

[26] C.H. Choi, S.H. Park, S.I. Woo, N-doped carbon prepared by pyrolysis of dicyandiamide with various MeCl2·xH2O (Me=Co, Fe, and Ni) composites: Effect of type and amount of metal seed on oxygen reduction reactions, Appl. Catal. B Environ. 119–120 (2012) 123–131. doi:10.1016/j.apcatb.2012.02.031.

[27] M. Borghei, P. Kanninen, M. Lundahl, T. Susi, J. Sainio, I. Anoshkin, A. Nasibulin, T. Kallio, K. Tammeveski, E. Kauppinen, V. Ruiz, High oxygen reduction activity of few-walled carbon nanotubes with low nitrogen content, Appl. Catal. B Environ. 158 (2014) 233–241. doi:10.1016/j.apcatb.2014.04.027.

[28] F. Jaouen, J.-P. Dodelet, Average turn-over frequency of O2 electro-reduction for Fe/N/C and Co/N/C catalysts in PEFCs, Electrochim. Acta. 52 (2007) 5975–5984. doi:https://doi.org/10.1016/j.electacta.2007.03.045.

[29] G. Wei, J. Wainright, R. Savinell, Catalytic activity for oxygen reduction reaction of catalysts consisting of carbon, nitrogen and cobalt, J. New Mater. Electrochem. Syst. 129 (2000) 121–129.

[30] K. Artyushkova, S. Levendosky, P. Atanassov, J. Fulghum, XPS Structural studies of nano-

composite non-platinum electrocatalysts for polymer electrolyte fuel cells, Top. Catal. 46 (2007) 263–275. doi:10.1007/s11244-007-9002-y.

[31] A.H.A. Monteverde Videla, L. Osmieri, M. Armandi, S. Specchia, Varying the morphology of Fe-N-C electrocatalysts by templating Iron Phthalocyanine precursor with different porous SiO2 to promote the Oxygen Reduction Reaction, Electrochim. Acta. 177 (2015) 43–50. doi:10.1016/j.electacta.2015.01.165.

[32] H.S. Oh, H. Kim, The role of transition metals in non-precious nitrogen-modified carbon-based electrocatalysts for oxygen reduction reaction, J. Power Sources. 212 (2012) 220–225. doi:10.1016/j.jpowsour.2012.03.098.

[33] S.H. Liu, J.R. Wu, Influence of nitrogen and iron precursors on the synthesis of FeN x/carbons electrocatalysts toward oxygen reduction reaction in acid solution, Electrochim. Acta. 135 (2014) 147–153. doi:10.1016/j.electacta.2014.04.167.

[34] A. Dorjgotov, J. Ok, Y. Jeon, S.-H. Yoon, Y.G. Shul, Nitrogen-doped ordered porous carbon catalyst for oxygen reduction reaction in proton exchange membrane fuel cells, J. Solid State Electrochem. 17 (2013) 2567–2577. doi:10.1007/s10008-013-2135-y.

[35] J. Masa, W. Xia, M. Muhler, W. Schuhmann, On the Role of Metals in Nitrogen-Doped Carbon Electrocatalysts for Oxygen Reduction, Angew. Chemie - Int. Ed. 54 (2015) 10102–10120. doi:10.1002/anie.201500569.

[36] H. Zhang, H. Kong, X. Yuan, Q. Jiang, J. Yang, Influence of metal precursors on the catalytic activity and structure of non-precious metal electrocatalysts for oxygen reduction reaction, Int. J. Hydrogen Energy. 37 (2012) 13219–13226. doi:10.1016/j.ijhydene.2012.03.049.

[37] S. Ratso, I. Kruusenberg, A. Sarapuu, P. Rauwel, R. Saar, U. Joost, J. Aruväli, P. Kanninen, T. Kallio, K. Tammeveski, Enhanced oxygen reduction reaction activity of iron-containing nitrogen-doped carbon nanotubes for alkaline direct methanol fuel cell application, J. Power Sources. 332 (2016) 129–138. doi:10.1016/J.JPOWSOUR.2016.09.069.

[38] Y. Yao, B. Zhang, J. Shi, Q. Yang, Preparation of Nitrogen-Doped Carbon Nanotubes with Different Morphologies from Melamine-Formaldehyde Resin, (2015). doi:10.1021/acsami.5b01233.

[39] Q. Zhao, Q. Ma, F. Pan, J. Guo, J. Zhang, Facile synthesis of N-doped carbon nanosheet-encased cobalt nanoparticles as efficient oxygen reduction catalysts in alkaline and acidic media, Ionics (Kiel). (n.d.). doi:10.1007/s11581-016-1748-4.

[40] L. Osmieri, A.H.A. Monteverde Videla, S. Specchia, Optimization of a Fe–N–C electrocatalyst supported on mesoporous carbon functionalized with polypyrrole for oxygen reduction reaction under both alkaline and acidic conditions, Int. J. Hydrogen Energy. 41 (2016) 19610–19628. doi:10.1016/j.ijhydene.2016.05.270.

[41] A. Sarapuu, L. Samolberg, K. Kreek, M. Koel, L. Matisen, K. Tammeveski, Cobalt- and iron-containing nitrogen-doped carbon aerogels as non-precious metal catalysts for electrochemical reduction of oxygen, J. Electroanal. Chem. 746 (2015) 9–17. doi:10.1016/j.jelechem.2015.03.021.

[42] A.H.A. Monteverde Videla, D. Sebastián, N.S. Vasile, L. Osmieri, A.S. Aricò, V. Baglio, S. Specchia, Performance analysis of Fe–N–C catalyst for DMFC cathodes: Effect of water saturation in the cathodic catalyst layer, Int. J. Hydrogen Energy. 41 (2016) 22605–22618. doi:10.1016/J.IJHYDENE.2016.06.060.

[43] E. Negro, A.H.A.M. Videla, V. Baglio, A.S. Aricò, S. Specchia, G.J.M. Koper, Fe–N supported on graphitic carbon nano-networks grown from cobalt as oxygen reduction catalysts for low-temperature fuel cells, Appl. Catal. B Environ. 166–167 (2015) 75–83. doi:10.1016/J.APCATB.2014.10.074.

[44] X. Li, G. Liu, B.N. Popov, Activity and stability of non-precious metal catalysts for oxygen reduction in acid and alkaline electrolytes, J. Power Sources. 195 (2010) 6373–6378. doi:10.1016/j.jpowsour.2010.04.019.

[45] H. Ghanbarlou, S. Rowshanzamir, M.J. Parnian, F. Mehri, Comparison of nitrogen-doped graphene and carbon nanotubes as supporting material for iron and cobalt nanoparticle electrocatalysts toward oxygen reduction reaction in alkaline media for fuel cell applications, Int. J. Hydrogen Energy. 41 (2016) 14665–14675. doi:10.1016/j.ijhydene.2016.06.005.

[46] A.H.A. Monteverde Videla, S. Ban, S. Specchia, L. Zhang, J. Zhang, Non-noble Fe-NXelectrocatalysts supported on the reduced graphene oxide for oxygen reduction reaction, Carbon N. Y. 76 (2014) 386–400. doi:10.1016/j.carbon.2014.04.092.

CHAPTER 4

Performance of direct formic acid fuel cell using transition metal-nitrogen-doped carbon nanotubes as cathode catalyst

4.1 Introduction

Fe− and Co− nitrogen-doped carbon catalyst that was proved to exhibits high methanol tolerance and promising as the cathode catalyst for DMFC [1–8]. Previous studies reported on the performance of single DMFC using Fe−NC catalyst in the cathode and the comparison of the performance with the conventional Pt/C cathode catalyst are summarized in Table 4-1. The effect of operating conditions such as cell operating temperature and methanol concentration on the cell performance were investigated in the literatures [5,9–11]. As found in the studies reported by D. Sebastian et al., an optimum temperature and methanol concentration was obtained at 90 °C and 5 M, respectively for DMFC with Fe−NC cathode catalyst [5,9,10]. For the DMFC equipped with conventional Pt/C cathode, the maximum power density is still higher at that optimum operating condition. Nevertheless, it is remarkable that there is slightly changes in open circuit voltage (OCV) values with the increase of methanol concentration for Fe−NC cathode catalyst whereas significant decrease of OCV for Pt−based cathode as the methanol concentration increase which indicates the detrimental effect of methanol crossover [5]. In addition, the DMFC performance with Fe–NC cathode catalysts is found to be lower than the conventional Pt/C catalyst at 90 °C operating temperature and 2 M methanol concentration as reported by L.Osmieri et al. [12]. In summary, the higher cell performance for the Fe−NC catalyst in the DMFC operation is related to the superior methanol tolerance properties than the conventional Pt/C catalyst [10]. Although these studies have been very useful for reducing the cost of DMFC, its performance remains low. Besides that, it was also found that there is an optimum operating condition especially the operating

temperature and the fuel (methanol) concentration even though the developed non-precious metal catalysts have better tolerance toward methanol as compared with the conventional Pt/C catalyst. The performance of NPM catalyst seems to exhibit better than the conventional Pt/C at higher methanol concentration and higher operating temperature as shown in Table 4-1.

Table 4-1 Comparison of single DMFC performance using Fe− or Co−NC and Pt/C cathode catalyst

Reference	Operating temperature (°C)	Methanol concentration (M)	Oxygen flow rate	Cathode catalyst	Open circuit voltage (OCV)	Maximum power density (mW cm^{-2})
D. Sebastian et al. [5]	90	5	100 ml min^{-1} (humidified)	Fe−NC Pt/C	0.75 ~0.60	35 65
D.Sebastian et al. [10]	90	5	100 ml min^{-1} (humidified)	Fe−NC Pt/C	- -	~62 ~60
D. Sebastian et al. [10]	90	10	100 ml min^{-1} (humidified)	Fe−NC Pt/C	0.82 0.50	60 ~42
D. Sebastian et al. [10]	110	17	100 ml min^{-1} (humidified)	Fe−NC Pt/C	0.78 0.45	58 26
Osmieri et al. [12]	90	2	200 Nml min^{-1} (dry)	Fe−NC Pt/C	0.70 0.60	19.6 30.9

In DFAFC operation, the single cell performance on NPM cathode catalyst is still limited [13]. So far, no studies have been reported on the single DFAFC operation of Fe- and Co-based catalysts to the best of our knowledge. Since the cathode reaction of DMFC is similar to that of DFAFC, it is expected that any improvements to the DMFC cathode will be applicable to the DFAFC cathode [14]. As reported in Chapter 3, the Fe−NCNT and Co−NCNT catalyst synthesized showed better tolerance toward formic acid than the commercial Pt/C catalyst in acidic medium thus, indicates these catalysts are promising cathode catalyst for DFAFC application. Therefore, in this chapter, we apply both non-precious metal catalyst as the DFAFC cathode. The performance in PEFC and DFAFC with Fe–NCNT and Co–NCNT as cathode catalysts are then evaluated under

different operating conditions to determine the optimum value and compared with those using the Pt/C catalyst. The comparison with the other literatures reported on DLFC with TM−NC cathode catalyst was discussed as well.

4.2 Experimental method

Detail procedure for the membrane electrode assemblies (MEA) fabrication was explained in Chapter 2. Three sets of MEA prepared and measured in this study, as listed in Table 4-2.

Table 4-2 Membrane electrode assemblies used for single cell measurement

Membrane electrode assembly (MEA)	**Anode catalyst**	**Cathode catalyst**
MEA-Fe−NCNT	Pd/C	Fe–NCNT (4.6 mg cm^{-2})
MEA-Co−NCNT	Pd/C	Co–NCNT (3.3 mg cm^{-2})
MEA-Pt/C	Pd/C	Pt/C (2.0 mg_{Pt} cm^{-2})

Before conducting the performance test, the single cell was pretreated by feeding humidified hydrogen to the anode side and dry oxygen to the cathode side. Then, the i−V measurement was recorded in the hydrogen-oxygen operation (PEFC). For the DFAFC operation, the MEAs were operated at the operating temperature of 60°C, 5 M formic acid concentration, and 500 ml min^{-1} dry oxygen flow rate as a pre-treatment for the formic acid operation. For the performance test, 3, 5, 7, and 10 M formic acid was supplied to the anode at 5 ml min^{-1}, and dry oxygen was supplied to the cathode at different flow rates: 300, 500, and 700 ml min^{-1}. This condition was tested at two different operating temperatures: 30°C and 60°C.

4.3 Result and discussion

4.3.1 Comparisons of the PEFC and DFAFC performance

The polarization and power density curves for the synthesized catalysts Fe–NCNT and Co–NCNT and for the commercial Pt/C catalyst, as the cathode for PEFC and DFAFC operations, are shown in Figure 4-1 (a) and Figure 4-1 (b), respectively, and these results are summarized in Table 4-3. DFAFC is operated at 60°C with 5 M formic acid and 500 ml min^{-1} dry oxygen flow rate. In the PEFC operation, the highest power density is obtained at the commercial Pt/C cathode catalyst (509.3 mW cm^{-2}), followed by Co–NCNT and Fe–NCNT, which give 164.0 mW cm^{-2} and 94.9 mW cm^{-2}, respectively. For the PEFC operation, the open circuit voltage (OCV) value for Fe–NCNT and Co–NCNT is 0.69 V and 0.77 V, respectively. These values are lower than that for the commercial Pt/C catalyst, which is 0.88 V. In other literature, the maximum power density value obtained for a Fe–NC catalyst synthesized from Fe (II)-phthalocyanine in PEFC at 60°C was 105 mW cm^{-2} [15]. A single PEFC performance test using a Co-based catalyst done by Y. Ma et al. at 80°C gave a maximum power density of 200 mW cm^{-2}, which is one fourth of that for the commercial Pt/C catalyst [16]. The Fe–NCNT and Co–NCNT catalysts in this study show maximum power densities of 94.9 mW cm^{-2} and 164.0 mW cm^{-2}, respectively, at 60°C operating temperature in PEFC. These results indicate that the Fe–NCNT and Co–NCNT catalysts synthesized in this study have comparable performances with those reported in previous studies in PEFC, despite their lower performance than the conventional Pt/C catalyst.

With regard to the DFAFC operation shown in Figure 4-1 (b), it is observed that DFAFC with Co–NCNT as the cathode catalyst gives the highest maximum power density, 142.4 mW cm^{-2}, than any other catalysts. This value indicates that it performs better than the commercial Pt/C catalyst as the cathode catalyst in DFAFC, which gives a maximum power density of 128.9

mW cm^{-2} under similar operating conditions. Comparing the PEFC and DFAFC operations, all catalysts tested here experience decay in the OCV value. However, the OCV reduction for Fe–NCNT and Co–NCNT is less than that experienced by the single cell with the commercial Pt/C catalyst. This indicates a higher formic acid tolerance of the non-Pt-based catalysts synthesized in this study than the commercial Pt/C catalyst. As shown in Table 4-3, the Co−NCNT and Pt/C cathode catalyst have comparable cell resistance with the other DFAFC operation reported in A. Zainoodin et al. with the cell resistance of ~ 200 $m\Omega \cdot cm^2$ for the ultrasonic spray method that was used in this study to prepare the MEA [17]. However, because of the highest catalyst loading used for Fe–NCNT as compared with the other catalysts, the resistance for the single cell with the Fe–NCNT cathode catalyst is the highest. A thicker cathode electrode may cause water saturation and flooding, thus hindering the diffusion of oxygen to the active sites of the catalyst [10,18]. The corresponding I–R corrected polarization and the corresponding power density curves are presented in Figure 4-1 (c). From these curves, it can be concluded that Co–NCNT still gives the best power density even though the catalyst loading used is similar for all catalyst. Although the performance of the single cell with Fe–NCNT as the cathode catalyst is the lowest in both PEFC and DFAFC operations, it should still be further investigated. As it is less expensive than Pt, it relies on very abundant resources, and it remains a promising cathode catalyst for DLFC application [10,19]. The power curve is also calculated in mW per mg catalyst used which is shown in Figure 4-2. The maximum power obtained for DFAFC with Co−NCNT cathode is lower than that Pt/C cathode catalyst which is 43.2 mW $mg^{-1}_{catalyst}$ and 64.5 mW $mg^{-1}_{catalyst}$ for Co−NCNT and Pt/C, respectively. As the Fe and Co is less expensive than the Pt, further study on optimization of the catalyst loading can be done to reach the similar or even higher cell performance than the Pt/C.

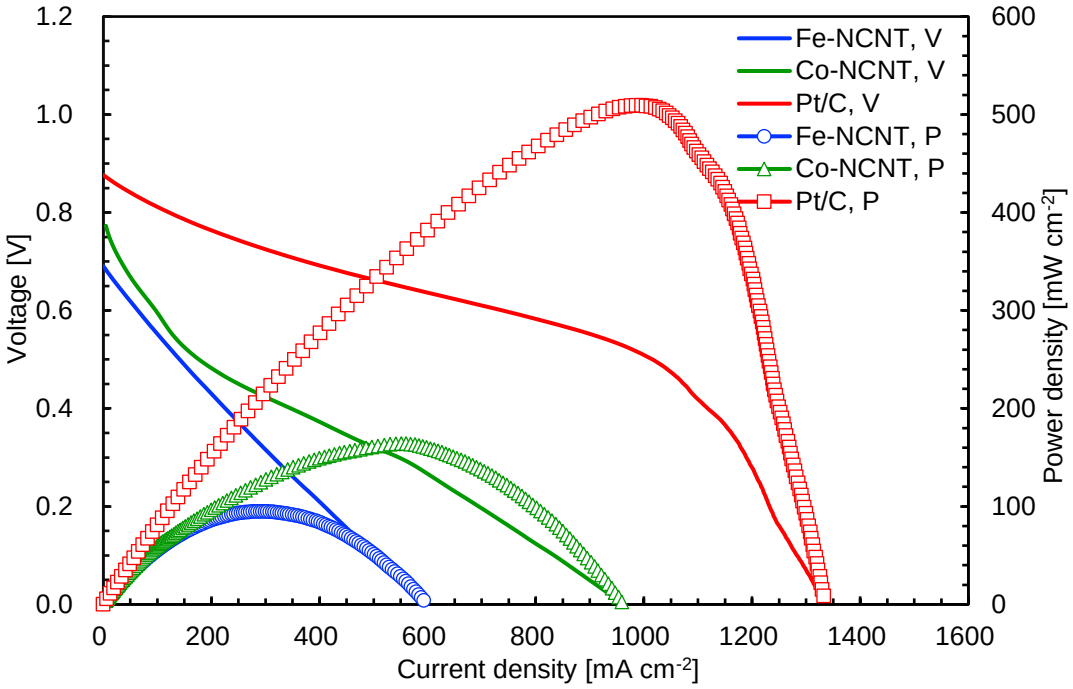

(a) PEFC

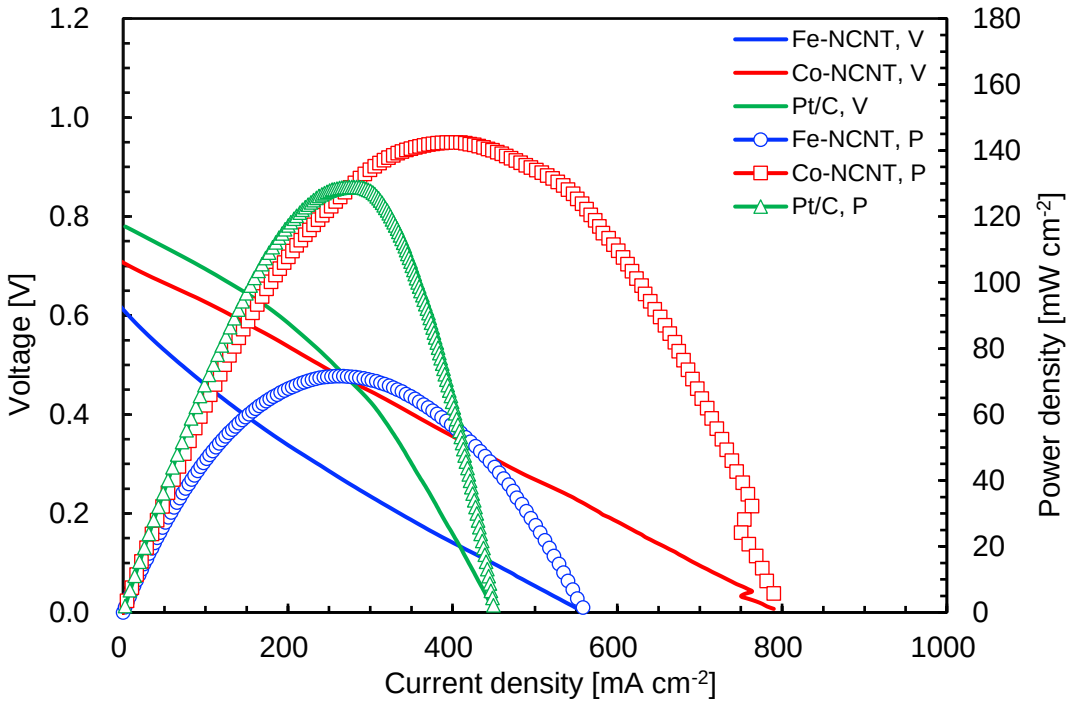

(b) DFAFC

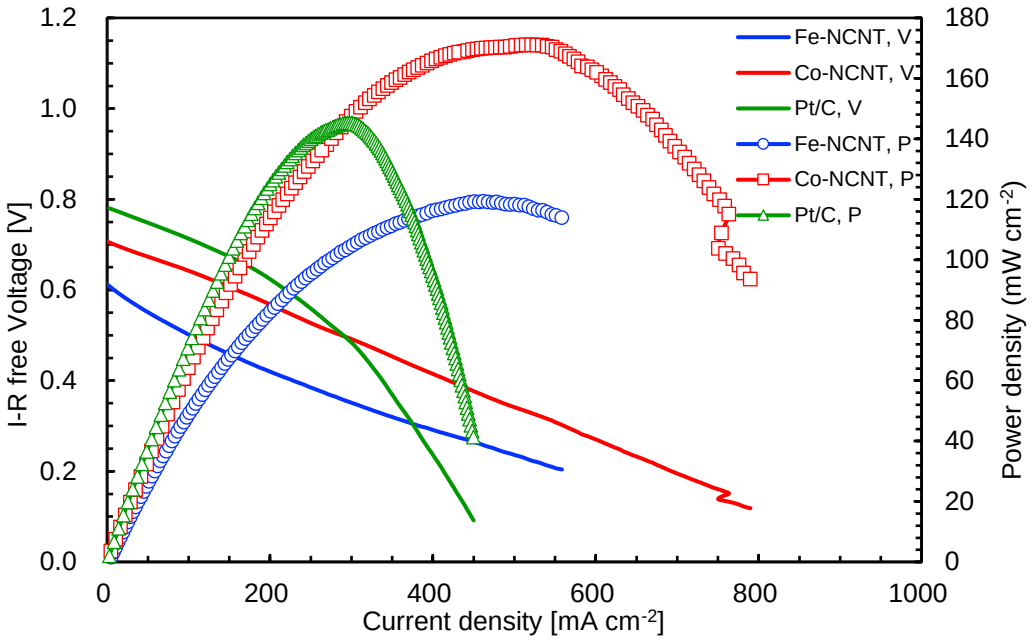

(c) DFAFC (I-R free voltage)

Figure 4-1 Polarization curve and power density curve for the (a) PEFC, (b) DFAFC, and (c) DFAFC (I–R free voltage) operations using Fe–NCNT, Co–NCNT, and commercial Pt/C as the cathode catalysts at 60°C operating temperature

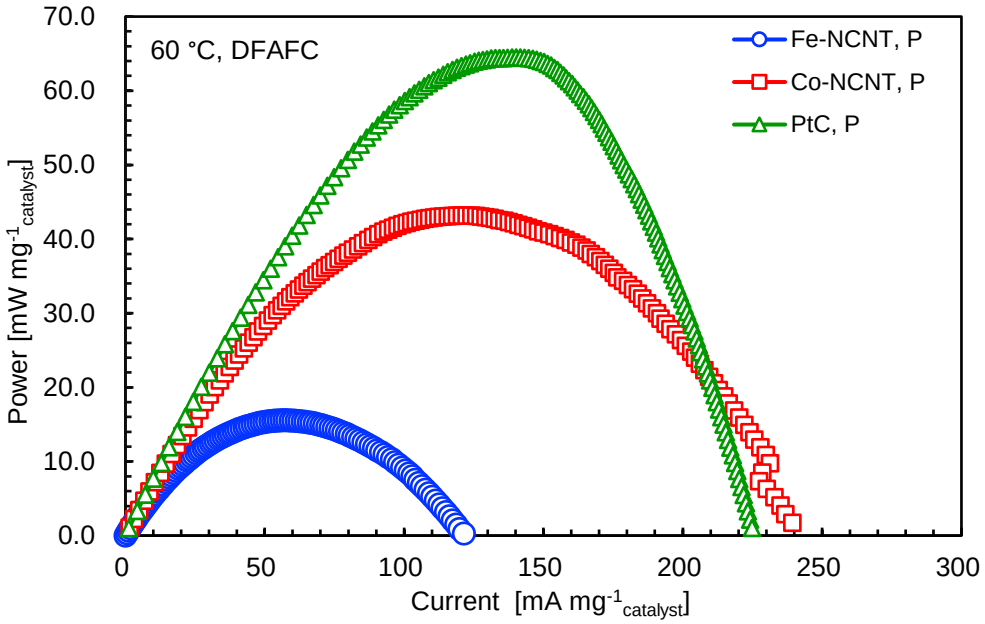

Figure 4-2 Specific power curve for DFAFC operation at 60 °C operating temperature and 5 M formic acid concentration

Table 4-3 Summary of single cell performance result for PEFC and DFAFC operation at 60°C and 5 M formic acid concentration

Operation	Catalyst	Open circuit voltage, OCV (V)	Cell resistance ($m\Omega \cdot cm^2$)	Max. power density ($mWcm^{-2}$)
PEFC	Fe–NCNT	0.69	407	94.9
	Co–NCNT	0.77	184	164.0
	Pt/C	0.88	150	509.3
DFAFC	Fe–NCNT	0.63	407	71.5
	Co–NCNT	0.71	155	142.4
	Pt/C	0.78	174	128.9

4.3.2 Effect of operating condition on DFAFC performance

Based on the single cell test at 60°C with 5 M formic acid concentration as the feed, the Co–NCNT catalyst shows the best performance, compared to the Fe–NCNT catalyst and the commercial Pt/C catalyst. Thus, we investigate the effect of the operating conditions on the DFAFC for the performance of the Co–NCNT catalyst. The cell performance is measured at 30°C and 60°C, formic acid concentrations from 3 M to 10 M, and three oxygen flow rates: 300 ml min^{-1}, 500 ml min^{-1}, and 700 ml min^{-1}. Figures 4-3 and 4-4 show the polarization and power density curves for DFAFC with the Co–NCNT catalyst at the cathode at 30°C and 60°C operating temperatures, respectively. The catalyst loading is 3.3 mg cm^{-2}. At 30°C operating temperature, the polarization and power density curves show a positive trend with increasing formic acid concentration, especially in the high current density region for all oxygen flow rates. The highest maximum power density achieved is 80.4 $mWcm^{-2}$ at 10 M formic acid concentration and 700 ml min^{-1} oxygen flow rate. Based on the different O_2 flow rates at 30°C operation, it is observed that, for 3 M formic acid concentration, the maximum power density is slightly decreased from 49.0

mW cm^{-2} to 44.7 mW cm^{-2} as the O_2 flow rate increases from 300 ml min^{-1} to 500 ml min^{-1} and slightly increased to 46.0 mW cm^{-2} as the O_2 flow rate increases from 500 ml min^{-1} to 700 ml min^{-1}. However, for 5, 7, and 10 M formic acid, the power density increases with the O_2 flow rate. In the DFAFC operation using a non-Pt catalyst at the cathode (Pd/C catalyst) done by A. Mikolajczuk-Zychora et al., the maximum power density achieved was approximately 60 mW cm^{-2} at 30 °C operating temperature, 3 M formic acid and 125 ml min^{-1} O_2 flow rate, which is higher than that achieved in this study (49.0 mW cm^{-2}) under the similar operating temperature and formic acid concentration [13].

The effect of the O_2 flow rate on the performance at 60°C is different, with the power density of DFAFC with 10 M formic acid decreasing at 700 ml min^{-1} O_2 flow rate. As for DFAFC operation, usage of dry oxygen in the cathode is expected. Thus, the decrease of the power density at high formic acid concentration and high O_2 flow rate may be caused by the drying of the cathode and the Nafion membrane. Although higher oxygen flow rates can increase the mass transport of oxygen and enhance the activity of the ORR, the greater amount of oxygen will dry up the Nafion membrane and decrease the proton transport ability [20,21].

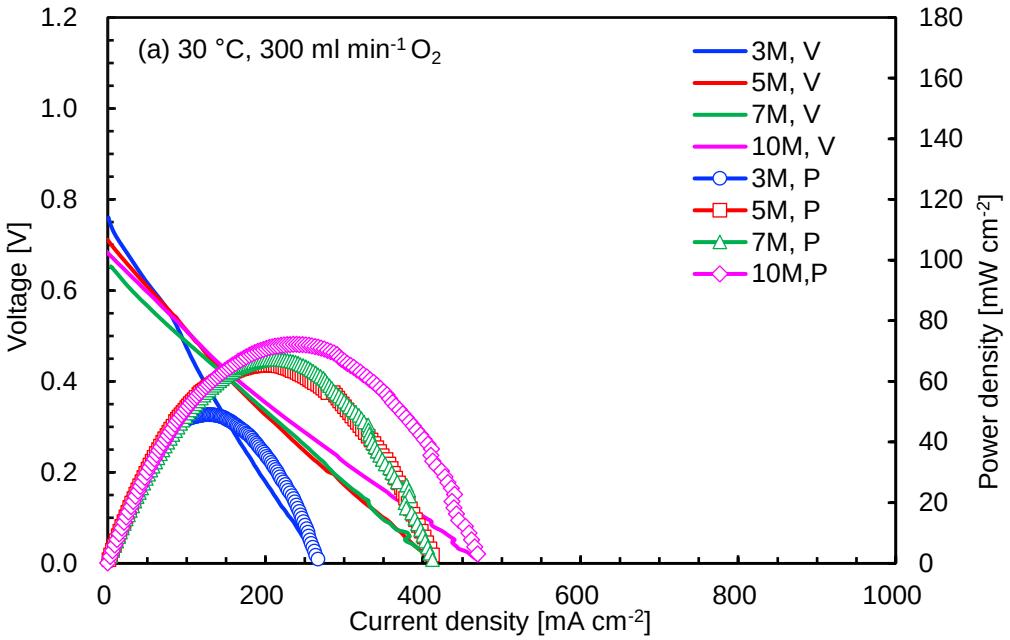
(a) 30 °C, 300 ml min-1 O2
3M, V
5M, V
7M, V
10M, V
3M, P
5M, P
7M, P
10M,P
Voltage [V]
Power density [mW cm-2]
Current density [mA cm-2]
0.0
0.2
0.4
0.6
0.8
1.0
1.2
0
20
40
60
80
100
120
140
160
180
0
200
400
600
800
1000

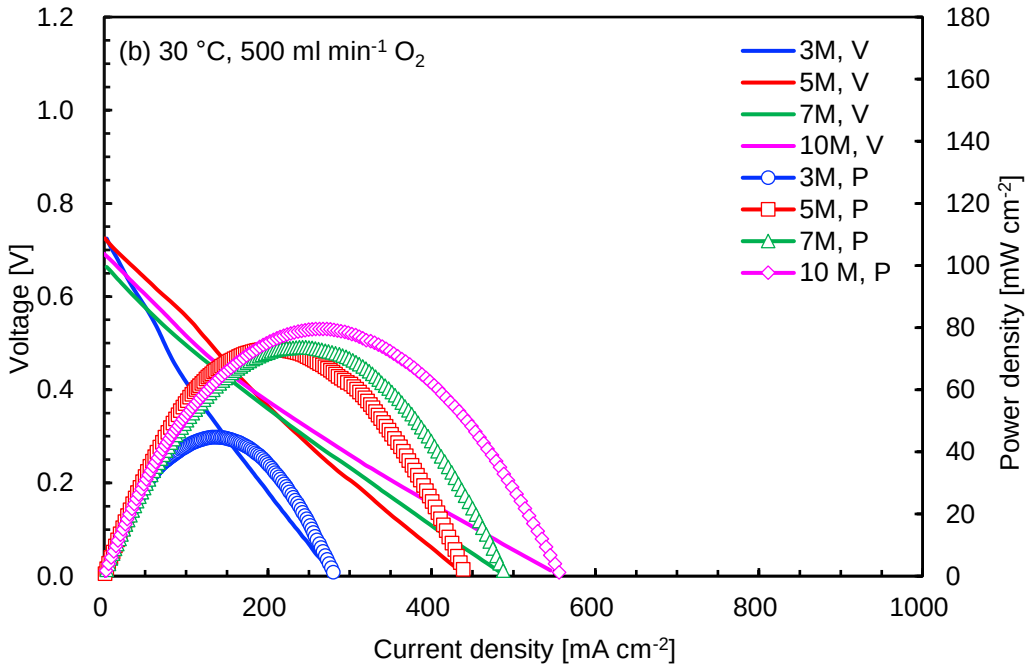
(b) 30 °C, 500 ml min-1 O2
3M, V
5M, V
7M, V
10M, V
3M, P
5M, P
7M, P
10 M, P
Voltage [V]
Power density [mW cm-2]
Current density [mA cm-2]
0.0
0.2
0.4
0.6
0.8
1.0
1.2
0
20
40
60
80
100
120
140
160
180
0
200
400
600
800
1000

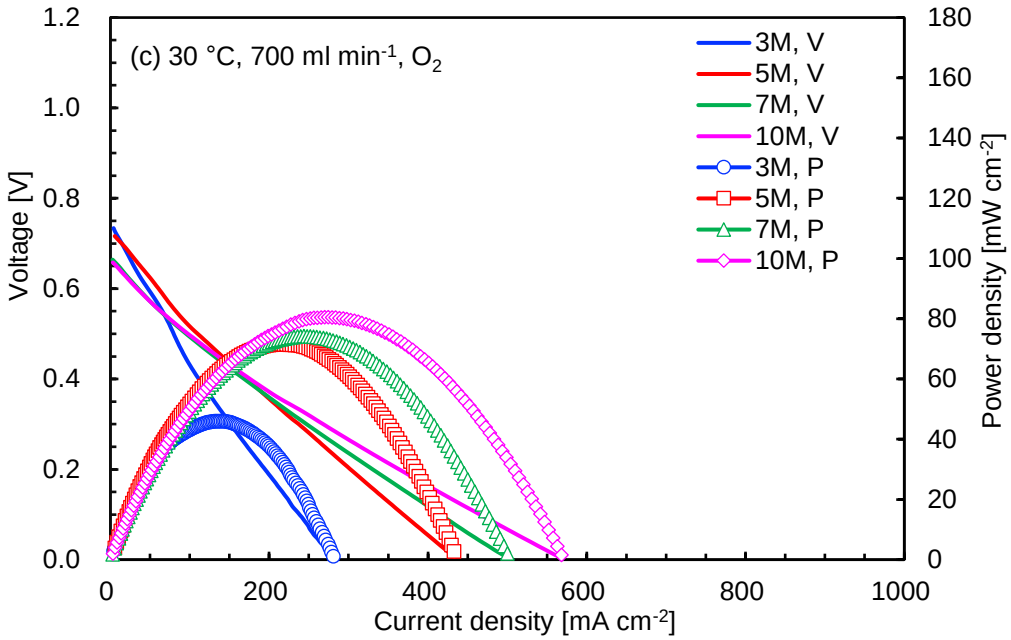

Figure 4-3 Polarization curve and power density curve single cell using Co–NCNT as the cathode catalyst in the DFAFC operation at 30°C with various formic acid concentrations and oxygen flow rates

At 60°C operating temperature, the optimum operating condition achieved by the DFAFC is at 7 M formic acid concentration and 700 ml min^{-1} O_2 flow rate; the highest maximum power density obtained is 160.7 mW cm^{-2}. As the formic acid concentration increases above 10 M, the maximum power density decreases for all O_2 flow rates. From the polarization curve, it can be observed that the OCV is only slightly affected by the formic acid concentration changes. The changes in the maximum power density and the OCV value with the formic acid concentration are further discussed in the below.

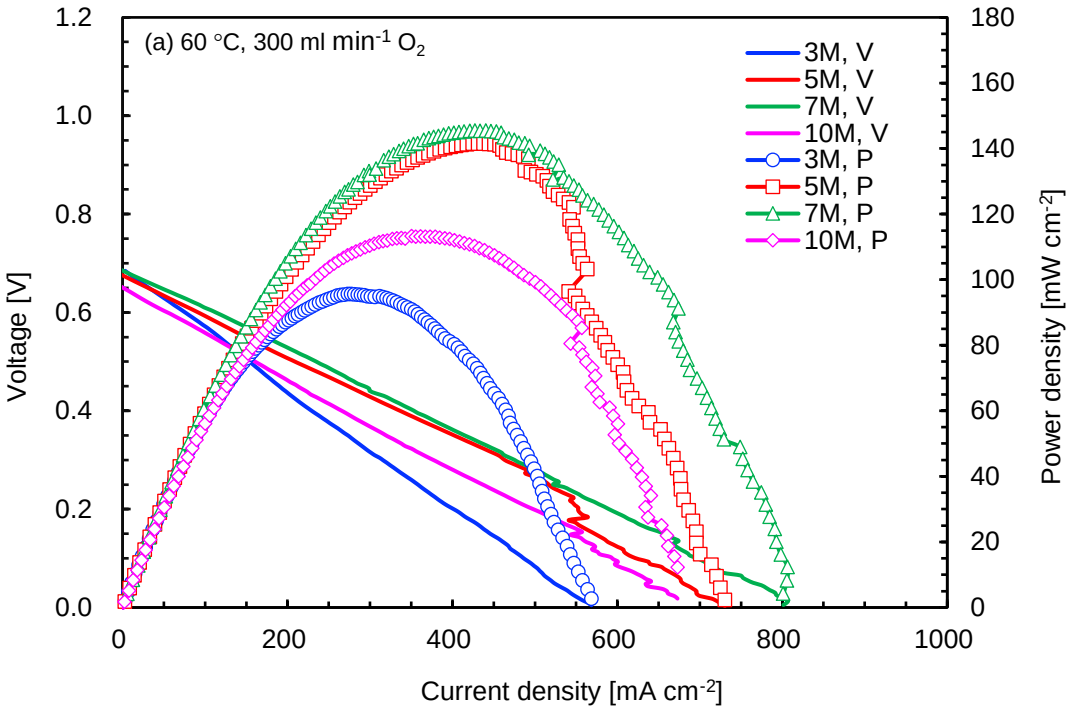
(a) 60 °C, 300 ml min-1 O2
3M, V
5M, V
7M, V
10M, V
3M, P
5M, P
7M, P
10M, P
Voltage [V]
Power density [mW cm-2]
Current density [mA cm-2]
0.0
0.2
0.4
0.6
0.8
1.0
1.2
0
20
40
60
80
100
120
140
160
180
0
200
400
600
800
1000

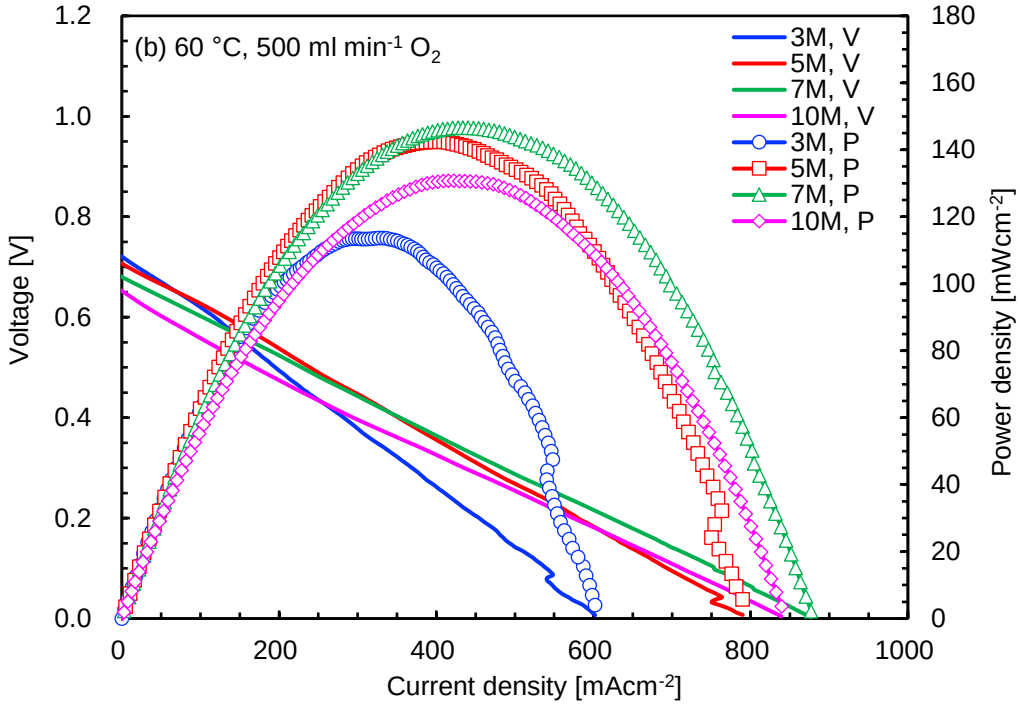
(b) 60 °C, 500 ml min-1 O2
3M, V
5M, V
7M, V
10M, V
3M, P
5M, P
7M, P
10M, P
Voltage [V]
Power density [mWcm-2]
Current density [mAcm-2]
0.0
0.2
0.4
0.6
0.8
1.0
1.2
0
20
40
60
80
100
120
140
160
180
0
200
400
600
800
1000

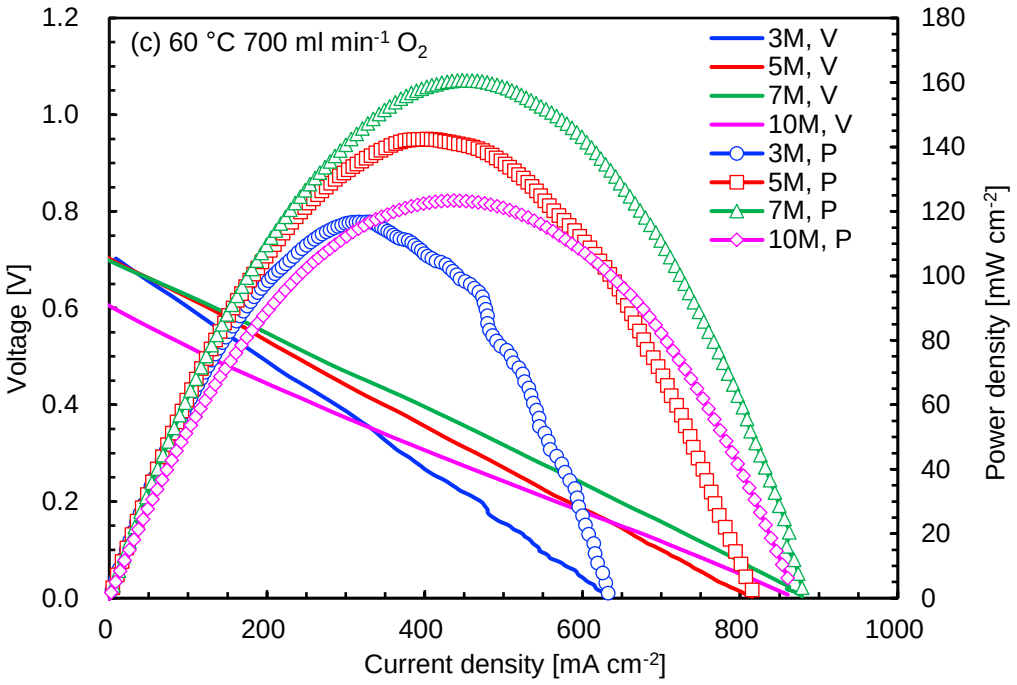

Figure 4-4 Polarization curve and power density curve single cell using Co–NCNT as the cathode catalyst in the DFAFC operation at 60°C with various formic acid concentrations and oxygen flow rates

In order to observe clearly the changes in the maximum power density and the OCV with changing formic acid concentration, the polarization and power density curves shown in Figure 4-3 and 4-4 are summarized and presented in Figure 4-5. From Figure 4-5 (a), as the temperature increases from 30°C to 60°C, the performance of the cell also increases. This is because a higher temperature increases the electrode kinetics controlling the anodic, cathodic, and membrane ionic conductivities, which contribute to an increase in cell performance [5]. Comparing the values derived under these operating temperatures, the maximum power density increases as the formic acid concentration increases up to 10 M at 30°C, but there is an optimum value of the maximum power density at 60°C operating temperature, 7 M formic acid concentration, and 700 ml min^{-1} oxygen flow rate. Performance decreases at 10 M formic acid concentration at 60^{o}C perhaps due

to the decrease in the oxygen availability at the cathode caused by the migration of the formic acid solution from the anode to the cathode through the membrane, which also results in the decrease of the OCV value at 10 M formic acid concentration, as shown in Figure 4-5 (c). This phenomenon occurs because the crossover flux of formic acid from the anode to the cathode through the membrane is increased with the operating temperature and the formic acid concentration [22]. In this study, for the operating temperature of 30 °C, the OCV decreases from 30 mV to 60 mV as the formic acid concentration increases above 5 M for all O_2 flow rates, whereas at 60 °C, the OCV decreases to 10 mV as the formic acid concentration increases above 5 M for 300 and 500 ml min^{-1} O_2 flow rate values. For the 700 ml min^{-1} O_2 flow rate and at 60°C, the OCV decreases of 40 mV when a formic acid concentration greater than 7 M is applied. This slight decay in both operating temperatures reflects the high tolerance of the cathode catalyst toward formic acid. The slight decrease in the OCV at higher feed concentration was also observed in the DMFC test conducted by J.C. Park and C.H. Choi, where the OCV slightly decreased with increasing methanol concentration using a Fe/Co–N–C catalyst at the cathode. These authors concluded that the slight decrease was not due to the competitive MOR in the cathode, as the catalyst showed high methanol tolerance [18].

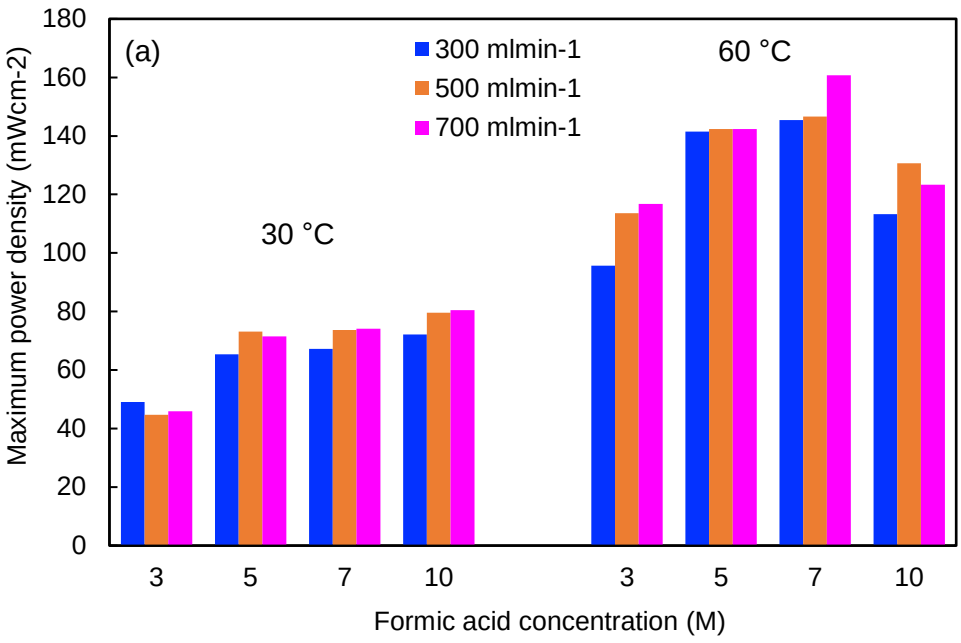
(a)
300 mlmin-1
500 mlmin-1
700 mlmin-1
30 °C
60 °C
Maximum power density (mWcm-2)
180
160
140
120
100
80
60
40
20
0
3
5
7
10
3
5
7
10
Formic acid concentration (M)

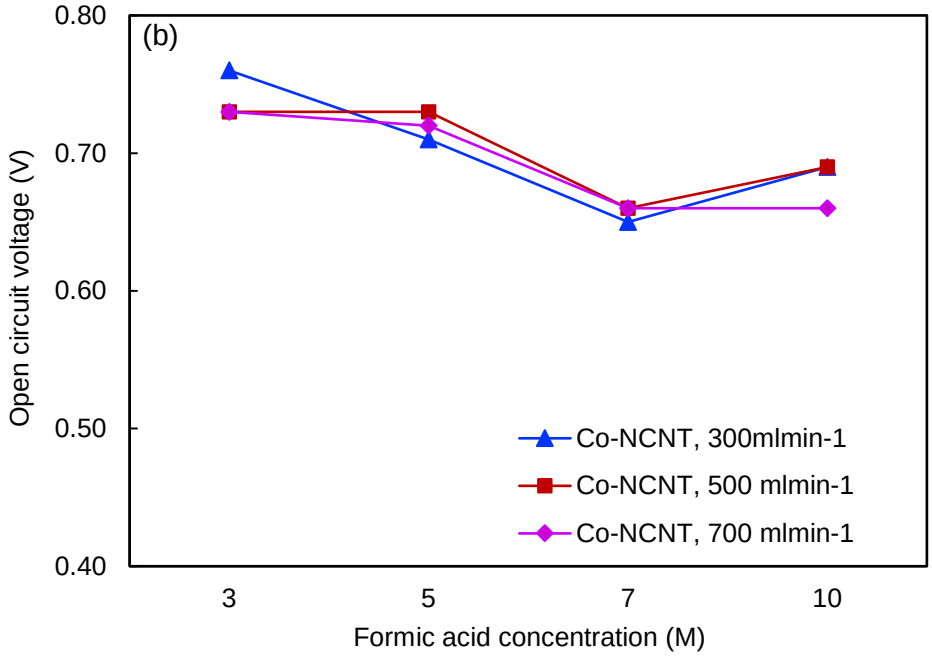
(b)
Open circuit voltage (V)
0.80
0.70
0.60
0.50
0.40
Co-NCNT, 300mlmin-1
Co-NCNT, 500 mlmin-1
Co-NCNT, 700 mlmin-1
3
5
7
10
Formic acid concentration (M)

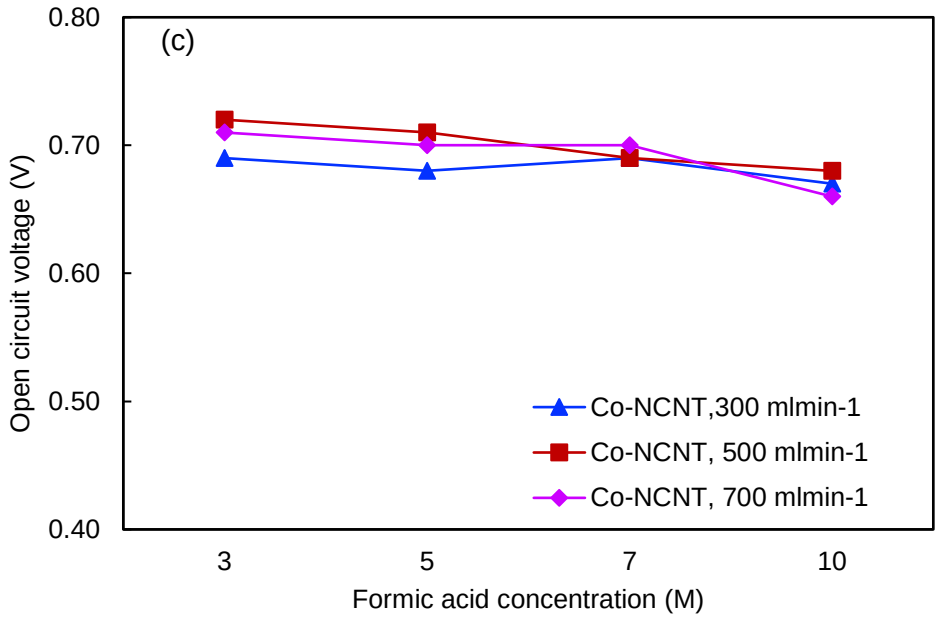

Figure 4-5 Maximum power density (a) and open circuit voltage (b and c) in DFAFC as a function of the formic acid concentration at 30°C and 60°C operating temperatures

4.3.3 Comparisons of performance with other DLFC

Next, we compare the performance obtained for the single DFAFC using the Fe–NCNT and the Co–NCNT cathode catalysts with the other types of DLFCs especially in DMFC operation. Moreover, no studies reported on the single DFAFC operation using the transition metal−nitrogen-doped carbon (TM−NC) based as the cathode catalyst. The present findings for the optimum feed concentration corroborate those of other studies[10,12,23] on the DMFC with a transition metal–nitrogen–carbon as the cathode catalyst. Table 4-4 presents the performance data obtained for the direct methanol fuel cell (DMFC) operation using a transition metal–nitrogen–carbon material catalyst as the cathode catalyst, particularly Fe and Co. The DMFCs listed in Table 4-4 are actively fed with a methanol solution and O_2 at the anode and the cathode, respectively. From the data presented in Table 4-4, the maximum power density achieved in this study is the best compared

with those from other studies on DMFC utilizing Fe- and Co-based catalysts at the cathode. It is noteworthy that DFAFC using both the Fe–NCNT and Co–NCNT catalysts in this study exhibits the highest maximum power density at 60°C, whereas in other studies, only 90°C operating temperature was applied.

D. Sebastian et al. evaluated the effect of the cathode catalyst (Fe–NCB) loading on the performance of a DMFC operated at 90°C with 10 M methanol. The highest maximum power density was achieved by the single cell using 4 mg cm^{-2} Fe–N−CB and PtRu loading at the cathode and anode, respectively [10]. Fe–NCNT synthesized by pyrolysis of MWCNT and Fe–Phen complex in the study by Osmieri et al. gave the maximum power density of 7.7 $mWcm^{-2}$ at 90°C which lower than that achieved by the other mesoporous carbon support (Fe-NMPC) [12]. This indicates the non-Pt catalysts synthesized in this study are promising for DFAFC application. Based on the comparison with the DMFC, the performance obtained in this study is the highest. This is in accordance with the performance using the Pt-based catalyst as the cathode catalyst, where all reported DFAFCs showed better performance than DMFC due to the high kinetic rate of formic acid oxidation and low fuel crossover than DMFC [24].

Table 4-4 Summary of performance for DMFC with Fe– and Co–based catalysts at the cathode

Operation	Cathode catalyst	Open circuit voltage (V)	Max. power density ($mWcm^{-2}$)	Feed concentration (M)	Oxygen/ air	Operating temperature (°C)	Reference
DMFC	Fe–NCB 4 mg cm^{-2}	0.82	60	10	Humidified oxygen 100 ml min^{-1}	90	[10]
DMFC	Fe–NCNT 2.5 mg cm^{-2}	0.57	7.7	2	Dry oxygen 200 Nml min^{-1} 3 bar backpressure	90	[12]
DMFC	Fe−NMPC 2.5 mg cm^{-2}	0.64	22.6	2	Dry oxygen 200 Nml min^{-1} 3 bar backpressure	90	[12]
DMFC	Co–NC 10 mg cm^{-2}	~0.50	53.2	2	Oxygen 100 ml min^{-1}	60	[23]
DFAFC	Fe–NCNT 4.6 mg cm^{-2}	0.63	71.5	5	Dry Oxygen 500 ml min^{-1}	60	This study
DFAFC	Co–NCNT 3.3 mg cm^{-2}	0.70	160.7	7	Dry oxygen 700 ml min^{-1}	60	This study

4.4 Conclusions

Single-cell tests for the Fe–NCNT and Co–NCNT catalysts at the cathode were conducted in the PEFC and DFAFC operations. The OCV difference between the PEFC and DFAFC operation for both TM–N−CNT catalysts is lower than that for the Pt/C catalyst, reflecting their high formic acid tolerance characteristic. At 60°C operating temperature with 5 M formic acid concentration and 500 ml min^{-1} dry oxygen flow rate, DFAFC with the Co–NCNT cathode catalyst gave the highest maximum power density. The effects of the operating temperature, the formic acid concentration, and oxygen flow rate on the performance of DFAFC with Co–NCNT as the cathode catalyst were then determined. The maximum power density achieved by the DFAFC was 160.7 mW cm^{-2} at 60°C and 7 M formic acid concentration. As compared with the DMFC operation in other studies,

DFAFC measured in this study gave the highest maximum power density with both TM–NCNT catalysts at the cathode. Therefore, it can be concluded that the Fe–NCNT and Co–NCNT catalysts used in this study showed high performance in the DFAFC operation. However, it is necessary for further optimize the other catalyst parameters such as catalyst loading and ionomer loading in the catalyst in future to enhance the cell performance. The durability test in the DFAFC operation with the TM−NCNT catalysts also should be done in future as the catalyst showed better durability than the conventional Pt/C catalyst in DMFC operation.

4.5 References

[1] N.A. Karim, S.K. Kamarudin, K.S. Loh, Performance of a novel non-platinum cathode catalyst for direct methanol fuel cells, Energy Convers. Manag. 145 (2017) 293–307. doi:10.1016/j.enconman.2017.05.003.

[2] N.A. Karim, S.K. Kamarudin, Novel heat-treated cobalt phthalocyanine/carbon-tungsten oxide nanowires (CoPc/C-W18O49) cathode catalyst for direct methanol fuel cell, J. Electroanal. Chem. 803 (2017) 19–29. doi:10.1016/j.jelechem.2017.08.050.

[3] S. Ratso, I. Kruusenberg, A. Sarapuu, M. Kook, P. Rauwel, R. Saar, J. Aruväli, K. Tammeveski, Electrocatalysis of oxygen reduction on iron- and cobalt-containing nitrogen-doped carbon nanotubes in acid media, Electrochim. Acta. 218 (2016) 303–310. doi:10.1016/j.electacta.2016.09.119.

[4] L. Lin, Q. Zhu, A. Xu, Noble-Metal-Free Fe − N/C Catalyst for Highly E ffi cient Oxygen Reduction Reaction under Both Alkaline and Acidic Conditions, J. Am. Chem. Soc. 136 (2014) 11027–11033. doi:10.1021/ja504696r.

[5] D. Sebastián, V. Baglio, A.S. Aricò, A. Serov, P. Atanassov, Performance analysis of a non-platinum group metal catalyst based on iron-aminoantipyrine for direct methanol fuel cells,

Appl. Catal. B Environ. 182 (2016) 297–305. doi:10.1016/j.apcatb.2015.09.043.

[6] R. Janarthanan, A. Serov, S.K. Pilli, D.A. Gamarra, P. Atanassov, M.R. Hibbs, A.M. Herring, Direct Methanol Anion Exchange Membrane Fuel Cell with a Non-Platinum Group Metal Cathode based on Iron-Aminoantipyrine Catalyst, Electrochim. Acta. 175 (2015) 202–208. doi:10.1016/j.electacta.2015.03.209.

[7] R. Zhang, Y. Peng, Z. Li, K. Li, J. Ma, Y. Liao, L. Zheng, X. Zuo, D. Xia, Oxygen Electroreduction on Heat - treated Multi - walled Carbon Nanotubes Supported Iron Polyphthalocyanine in Acid Media, Electrochim. Acta. 147 (2014) 343–351. doi:10.1016/j.electacta.2014.09.064.

[8] Y. Liu, J. Ruan, S. Sang, Z. Zhou, Q. Wu, Iron and nitrogen co-doped carbon derived from soybeans as efficient electro-catalysts for the oxygen reduction reaction, Electrochim. Acta. 215 (2016) 388–397. doi:10.1016/J.ELECTACTA.2016.08.090.

[9] D. Sebastián, A. Serov, K. Artyushkova, P. Atanassov, A.S. Aricò, V. Baglio, Performance, methanol tolerance and stability of Fe-aminobenzimidazole derived catalyst for direct methanol fuel cells, J. Power Sources. 319 (2016) 235–246. doi:10.1016/j.jpowsour.2016.04.067.

[10] D. Sebastián, A. Serov, I. Matanovic, K. Artyushkova, P. Atanassov, A.S. Aricò, V. Baglio, Insights on the extraordinary tolerance to alcohols of Fe-N-C cathode catalysts in highly performing direct alcohol fuel cells, Nano Energy. 34 (2017) 195–204. doi:10.1016/J.NANOEN.2017.02.039.

[11] A.H.A. Monteverde Videla, D. Sebastián, N.S. Vasile, L. Osmieri, A.S. Aricò, V. Baglio, S. Specchia, Performance analysis of Fe–N–C catalyst for DMFC cathodes: Effect of water saturation in the cathodic catalyst layer, Int. J. Hydrogen Energy. 41 (2016) 22605–22618.

doi:10.1016/J.IJHYDENE.2016.06.060.

[12] L. Osmieri, R. Escudero-Cid, M. Armandi, A.H.A. Monteverde Videla, J.L. García Fierro, P. Ocón, S. Specchia, Fe-N/C catalysts for oxygen reduction reaction supported on different carbonaceous materials. Performance in acidic and alkaline direct alcohol fuel cells, Appl. Catal. B Environ. 205 (2017) 637–653. doi:10.1016/j.apcatb.2017.01.003.

[13] A. Mikolajczuk-zychora, A. Borodzinski, P. Kedzierzawski, B. Mierzwa, Highly active carbon supported Pd cathode catalysts for direct formic acid fuel cells, Appl. Surf. Sci. 388 (2016) 645–652. doi:10.1016/j.apsusc.2016.02.065.

[14] S.L. Blair, W.L. (Simon) Law, Electrocatalysis in Other Direct Liquid Fuel Cells, Electrocatal. Direct Methanol Fuel Cells. (2009). doi:doi:10.1002/9783527627707.ch14.

[15] L. Osmieri, R. Escudero-Cid, A.H.A. Monteverde Videla, P. Ocón, S. Specchia, Performance of a Fe-N-C catalyst for the oxygen reduction reaction in direct methanol fuel cell: Cathode formulation optimization and short-term durability, Appl. Catal. B Environ. 201 (2017) 253–265. doi:10.1016/J.APCATB.2016.08.043.

[16] Y. Ma, H. Zhang, H. Zhong, T. Xu, H. Jin, Y. Tang, Z. Xu, Cobalt based non-precious electrocatalysts for oxygen reduction reaction in proton exchange membrane fuel cells, Electrochim. Acta. 55 (2010) 7942–7947. doi:10.1016/j.electacta.2010.03.087.

[17] A.M. Zainoodin, T. Tsujiguchi, M.S. Masdar, S.K. Kamarudin, Y. Osaka, A. Kodama, Performance of a direct formic acid fuel cell fabricated by ultrasonic spraying, Int. J. Hydrogen Energy. 43 (2018) 6413–6420. doi:10.1016/J.IJHYDENE.2018.02.024.

[18] J.C. Park, C.H. Choi, Graphene-derived Fe/Co-N-C catalyst in direct methanol fuel cells: Effects of the methanol concentration and ionomer content on cell performance, J. Power Sources. 358 (2017) 76–84. doi:10.1016/J.JPOWSOUR.2017.05.018.

[19] F.J. Pérez-Alonso, M.A. Salam, T. Herranz, J.L. Gómez De La Fuente, S.A. Al-Thabaiti, S.N. Basahel, M.A. Peña, J.L.G. Fierro, S. Rojas, Effect of carbon nanotube diameter for the synthesis of Fe/N/multiwall carbon nanotubes and repercussions for the oxygen reduction reaction, J. Power Sources. 240 (2013) 494–502. doi:10.1016/j.jpowsour.2013.04.086.

[20] S. Chen, F. Ye, W. Lin, Effect of operating conditions on the performance of a direct methanol fuel cell with PtRuMo/CNTs as anode catalyst, Int. J. Hydrogen Energy. 35 (2010) 8225–8233. doi:10.1016/J.IJHYDENE.2009.12.085.

[21] G. Liu, H. Zhou, X. Ding, X. Li, D. Zou, X. Li, X. Wang, J.K. Lee, Effect of fabrication and operating parameters on electrochemical property of anode and cathode for direct methanol fuel cells, Energy Convers. Manag. 122 (2016) 366–371. doi:10.1016/j.enconman.2016.06.008.

[22] N. V Rees, R.G. Compton, Sustainable energy: a review of formic acid electrochemical fuel cells, J. Solid State Electrochem. 15 (2011) 2095–2100. doi:10.1007/s10008-011-1398-4.

[23] Y. Wei, C. Shengzhou, L. Weiming, Oxygen reduction on non-noble metal electrocatalysts supported on N-doped carbon aerogel composites, Int. J. Hydrogen Energy. 37 (2012) 942–945. doi:10.1016/J.IJHYDENE.2011.03.103.

[24] W. Cai, L. Liang, Y. Zhang, W. Xing, C. Liu, Real contribution of formic acid in direct formic acid fuel cell : Investigation of origin and guiding for micro structure design, Int. J. Hydrogen Energy. 38 (2012) 212–218. doi:10.1016/j.ijhydene.2012.09.155.

CHAPTER 5

5.1 Conclusions

In summary, transition metal−nitrogen doped−carbon nanotubes catalyst namely, Fe-NCNT and Co−NCNT for DFAFC cathode catalyst were synthesized in this study. Their ORR catalytic activity and single DFAFC performance were evaluated. At first, the effect of pyrolysis step of each catalyst on the ORR activity in acidic and alkaline medium was determine. It was found that the effect of pyrolysis is different on the ORR activity in acidic and alkaline medium. Catalyst from first pyrolysis, Fe−NCNT1 and Co−NCNT1 perform better than other samples in acidic medium. For alkaline medium, acid-treated combined with second pyrolyzed Fe-containing catalyst (Fe−NCNT2A) and twice pyrolyzed Co-containing catalyst (Co−NCNT2) perform better in alkaline medium. It can be concluded that Fe−NCNT catalyst was found to be more active for ORR in acidic medium whereas Co−NCNT catalyst is more active for ORR in alkaline medium. In comparison with commercial Pt/C catalyst, the ORR activity of these Fe−NCNT and Co−NCNT catalysts are still lower, but they have better fuel tolerance than that commercial Pt/C catalyst in acidic and alkaline medium. The Co−NCNT catalyst exhibits superior stability than Fe−NCNT and comparable with commercial Pt/C catalyst in both medium. These characteristics make the TM−NCNT catalyst prepared in this study as a promising for fuel cell application either in acidic or alkaline condition.

Therefore, single cell performance test was carried out by using Fe−NCNT and Co−NCNT as the cathode catalyst. Single cell tests for the Fe–NCNT and Co–NCNT catalysts at the cathode were conducted in the PEFC and DFAFC operations. The OCV difference between the PEFC and DFAFC operation for both TM–NCNT catalysts is lower than that for the Pt/C catalyst, reflecting

their high formic acid tolerance characteristic. At 60°C operating temperature with 5 M formic acid concentration and 500 ml min^{-1} dry oxygen flow rate, DFAFC with the Co–NCNT cathode catalyst gave the highest maximum power density. The effects of the operating temperature, the formic acid concentration, and oxygen flow rate on the performance of DFAFC with Co–NCNT as the cathode catalyst were then determined. The maximum power density achieved by the DFAFC was 160.7 mW cm^{-2} at 60°C and 7 M formic acid concentration. As compared with the DMFC operation in other studies, DFAFC measured in this study gave the highest maximum power density with both TM–NCNT catalysts at the cathode. It can be concluded that the Fe–NCNT and Co–NCNT catalysts used in this study showed high performance in the DFAFC operation. Therefore, the aim to obtain high performance in direct liquid fuel cell (DLFC) operation was achieved in this study. However, it is necessary for further optimize the other catalyst parameters such as catalyst loading and ionomer loading in the catalyst in future to enhance the cell performance. The durability test in the DFAFC operation with the TM−NCNT catalysts also should be done in future as the catalyst showed better durability than the conventional Pt/C catalyst in DMFC operation. The performance of single direct formate fuel cell (DFFC) using those catalysts at the cathode also should be measured as they show good ORR activity and fuel tolerance in alkaline medium.

ACKNOWLEDGMENT

First of all, praises to Allah for everything that He granted. I am so grateful for giving me the opportunity, patience and perseverance throughout this research journey.

I would like to express my deepest appreciation to my supervisor, Dr. Takuya Tsujiguchi for his guidance, earnest supervision during my study in Kanazawa University. Besides, he always gives moral support, teach me well regarding the research area and very helpful supervisor in solving the any problem faced during my research work.

I would like to thank Professor Akio Kodama and Dr. Yugo Osaka for giving advices and comments for improving my knowledge about my research area. Many thanks to my laboratory member especially, Norraihanah Mohamed Aslam and Ryouta Mochizuki who always giving me assistance and support in these three years. Thank you to other laboratory members as well for giving cooperation and helping me in improving my Japanese language.

A lot of thanks to Kanazawa University staff, Malaysian students as well as the students from other countries for their kindness and help in my daily life in Japan.

A lot of thanks to Ministry of Education, Culture, Sports, Science and Technology for the scholarship in these three years.

Finally, special thanks to my family for the encouragement, support and continuous pray to ease my life journey.

LIST OF PUBLICATION AND PRESENTATION RELATED TO THE THESIS

Publication:

1. Fahimah Abd Lah Halim[1], Takuya Tsujiguchi[*2], Yugo Osaka[2], Akio Kodama[2]. Performance of direct formic acid fuel cell using transition metal–nitrogen-doped carbon nanotubes as cathode catalysts. International Journal of Energy Research. 2019.

Conference paper:

1. Fahimah Abd Lah Halim[1], Takuya Tsujiguchi[*2], Yugo Osaka[2], Akio Kodama[2]. Study on formic acid tolerance of transition metal-containing nitrogen-doped carbon nanotubes for the cathode of the direct formic acid fuel cell. The 6th International Conference on Nuclear and Renewable Energy Resources (NURER2018). 30 Sep. - 03 Oct. 2018. Jeju, Korea.